Structure-Property Relationships of Electron Beam Cured Systems Containing Bis-GMA

by

Danny C. Thompson

Thesis submitted to the Faculty of the

Virginia Polytechnic Institute and State University

in partial fulfillment of the requirements for the degree of

Master of Science

in

Chemical Engineering

APPROVED:

Garth L. Wilkes, Chairman

James E. McGrath

Donald G. Baird

September, 1986

Blacksburg, Virginia

Structure-Property Relationships of Electron Beam Cured Systems Containing Bis-GMA

by

Danny C. Thompson

Garth L. Wilkes, Chairman

Chemical Engineering

(ABSTRACT)

Structure-property relationships were investigated for the bis-glycidyl methacrylate derivatives of bisphenol-A crosslinked by electron beam irradiation. This material, commonly called bis-GMA, is a viscous liquid at room temperature which crosslinks to form a glassy network when a 3 to 5 mil coating is irradiated with sufficient energy. The major parameters which were systematically varied in this study were radiation dosage, dose rate, aging time after irradiation, and post-cure annealing at higher temperatures.

Measurements were conducted first to quantify the crosslinking reaction, then to characterize the physical properties of the resulting networks. Extraction by a solvent was done to determine the degree of network formation through the equilibrium swelling ratio and the gel weight fraction after drying. Another method utilized FTIR to monitor the disappearance of double bonds as the crosslinking reaction proceeded. In order to characterize the physical properties, differential scanning calorimetry (DSC) and dynamic mechanical spectroscopy were done to determine the glass transition temperature.

It was found that the network density or amount of cure is proportional to the irradiation dosage, with an upper limit reached above some critical dosage. Dose rate was not found to influence the degree of cure greatly. The crosslinking reaction often became diffusion limited as vitrification occurred. These phenomena were discussed in terms of the well-known Time-Temperature-Transformation diagram. Free radicals trapped in these networks exhibited a finite lifetime. Post-curing can be achieved by annealing at a temperature above the

T_g of the network, as shown by the increase of the glass transition temperature from DSC and dynamic mechanical results.

Bis-GMA was mixed with rubbery modifier materials with acrylate and methacrylate functional ends in order to toughen the bis-GMA networks. It was observed that the acrylate end groups were more reactive in EB cured systems than analogous methacrylates probably due to their higher polymerization enthalpy and less steric hindrance. Phase separation, which would provide rubber toughening without depressing the high glass transition temperature, was not achieved by irradiation with the modifying materials at the molecular weights used in this study, but the mixtures were toughened as shown by the dynamic mechanical data.

Acknowledgements

I would first like to thank my advisor, Dr. Garth Wilkes, for his direction and his tireless effort. The hard work is making me a better scientist.

I would also like to thank;

Dr. Joo H. Song, post-doctoral fellow in our lab, for performing SEM tests, and for being there during the early part of this project as we learned together.

Dr. Dillip Mohanty, for assistance with the end-capping reaction.

Dr. D.G. Baird and Dr. J.E. McGrath, my committee members, for their helpful discussions and willingness to serve.

Vic Thalacker, Tom Simpson, and the 3M Company for their financial support and for allowing me to learn from their E-Beam team.

The "lunch bunch"; Greg, Tom, Chun-Wah, and Kim, for those "never a dull moment lunches" and the comedy we called softball.

The guys in the lab and my many friends at Wesley for their support and encouragement.

Finally, my love and thanks to Mom and Dad for their love, thoughtfulness, and encouragement.

Table of Contents

List of Illustrations

List of Tables

1.0 Introduction

Coating processes have gained prominence in industry for large scale application of adhesives or other polymeric formulations onto a substrate (e.g., polymeric, paper, metal, etc.). Formulations have historically consisted of polymer "binders", surfactants, adhesives, and fillers suspended in solvents. Thermal ovens are widely used to evaporate carrier solvents as well as initiate crosslinking in reactive systems.

More recently, solventless coatings have emerged to significance in industry. Development of solventless coatings using radiation crosslinking was expedited during the 1970's to help offset energy costs and stiffer pollution regulations. This momentum has been carried into the 1980's, as more economical radiation sources are becoming available, and in many cases, radiation crosslinked materials possess certain desirable physical properties.

Radiation for the curing of polymers is generated in the form of infrared (IR), ultraviolet (UV), electron beam (EB), or gamma rays (γ-rays). Electrical energy is the primary source of IR, UV, and EB radiation, while a radioactive isotope such as cobalt-60 (Co^{60}) is required to generate gamma rays. Although the research discussed in this thesis utilizes only electron beam irradiation, a brief discussion of all the forms mentioned above is given for comparison and contrast.

1.1 Sources for Radiation Curing

1.1.1 Infrared

The photon energy for infrared sources ranges from 0.01 to 1 electron volt (eV), well below that required to break chemical bonds. That being the case, infrared radiation is generally absorbed in molecules through rotational, vibrational, or translational energy modes. Curing proceeds similarly to that experienced in conventional thermal ovens. As such, IR curing suffers from the same inefficiencies as thermal curing, with energy being lost to the substrate and to the surroundings. Another inefficiency arises due to the fact that the crosslinking medium only absorbs a few wavelengths. Since most IR sources provide a wide distribution of wavelengths, much of the energy may pass through the target unabsorbed.

Infrared radiation might be preferred, however, where heat sensitive coatings are applied to odd geometrical shapes. Both EB and UV generally cure through chemical bond-breaking mechanisms, such that the initiation process might not be uniformly distributed through non-uniform geometries. Since the IR induces thermal initiation, only thermal conduction is required. In general, IR has many limiting variables which include cure speed, coating thickness, and substrate material, so its applications are likely to be few as compared to UV or EB.

1.1.2 Ultraviolet

Ultraviolet sources produce radiation in the range of 200 to 400 nm, with photon energies of 3 to 6 eV. A distribution of wavelengths usually exists such that infrared radiation is also present. A filter may be used to reduce the IR light. The UV light energy is only sufficient to break certain bonds, particularly those of photoinitiators such as benzophenone or benzoin ethers.[1] The chemical structures for a few common photoinitiators are shown in Figure 1. Free radicals are generated within the initiators which can begin the chain reaction to crosslink the monomers and oligomers. Since many reactions can occur from just one initial free radical, UV cure is much more energy efficient than IR curing.

Applications where ultraviolet light sources are used are numerous and new developments continue in the field. Much work has been done to crosslink printing inks on paper, fabrics, metal, glass, and wood via UV irradiation [1]. UV crosslinking of thin industrial coatings is also a rapidly growing field. Epoxy UV-curable formulations as well as acrylated urethane formulations are commonly used in these coatings.

A few characteristics of UV curing are worth mentioning. First, line speeds are inversely proportional to coating thickness. Assuming that one 200 Watt per inch lamp is used, coating speeds range from 15 feet per minute at 5 mils to 100 feet per minute at 0.1 mils. Secondly, the process is cooler than IR curing, as a temperature rise of 15 to 20°C is reported by Ramler for conventional systems [2]. More discussion will be given concerning the temperature rise during curing in a later section. A third characteristic of UV curing is the difficulty observed with achieving adequate adhesion, which is often associated with coating shrinkage. Finally, the monomers in many of these formulations may be more likely to swell elastomeric machine parts (e.g., rubber rolls) than conventional solvents.

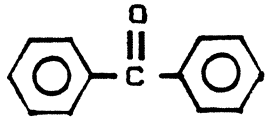

BENZOPHENONE

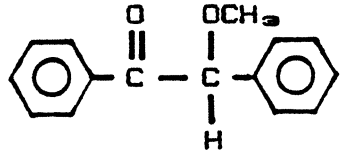

BENZOIN METHYL ETHER

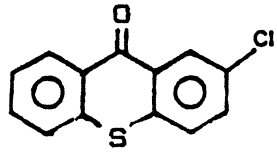

2-CHLOROTHIOXANTHONE

Figure 1. Common UV/Visible Initiators: Chemical structures of a few common initiators [1].

1.1.3 Electron Beam

Electrons differ from photons in that the electrons have mass and charge and their energies are high enough to break chemical bonds. Since some of these bonds break to form ionic species, the term "ionizing radiation" is often used to characterize EB (and γ-ray) radiation. In addition, the initiations usually generate free radicals which can initiate chain polymerization reactions. Thus, by introducing monomers or oligomers containing vinyl groups or other reactive species, polymerization, branching, and crosslinking reactions can occur without the photosensitizers required in UV curing.

Electron beams are often generated by heating an electron-rich transition metal to high temperatures (e.g., Tungsten) which releases electrons. These electrons are further accelerated by a voltage potential through a titanium foil window onto the target. The window is designed to allow the electrons to escape yet accommodate a vacuum in the 10^{-6} Torr range inside the accelerator chamber. The energy of the electrons is equal to the acceleration voltage of the instrument, which can range from 0.15 to 10 MeV, depending on the EB device.

Several operating variables exist in electron beam curing which allow some flexibility in processing. First, the depth of penetration of electrons into the target is a function of the acceleration voltage and the density of the target material. Low voltage electron beams (150 to 180 kV) are limited to penetration depths of 3 to 5 mils (80 to 130 microns)in most polymeric materials. High voltage electrons, with energies to 10 MeV, can penetrate up to 3 centimeters. Another variable is the intensity of electrons, which is controlled by the temperature of the cathode and the current of the electrons. Finally, the dose and dose rate of EB radiation absorbed by a sample are functions of the current of the electrons and the line speed of the conveyor. A simple relationship for dosage is given by

$$D = \frac{KI}{S} \qquad (1.1)$$

D = Dose (Megarads)

I = Electron beam current (mA)

S = Line speed (feet per minute)

K = Machine constant (Megarad-feet/mA-min), determined by dosimetry

A rad is a unit of energy equal to $2.39(10^{-6})$ cal/gram (actually defined as 100 ergs per gram), and a megarad is simply 10^6 rads.

The electrons from the EB source cause chemical reactions by transferring their energy to the target material. This energy transfer happens in small steps, and the electrons can change directions many times in this process. The electrons can be deflected as they pass near another electron or a nucleus, giving up their energy. The energy transfer has been shown in terms of a depth-dose distribution curve, which is reproduced in Figure 2 on page 7. These curves are from a theoretical model produced by Nablo [3] and Becker et. al. [4]. Each curve represents a different electron beam voltage. The relative energy loss is plotted vs. penetration depth into the sample. The energy loss reaches a maximum well underneath the surface. As the electrons are deflected and slowed down, the probability of an inelastic collision increases [4]. So, the probability of a collision reaches a maximum as almost all of the electrons have slowed down enough that they transfer their excess energy to the material. Consequently, the energy loss drops off rapidly beyond this maximum. The energy transfer in electron beam curing is also proportional to the density of the target material. The depth-dose curve is often plotted vs. a thickness density product, expressed in mg/cm^2 or g/cm^2 [1].

Electron beam applications reflect the thickness limitations described earlier. Low energy electrons in the range of 150 to 300 keV are efficiently used to crosslink industrial coatings on wood or polymer substrates [2,6], thin films [7], and foamed plastic [8]. Higher energy

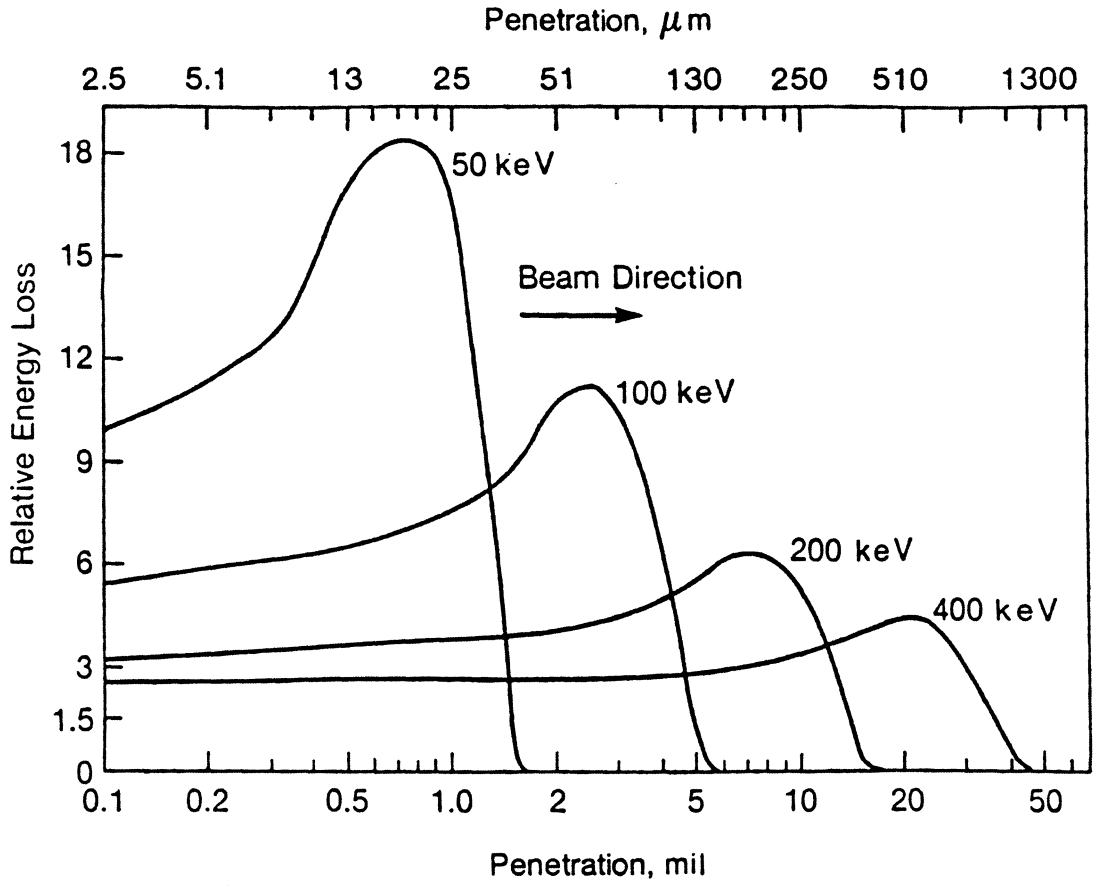

Figure 2. Depth-Dose Distribution Curve from a Theoretical Model by Nablo and Becker: The curves represent the absorbed dosage at different depths in the target material. This curve was calculated using values for polystyrene [3,4].

electrons are utilized in irradiating plastic sheets, tubing, wire and cable insulation [9], and even elastomeric structures to reinforce or replace automobile bumpers [10]. Electron beam crosslinking of polyethylene insulation for wire and cables has grown rapidly due to cost incentives and the improved physical properties of the material. Crosslinked polyethylene and ethylene-propylene-diene systems tend to char rather than flow at high temperatures, a desirable quality in electrical insulation, since voltage surges can cause relatively large temperature rises.

1.1.4 Gamma Rays

Gamma rays are produced from radioactive isotopes such as Co^{60}. They are far more penetrating than UV light or EB radiation. Their energy is transferred to an absorbing target primarily through Compton scattering. In this manner, the dose increases with increasing depth in the absorbing medium. This increase is exponential up to a limiting depth, with a mean free path near 30 cm in unit density material. As expected, γ-rays are used effectively where high depths of irradiation are needed. Examples are sterilization of cases of biomedical supplies, curing thick wood or plastic composites, polymerization or grafting of polymer materials, and in limited applications, sterilization of food [1].

Cobalt-60 gamma rays have two considerable disadvantages in industrial applications. First, the cobalt-60 isotope gives off radiation continuously, such that it can not be conveniently turned off with a switch as EB or UV sources. Secondly, the deeply penetrating Co^{60} gamma rays require thicker shielding than EB or UV radiation.

1.2 *Advantages of Irradiation*

Some of the advantages of each radiation source have been discussed throughout the previous sections. Many variables influence the cost and practicality of radiation curing and are important in choosing the radiation source to be used in desired applications. Some of the variables encountered in radiation-cured coating processes include the chemical formulation (epoxy, acrylates, vinyls, or polyethylene), desired physical properties, coating thickness, line speed, dosage requirement, initiator (if necessary), and substrate geometry.

Curing by infrared light will be used only in limited applications, since it offers few advantages over thermal heating. One such advantage is rapid heating which can be localized to certain areas in a coating. It could also be used to cure coatings on odd geometries, where only thermal conduction is required. Ultraviolet light sources may be used in many coating and printing processes. An initiator is required in the coating formulation. UV curing is best utilized where only a few lamps are required and line speeds are relatively slow. Significant cost savings can be realized if air can be substituted for nitrogen as the blanketing atmosphere. A 1978 study showed hourly utility costs were reduced from $12.30 to $4.80 by eliminating the nitrogen purge [1]. The above investigation assumed a 122 cm line with 10 UV lamps operating at 50 cm/sec.

Electron beam curing is characterized by a high capital cost, ranging from two-hundred thousand to one million dollars for a production line process. The advantages of EB curing are a potential for higher line speeds and thus, more production volume, high dosages, and no initiator requirement. Low energy electron beams are limited to thin films or coatings. In spite of the high equipment costs, electron beam curing has many applications in industry.

Gamma rays have the advantage of thick sample irradiation, and are used where thicknesses are above the EB limits, such as sterilization of medical materials or in wood impregnation. Gamma rays also require high equipment costs and more shielding than electron beams.

1.3 Crosslinking vs. Scission in Irradiated Polymers

Even with the different sources for irradiation, the most economically successful applications can be grouped into just two categories. One is sterilization of biomedical supplies, limited to gamma-ray or high energy EB as mentioned earlier. The other is modification of polymers via crosslinking or chain scission reactions. These reactions are most useful when small selective chemical changes occur in large molecules which lead to substantial physical changes. The mechanisms of crosslinking and chain-scission are paramount to radiation chemistry. Although much remains unresolved, it is appropriate to discuss some of the proposals from the literature as well as some of the early research which led to them.

Polymers tend to preferentially undergo crosslinking or degradation reactions when irradiated. Polymers which crosslink include polyethylene, polystyrene, isoprene, polyamides, and polydimethyl siloxane. Polymers which degrade include poly(isobutylene), poly(methyl methacrylate), and polytetrafluoroethylene (Teflon). More complete lists of crosslinking and degrading polymers are given in Table I. In many cases, a polymer may undergo both crosslinking and chain scission, so a table of this form is admittedly an oversimplification.This discussion assumes that no additives or stabilizer are present. The function of these will be discussed later.

The degree of crosslinking or scission a polymer will experience is often expressed in terms of G-values. The G-value for crosslinking, usually denoted G_x or G(x), is the number of

Table 1. Behavior of Solid Polymers under Irradiation

Behavior of Solid Polymers under Radiation [15]	
Polymers which crosslink	*Polymers which degrade*
Polyethylene	Polyisobutylene
Polystyrene	Polytetrafluoroethylene
Polyvinyl chloride	Polymonochlorotrifluorethylene
Polyvinyl alkyl ether	Poly-α-methyl styrene
Polyvinyl methyl ketone	
Chlorinated polyethylene	
Polyvinyl acetate	
Polyacrylonitrile	Polymethacrylonitrile
Polyacrylic acid and esters (polymethyl acrylate)	Polymethylacrylic acid and esters (polymethyl methacrylate)
Polyacrylamide	Polymethacrylamide
Rubber (Natural)	
Polybutadiene	
Neoprene (polychloroprene)	
Polyamides	
Copolymers	Cellulose
styrene-butadiene	cellulose derivatives
butadiene-acrylonitrile	Butyl rubber (copolymer)
styrene-acrylonitrile	
Polyphenyl siloxane	
Polydimethyl siloxane	

crosslinks formed per 100 eV of energy (2300 kcal/mol of repeat unit) absorbed. The G-value for polystyrene is only 0.05. However, G(x) for monomers such as methyl methacrylate which can undergo a chain reaction after irradiation may be as high as several thousand. An analogous G-value for chain scission is usually given the symbol G_s or G(s). Representative values for G(s) are 1.2 for poly(methyl methacrylate) and 10 for cellulose. Atactic polypropylene is a material which undergoes both chain scission and crosslinking, having G-values of 0.12 for crosslinking and 0.15 for chain scission.

1.3.1 Factors Which Influence Crosslinking and Scission

Irradiation-induced crosslinking of linear polymers, according to Charlesby, is a "seductively simple reaction" [11]. In fact, it is the heart of many industrial applications, yet surprisingly little is certain about its underlying mechanisms. The chain scission mechanisms are even more complex because polymer chains can be broken in many ways.

Some qualitative observations have been made for scission and crosslinking that have been quite helpful over the years. First, the degree of reaction (crosslinking or scission) is directly proportional to dosage up to some limit. Second, the effect of dose rate on polymer materials is generally small. Next, crosslinking does not always require unsaturated groups, because polymers such as polyethylene will crosslink with irradiation. However, as will be discussed later, there is a growing interest in prepolymers which contain unsaturated carbon bonds. Additionally, it is observed that crosslinking and degradation are not strong functions of the molecular weight of the material. Finally, the presence of certain inhibitors, such as oxygen or thioureas can severely limit the extent of reaction. It is well-advised to understand that these observations are oversimplified, and other factors can supercede these relationships. One such example which will play an important role in this author's research occurs when a

crosslinking network reaches diffusion limitations due to vitrification before all radicals can promote reaction.

The question of whether a polymer will crosslink or degrade is not a simple one. As early as 1954, Miller et. al. [12] suggested that vinyl polymers with one side group attached to a single carbon ($-CH_2-CHR_1-$ or $-CH_2-CH_2-$) tend to crosslink while polymers with two side groups ($-CH_2-CR_1R_2-$) tend to degrade. Here, hydrogen is not considered a side chain whereas Cl and F are. While the simplicity of this model is attractive, there are several exceptions. The most obvious of these is polypropylene. Although Miller's model predicts it will crosslink, the G-value for scission is slightly higher than that of crosslinking as mentioned previously. As such, the scission reaction overtakes the crosslinking reaction and the material degrades. Another example is cellulose which degrades upon irradiation, although none of the main chain carbons contain more than one side group. The reverse is true for siloxanes, analogous to polyisobutylene with two side methyl groups, as they crosslink with irradiation.

As mentioned above, a number of radiation curable prepolymers are now available for use in coatings, inks, etc. Many of these systems are terminated on each end with acrylate or other allyl species so they can crosslink via free-radical mechanisms. The "main chain" of a prepolymer can be varied to provide different physical properties. Often, polyethylene glycol (PEG) or poly(tetramethylene oxide) (PTMO) is used as the repeat unit. If only a few repeat units are present, the viscosity of the liquid is low such that it acts as a thinner or solvent. Higher molecular weight prepolymers with PEG or PTMO act as rubbery components. Main chain units with urethanes or aromatics such as derivatives of bisphenol-A can provide harder materials when cured by radiation.

The vinyl groups which crosslink in these prepolymers have a functionality of two. Since the chains have two vinyl groups, a three- dimensional network can result if both vinyls crosslink. A simplified sketch of the crosslinking scheme was given by Tripp and Nablo [13] and is presented here in Fig. 3. As shown in Fig. 3, irradiation of the prepolymer forms a network. As

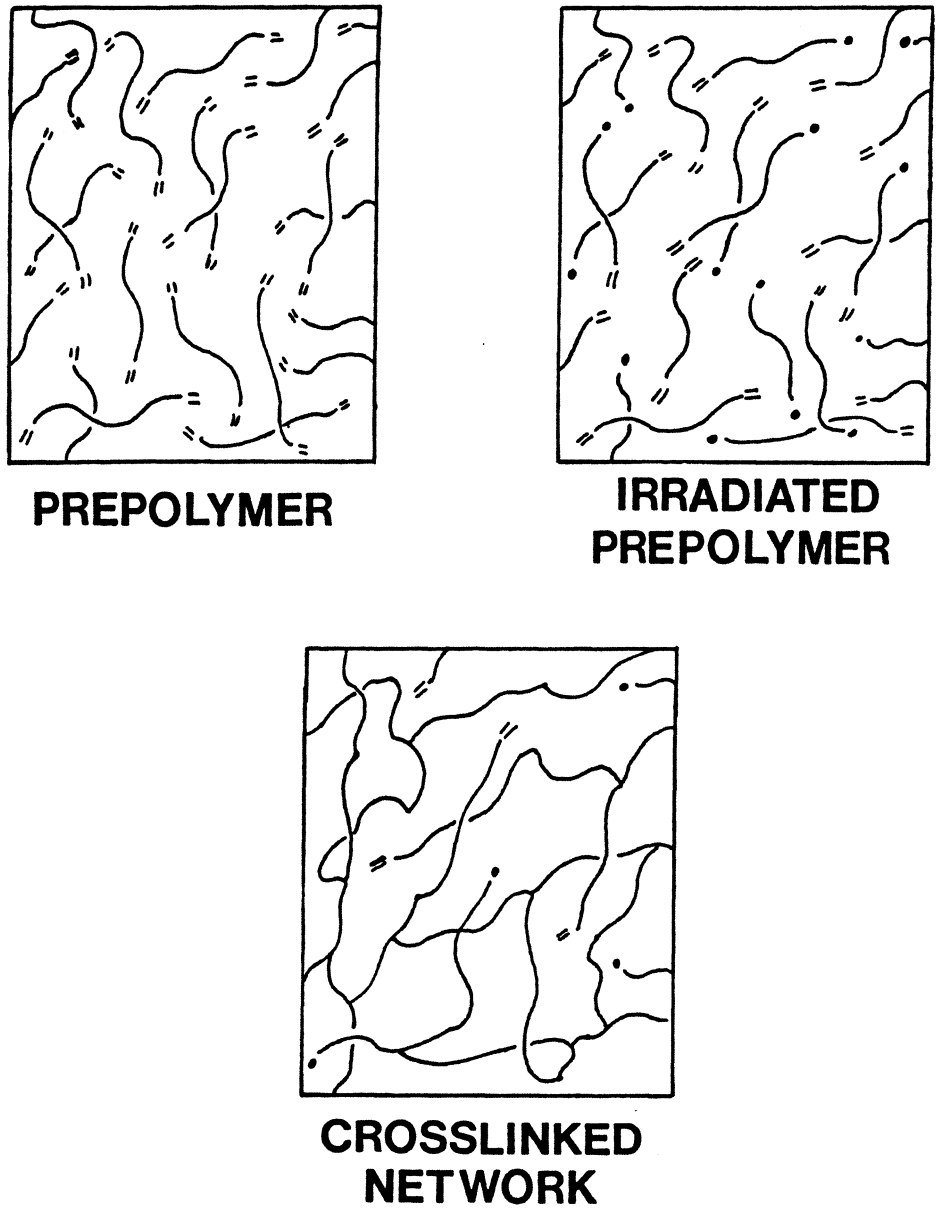

Figure 3. Prepolymer System Before and after Irradiation: This figure shows that the double bonds on the end of the oligomer chains are opened to form radical species during irradiation. The radicals can recombine with other radicals or double bonds to form crosslinks (from Tripp and Nablo, Ref. 13).

no process is perfect, there are residual double-bonds present in this network. The number of residual double-bonds is a function of dose, chemical reactivity of the system, and other variables mentioned previously. As with Miller's model for crosslinking vs. scission, this model is too simple to adequately describe electron beam curing of polymer systems. Thus, some depth into the mechanisms of crosslinking is in order.

1.3.2 Mechanisms of Crosslinking

The mechanisms of crosslinking of polymers can be separated into two categories. The first involves the mechanism for curing systems containing unsaturation, such as the prepolymers mentioned earlier. Many of these systems which are vinyl-terminated crosslink to form "model networks." Model networks have been extensively studied by Mark et. al. [14], and are characterized by the molecular weight of each chain being equal to that of the prepolymer. The second involves crosslinking of a polymer chain such as polyethylene or other crosslinkable material. Here, the crosslinking occurs randomly along the polymer chain, so models include the probabilities of reactions at each bond. This process has been modeled in detail by Charlesby [15]. Both the prepolymer crosslinking mechanisms and the longer chain polymer mechanisms will be discussed since the former is the subject of this author's research and the latter has been studied in more detail over the years.

1.3.3 Free Radical Crosslinking of Prepolymers

The mechanism of crosslinking in vinyl-terminated prepolymers parallels free radical polymerization of vinyl monomers such as styrene. Styrene can be polymerized with an ini-

tiator being thermally activated. The initiator links to a pi electron of the vinyl group as follows [16]

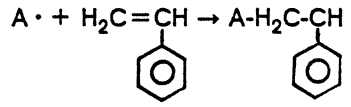

(1.2)

The initiated styrene can then add to other chains in a similar manner to propagate the reaction

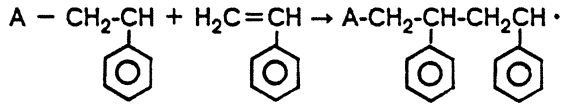

(1.3)

The reaction continues to form polymer chains until the double bonds are depleted or become unable to find other reactive bonds. Combination reactions can lead to termination of the network formation. Radicals which remain can become trapped in the polymer matrix. This can be explained in terms of a Time-Temperature-Transformation diagram which will be discussed later in this chapter.

Vinyl-terminated prepolymers react to radiation in much the same way. The electrons from the EB unit act as an initiator by transferring their energy to the chains. This energy is sufficient to break bonds to form free radicals. The simplest reaction of this type is the abstraction of a hydrogen atom as illustrated:

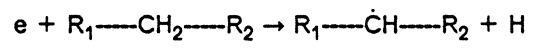

(1.4)

This event could occur almost anywhere along the prepolymer chain. However, it must be remembered that some bonds are more easily broken than others. Bond strengths generally range from 130 to 800 kJ/mol (1.5 to 8.3 eV). Some common bond energies as reported by Charlesby [15] and Mita [17] are presented in Table 2. Once the radicals are generated, they can initiate the chain reaction by adding across the double bonds. The reaction proceeds as

is shown in Fig. 4. The reaction continues until it is terminated by combination or disproportionation, or until the reactive species become diffusion limited.

1.3.4 Crosslinking of Longer Chain Polymers

1.3.4.1 Physical Model for Random Crosslinking of Polymers

Crosslinking of longer chain polymers by radiation has been nicely modeled by utilizing to some of the developments concerning polymer networks. A few assumptions that have generally been made are as follows:

1. Polymers consist of mono-functional (-A), di-functional (-A-), and higher-functional units (-A(-)- or -A(-)(-)-).

2. Crosslinks refer to tetrafunctional junction points which link two molecules together side-by-side (Fig. 5), or a tri-functional junction point where an end group is linked arbitrarily along the other chain, sometimes called a Y-junction (Fig. 6). Charlesby used the term "endlinking", but this term is more often used now to describe the linking of one chain end to another as in model networks.

3. Crosslinking occurs randomly along the polymer chains. In this way, longer chain molecules are more likely to crosslink within the chain to form tetrafunctional junctions than crosslinking at one end to form trifunctional links. The tetrafunctional linking points are often referred to as H-junctions. As mentioned before, individual bonds may be favored in these reactions due to lower bond energies.

Rather than reproducing the derivations of Charlesby [15], a few highlights resulting from this work will be discussed.

First, a few terms need definition. The crosslinking density is defined as the fraction of main-chain units crosslinked and is given the symbol q. Radiation dose is usually expressed

Table 2. Energies of Common Covalent Bonds [15,17]

BOND	MOLECULE	BOND ENERGY	
		kJ/Mol	*eV*
H-H	H_2	436	4.52
C-H	Paraffins	413	4.28
	Olefins	416	4.31
	Acetylene,HCN	403	4.18
	Benzene	421	4.37
$PhCH_2-H$	Toluene	356	3.69
C=C	Benzene	487	5.05
C=C	Olefins	588	6.09
C=C	Acetylenes	823	8.53
C-O	Alcohols,ethers	333	3.45
C=O	RCHO, R_1R_2CO	706	7.32
C-N	Amines, nitroparrafins	276	2.86
O-H	Alcohols	438	4.54
	Water	458	4.75

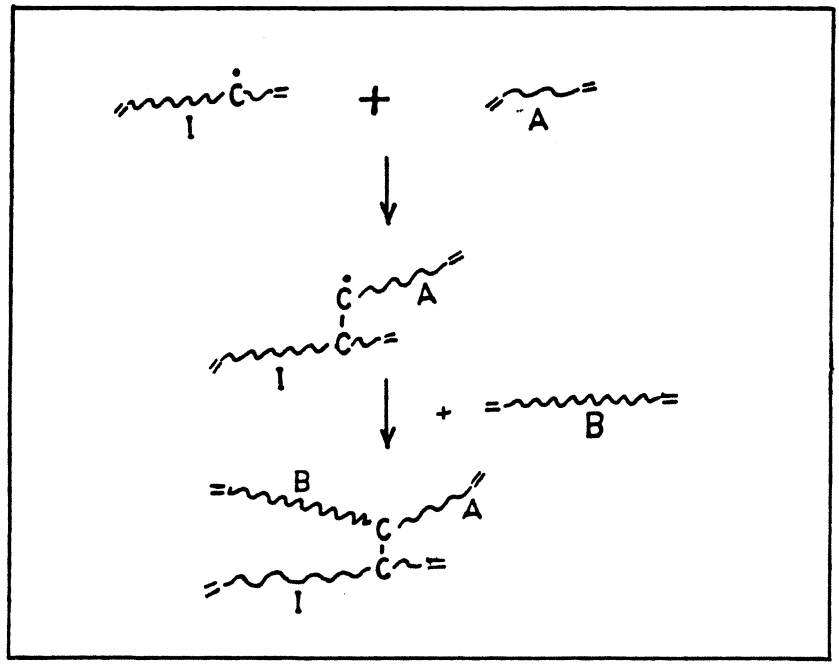

Figure 4. Propagation of Crosslinking Reaction via Radiation in a Prepolymer.: The mechanism shown above indicates that free radicals are formed as a result of irradiation. The radicals can combine with other radicals or double bonds to crosslink the chains.

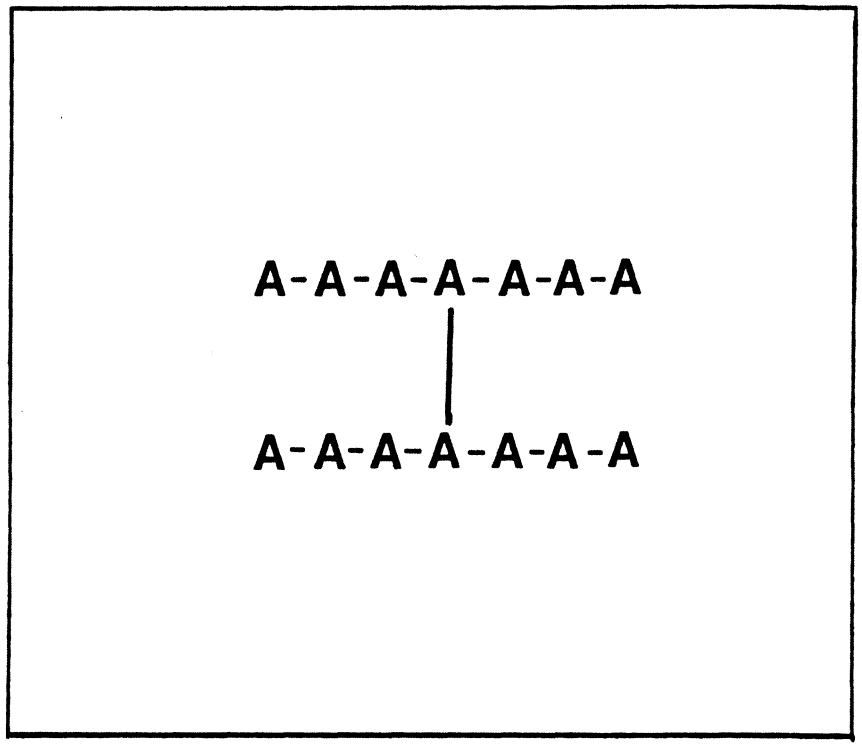

Figure 5. Tetrafunctional Junction Point in a Crosslinking Polymer, also Called an H-junction.: (from Charlesby, Ref. 15).

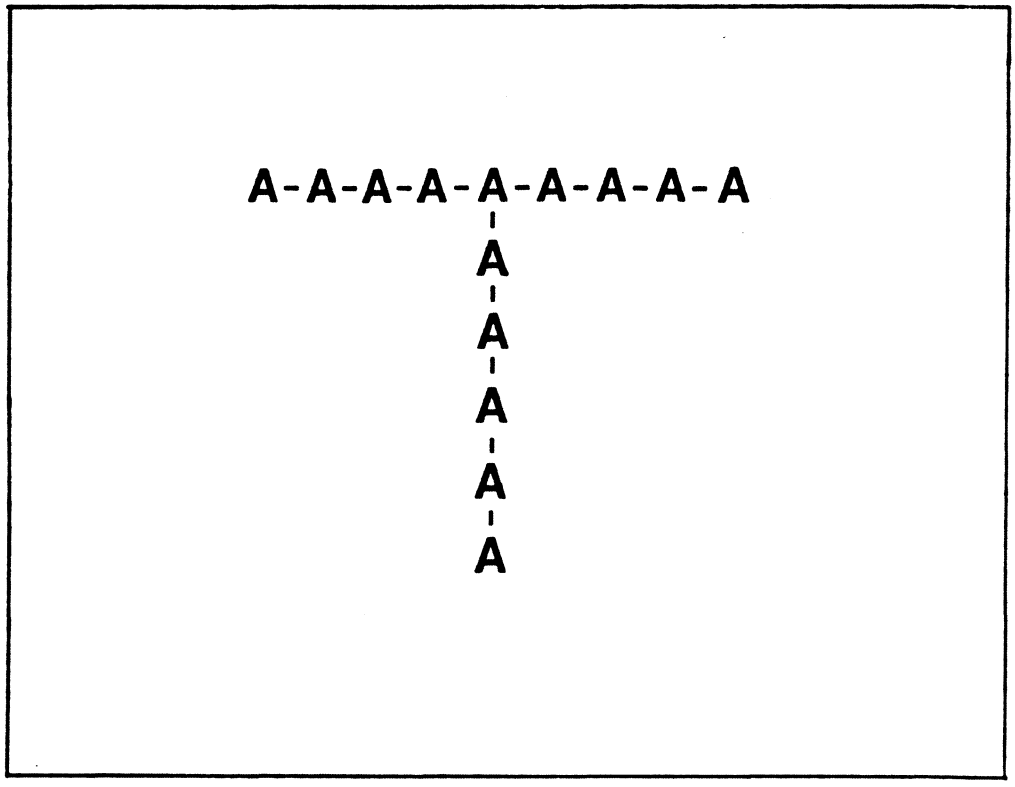

Figure 6. Trifunctional Junction Point at A', often Given the Term Y-junction.: (from Charlesby, ref. 15).

in megarad units and has the symbol r. For a polymer specimen containing A_1 chain units, the number of crosslinked units will be qA_1. The number average molecular weight between crosslinks, denoted by M_c is given by

$$M_c = w / q \qquad (1.5),$$

where w is the molecular weight of each of the A_1 units.

The M_c term is related to the irradiation dose and G value (G(x) = number of crosslinks per 100 eV absorbed) as follows:

$$M_c = w / q = 0.48 \times 10^6 / G(x)\, r \qquad (1.6)$$

where r is radiation dose expressed in megarads.

For these random polymer systems, the disturbing effects of the end groups has been ignored. Although this assumption is fine for determining M_c, the end effects are important for quantifying gel formation or solubility changes. For these effects, it is the average number of crosslinks per molecule which must be considered. Since the lengths of these molecules are not equivalent but are characterized by some distribution, this average number of crosslinks can be related to the number average, weight average, or higher order average molecular weight. Two terms have been defined to help characterize this gelation upon crosslinking, as follows:

1. *Crosslinking index* (γ) is the number of crosslinked units per *number* average molecule.

$$\gamma = \frac{q\,M_n}{w} = \frac{M_n}{M_c} = \frac{\sum_{\infty} n(M)\,M}{\sum_{\infty} n(M)} \tag{1.7}$$

2. *Crosslinking coefficient* (δ) is the number of cross-linked units per *weight* average molecule.

$$\delta = \frac{q\,M_w}{w} = \frac{M_w}{M_c} = \frac{\sum_{\infty} n(M)\,M^2}{\sum_{\infty} n(M)\,M} \tag{1.8}$$

By dividing the two equations, it is easy to see that (15)

$$\frac{\delta}{\gamma} = \frac{\frac{M_w}{M_c}}{\frac{M_n}{M_c}} = \frac{M_w}{M_n} \tag{1.9}$$

The gel point in a crosslinking system, as shown by Charlesby [15] is simply determined by the condition $\delta = 1$; that is, there is an average of one crosslink per molecule. As δ increases above one, molecules appear with theoretically more than an infinite degree of polymerization. These are in fact closed networks of three-dimensional character. The soluble fraction is one for any value of δ below one, then decreases as δ increases above one.

More development was done to characterize the sol fraction; that is, the extractable portion in an irradiated polymer which is swollen in a good solvent. The results can be described in terms of the famous Charlesby-Pinner equation, written in terms of the sol fraction (s) as

$$s + s^{1/2} = \frac{G(s)}{2G(x)} + \frac{50N_a}{D\overline{M}_{n0}G(x)} \tag{1.10}$$

Here, D is radiation dose in eV/gram and $\overline{M}_{n0}$ is the number average molecular weight of the monomer (before irradiation) and N_a is Avogadro's number. Underlying assumptions are

1. The molecular weight distribution is initially random.
2. Scission and crosslinking can occur randomly across the chain (weighted by the respective G values).
3. G values, G(s) and G(x), are constant with dose.

Upon inspection of equation 1.5 it is evident that a plot of $(s + s^{1/2})$ vs. 1/D should give a linear result with an intercept G(s)/G(x) and a slope proportional to 1/2G(x). An example of the Charlesby-Pinner plot is given in Fig. 7.

Plots of this type from experimental data are seldom linear. Polypropylene irradiated in high vacuum is one of very few exceptions. Another point in regard to this author's research is that end-capped prepolymers do not conform to the underlying assumptions of the Charlesby-Pinner theory, in that their crosslinking occurs primarily at the chain ends and not randomly throughout the chain. Thus, the Charlesby-Pinner equation is not applicable to the prepolymer systems discussed in this thesis.

1.3.4.2 Chemical Mechanisms

Quite a number of chemical mechanisms have been proposed to characterize radiation crosslinking of polymers. Although many try to model polyethylene for simplicity, some attempt to explain certain features of the chemical structure and its effect on radiation behavior. A few of the models will be discussed.

Sun [18] listed a series of reactions which are possible for irradiated long chain paraffin molecules. These serve as a model for polyethylene. They are:

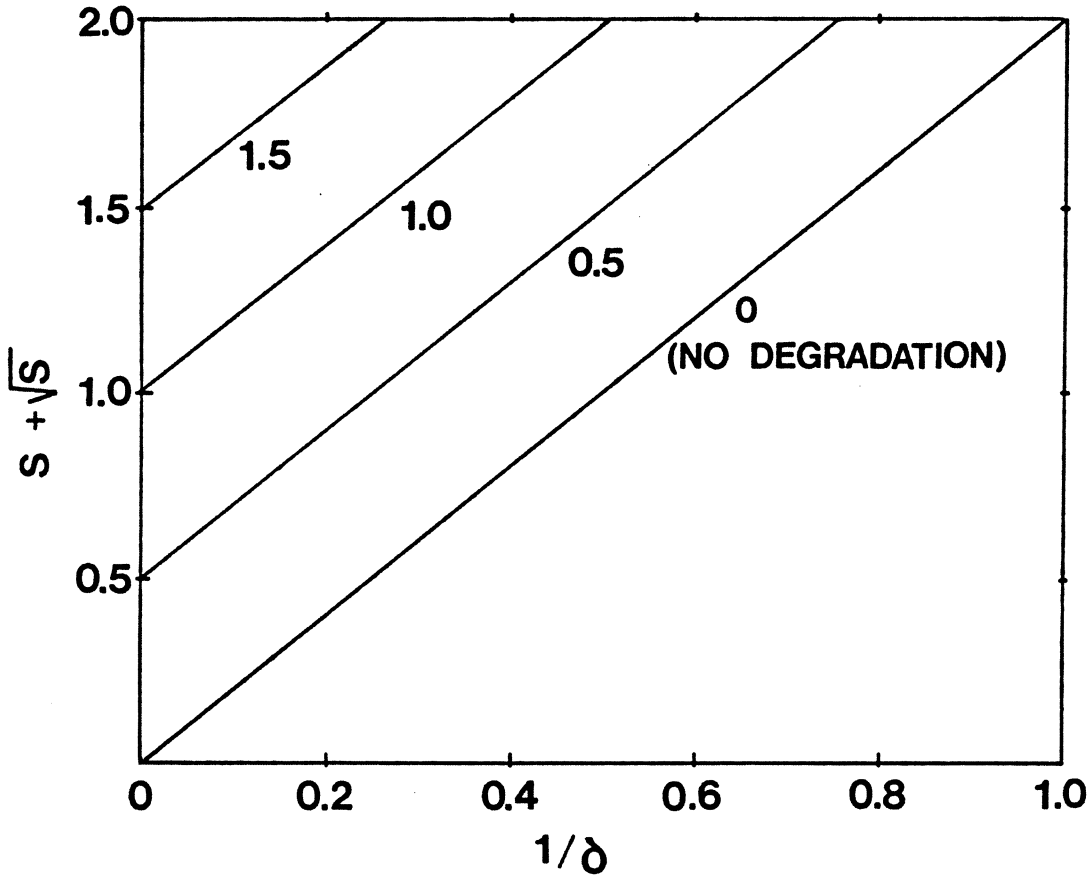

Figure 7. Charlesby-Pinner Plot Relating Sol Fraction to Irradiation Dose.: This plot is designed to portray simultaneous crosslinking and degradation. The sol fraction is determined (actually $s + s^{1/2}$) in terms of inverse dose [15].

1. Ionization and excitation.

2. Decomposition of excited molecules to give radicals and possibly ions.

3. Recapture of an electron by an ion, giving an excited molecule.

4. Molecular rearrangement within a molecule.

5. Migration of a radical along a molecular chain, and transfer between chains.

6. Combination of two radicals to give a crosslink or extended molecular weight by

$$R_1\bullet + R_2\bullet \rightarrow R_1R_2$$

7. Abstraction of a hydrogen to form a radical and eventually unsaturation,

$$R_1\overset{\bullet}{C}H\text{-}CH_2R_2 + H \rightarrow R_1CH{=}CHR_2 + H_2$$

8. Elimination of a double bond to form a radical

$$R_1CH{=}CHR_2 + H \rightarrow R_1CH_2\text{-}\overset{\bullet}{C}HR_2$$

9. Removal of hydrogen to leave unsaturation

$$R_1CH_2\text{-}CH_2R_2 \rightarrow R_1CH{=}CHR_2 + H_2$$

Reactions 1 and 2 have been established experimentally, while radical mobility, assumed for reactions 5 and 6, has little evidence to support it. Reactions 7, 8, and 9 are included in other models.

Reaction with a Neutral Molecule: Charlesby's first proposal stated that a hydrogen atom is liberated by radiation to form a radical molecule. This radical can react with a neighboring neutral molecule to eject a proton (hydrogen) and form a crosslink.

1) $R_1H \dashrightarrow R_1\bullet + H+$

2) $R_1\bullet + R_2H \dashrightarrow R_1R_2 + H+$

3) $H+ + H+ \dashrightarrow H_2$

Questions have been raised about step 2) because a radical such as $R_1\bullet$ is generally unable to eject a hydrogen from a stable molecule. It is possible that the radical formed from radiation is more unstable than thermally formed radicals, and could eject the hydrogen from a nearby molecule. Another possibility submitted later by Charlesby [15] is that ions are formed via irradiation, such that:

1) $R_1H \dashrightarrow R_1H+ + e$

2) $R_1H+ + R_2H \dashrightarrow R_1R_2 + H_2+$

3) $H_2+ + e \dashrightarrow H_2$

Mobility of Reactive Sites:

Dole and Keeling [19] proposed a mechanism to explain the preferential treatment given to the disappearance of vinylidene groups ($R_1R_2=CH_2$) in irradiated polyethylene. The vinylidene groups exist as the product of a secondary reaction, as only 0.043 groups exist per 100 carbon atoms. The number of vinylidene groups existing is a function of the type of catalyst used in the polymerization reaction as well as other conditions. However, these groups disappeared very rapidly when the polyethylene was irradiated. One third of the hydrogen atoms evolved were from the vinylidene groups. To explain this phenomenon, Dole and Keeling suggested a mobility of free free radicals as shown in Fig. 8. They also suggested that free radicals could be transferred to a nearby chain if the free energies were favorable.

Depolymerization Characteristics: A correlation was attempted to match radiation behavior and thermal behavior by Wall [20]. Particular attention was given to the thermal

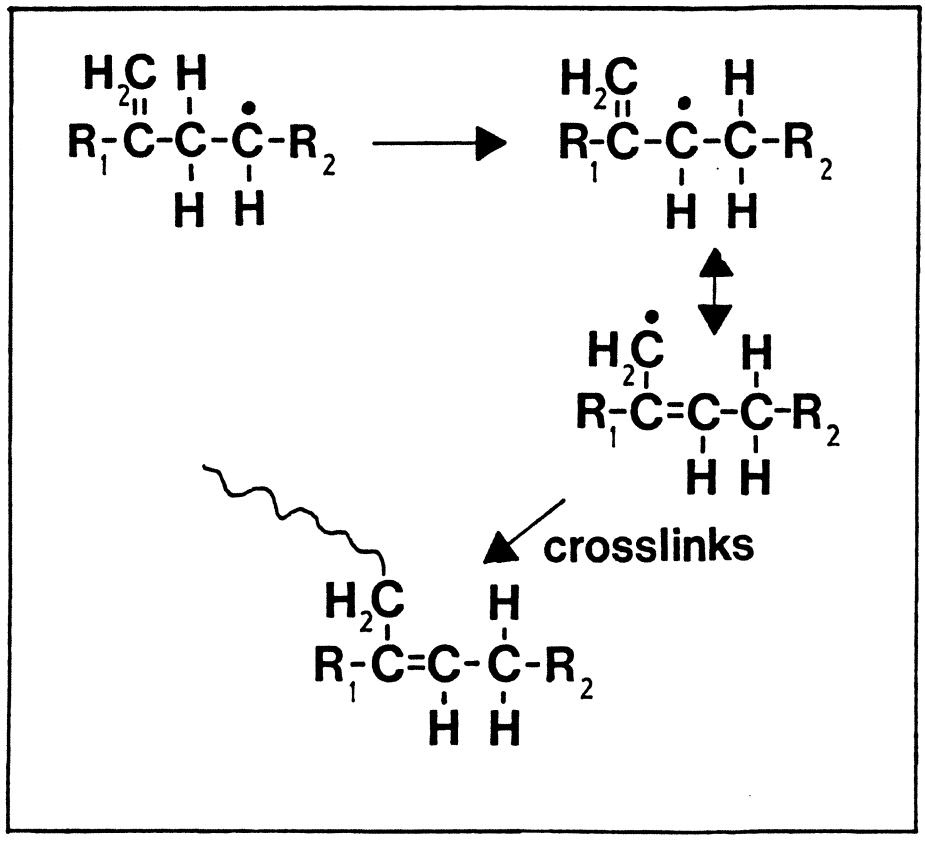

Figure 8. Schematic of Dole and Keeling's Model of Mobility of Active Sites: This model shows that mobility in the free radicals of irradiated species can lead to other crosslinks [19].

depolymerization of the polymer, the heat of polymerization, and monomer yield on pyrolysis. An α-methyl group favors depropagation during pyrolysis, while an α-hydrogen favors transfer reactions. The analogy suggests the α-methyl groups degrade under irradiation whereas the α-hydrogen groups crosslink (similar to Miller, sec. 1.2.3). Two exceptions are polyisobutylene, which gives very little monomer yield on pyrolysis, and polytetrafluoroethylene (PTFE or Teflon), which is thermally stable but degrades with irradiation.

Crosslinking via Unsaturation: Pearson [21] proposed that crosslinking in polyethylene takes place at points of unsaturation. The unsaturated groups can either be present in the original polymer or can be formed from irradiation. The reaction proceeds as shown in Fig. 9. This mechanism is not sufficient to explain the small difference in G values for crosslinking in saturated and unsaturated hydrocarbons, nor does it explain crosslinking in siloxanes which have no unsaturation.

Ionic Mechanism: Collyns and Weiss [22] proposed an ionic mechanism analogous to the free-radical mechanism assumed by Charlesby (see sec. 1.2.4.1). Crosslinking takes place when the carbonium ion comes close to a neutral carbon, as shown in Fig. 10. The ionic approach is similar to the free radical mechanism in accounting for unsaturation, as

$$-CH_2-\overset{\bullet}{C}H-CH_2- \longrightarrow -CH_2-\overset{\bullet}{C}=CH- + H_2$$

This model is different from Charlesby's [15] in that it states the crosslinking reaction only occurs when the active carbon atoms are close to each other. Since increasing the temperature gives more mobility to the chains, it increases the probability that the carbon groups get close together. This assumes that the mobility from temperature overcomes the competing distances due to the increase in free volume (decrease in density). This model predicts more crosslinking will occur at higher temperatures, which is observed in polyethylene.

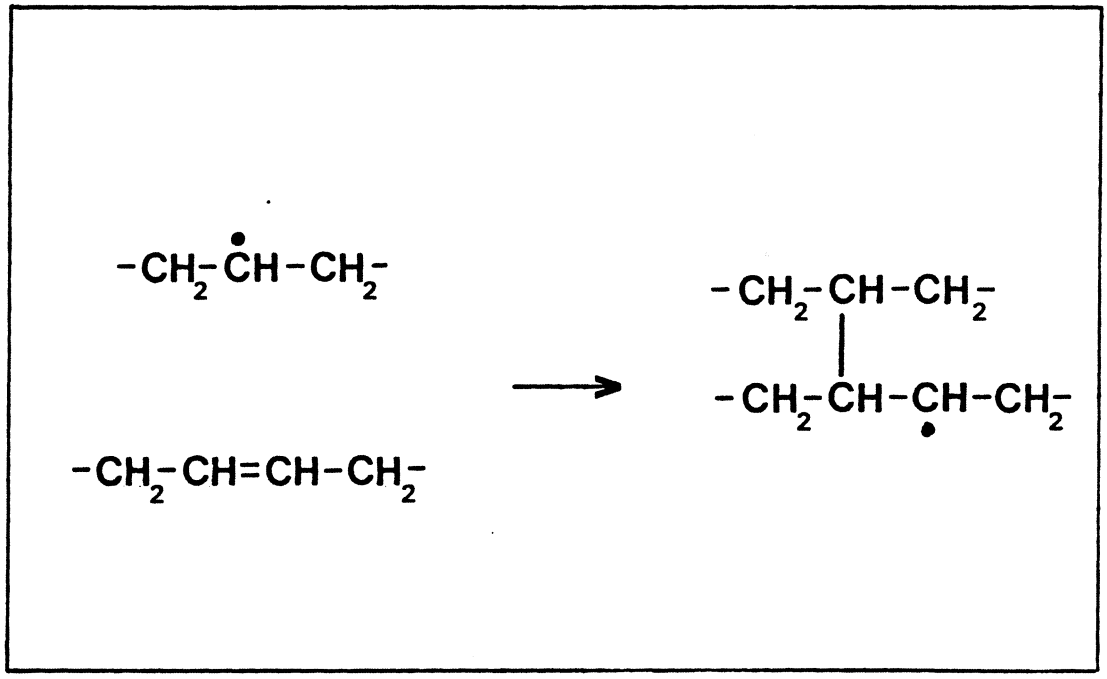

Figure 9. Crosslinking at Points of Unsaturation: (from Pearson, Ref. 21).

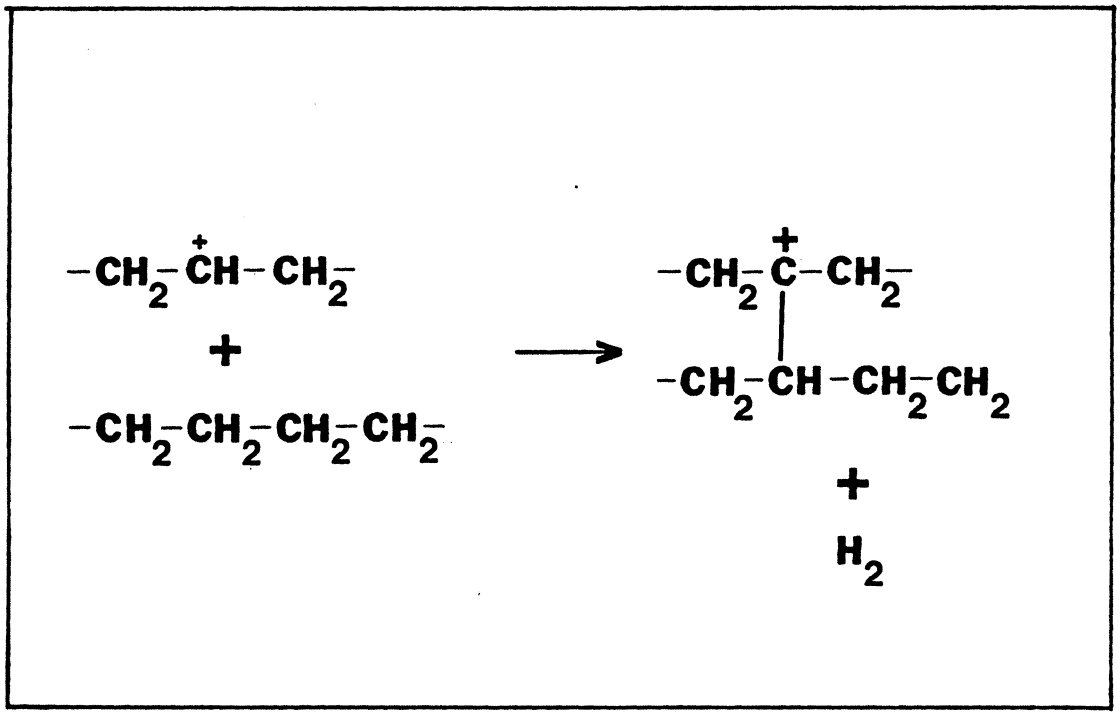

Figure 10. Crosslinking by Ionic Mechanism of Collyns and Weiss: The activated group in this mechanism is a carbonium ion. It can combine with another carbon atom to give hydrogen [22].

From the discussions of the models above, it is obvious that none of these models is adequate to describe the entirety of radiation crosslinking and degradation in polymers. The models do have significance in that many apply well to the situations of their intent (such as Wall's relating radiation behavior to thermal behavior). The number of mechanisms proposed reflects the amount of uncertainty that remains in this area.

1.4 Time-Temperature Effects in Glassy Polymers

The idea of diffusion limitations influencing the extent of curing in glassy polymers has appeared without previous explanation in this discussion. The extent of cure in glassy polymer networks is affected by the time and temperature of cure. This influence is present in networks cured by either thermal or radiation initiation. The difference in physical properties which are dependent of the degree of cure are qualitatively explained in terms of a Time-Temperature-Transformation (TTT) diagram [23,24]. The purpose of this section is to supply some explanation of the TTT diagram as well as discuss its implications to the final glassy properties of a network below its T_g. As an example, an application of these ideas to an epoxy network (the research of Kong et. al. [25]) will be reviewed shortly.

1.4.1 Time-Temperature-Transformation Diagram

Glassy polymers can have quite different morphologies or network topologies based on the time and temperature of their cure. Gillham and coworkers [26-28] have explained this idea by developing a Time-Temperature-Transformation diagram in terms of reactive networks. It

is reproduced in Fig. 11. As low molecular weight components or prepolymers crosslink to eventually form networks, their molecular weight as well as their glass transition temperature (T_g) increase. When the glass transition temperature reaches the curing temperature, diffusion is limited and the crosslinking reaction becomes severely slow. At this point the material undergoes vitrification and can be described as a glass.

Figure 11 shows six different physical states resulting from such systems which may form networks. They are the ungelled glass, liquid, gel, gelled glass, rubber, and charred polymer regions. A gel is simply a network of infinite molecular weight which may still contain some sol components. Reactive polymer systems possess these properties based on the time and temperature of cure. An isothermal cure beginning at temperature A (Fig. 11) can be traced by drawing a line parallel to the log time axis at A. The network begins as a liquid and crosslinks until the "ungelled glass" region is reached. At this point the rate of crosslinking is hindered by diffusion limitations and a gel is not achieved.

Another curing pathway occurs for temperatures between $_{gel}T_g$ and $T_{g\infty}$. For example, in isothermal curing at temperature B (see Fig. 11), the liquid crosslinks sufficiently to form a gel before the glassy region is reached. In this case, the glassy region reached at vitrification is the "gelled glass" region. At higher temperatures, such as C and D, a greater extent of reaction or gelation can occur before the glassy region is reached. This suggests the sol fraction present in the network at temperature C or D would be less than would be present at temperature B.

At temperatures above $T_{g\infty}$, as shown by point E, the network quickly crosslinks to form a gelled rubber. Since vitrification can not occur above $T_{g\infty}$, further reactivity will not be diffusion limited. However, after long times at sufficiently high temperatures the char region is reached indicating thermal degradation occurs. Some degradation can occur at temperatures below $T_{g\infty}$ as seen by observing the char region below $T_{g\infty}$ at sufficiently long times. The importance of degradation is highly dependent on the nature of the chemistry involved.

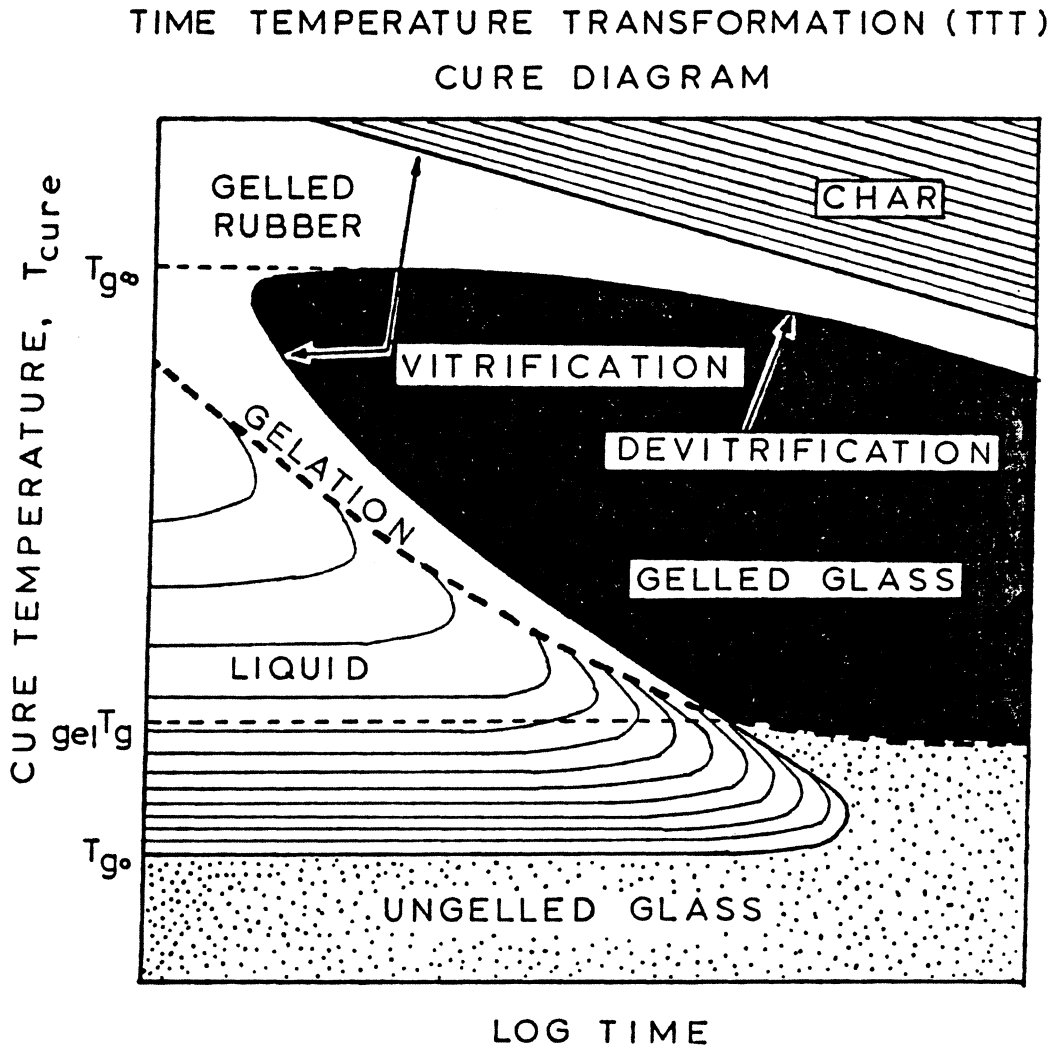

Figure 11. Time-Temperature-Transformation Diagram for Reactive Networks: This diagram details network formation by showing six physical states; the ungelled glass, gelled glass, liquid gel, rubber, and charred polymer regions [26-28].

The effects of time and temperature on a glassy polymer system have also been studied by Kong et. al. [25] and Orler et. al. [29]. The system investigated contained the diglycidyl ether of bisphenol-A, commonly called bis-GMA, and triethylene glycol dimethacrylate (TEGDMA). The chemical structures of these components are shown in Fig. 12. TEGDMA is a thin liquid at room temperature with a viscosity near 1 centipoise (cp). It forms a soft solid at room temperature when crosslinked by thermal initiation at higher temperatures. In contrast, bis-GMA has a viscosity near 10^6 cp at room temperature. It crosslinks by thermal or radiation curing to form a material which is a brittle glass at 25°C. A quartz filler is often added to this mixture for use in dental restorative resins [30]. The filled or unfilled system cures via peroxides to form a brittle solid at room temperature. Heat or photoinitiation (in the visible light region) has been used to speed the cure reaction and is compared to the systems cured at room temperature.

Kong et. al. used stress-strain, stress-relaxation, and differential scanning calorimetry (DSC) to investigate aging characteristics of the following compositions by weight:

1. 87% bis-GMA, 13% TEGDMA
2. 70% bis-GMA, 30% TEGDMA
3. 50% bis-GMA, 50% TEGDMA.

Isothermal curing of each system beginning at ambient revealed the component rich in bis-GMA (i.e., the 87/13 mixture) quickly ran into diffusion limitations, slowing down the reaction and limiting the peak temperature to about 35°C. The term isothermal in this case simply means that the temperature around the sample was kept constant. The actual temperature of the sample did rise during the cure due to the exothermic reaction. The 70/30 and 50/50 mixtures reached peak temperatures of 54 and 50°C respectively as determined by imbedded thermocouples.

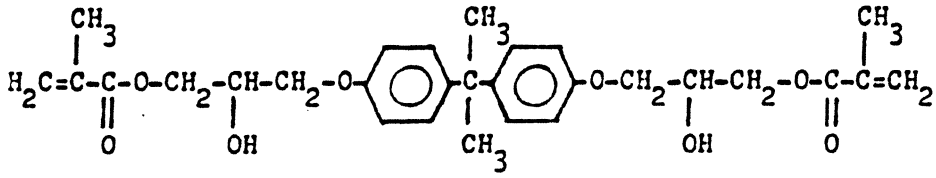

2,2-BIS [4(2-HYDROXY-3-METHACRYLOYLOXY-
PROPYLOXY)-PHENYL]-PROPANE

BIS-GMA

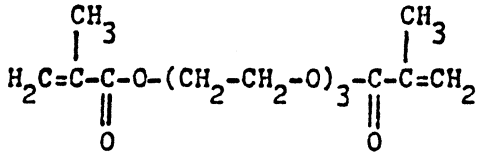

TRIETHYLENE GLYCOL DIMETHACRYLATE (TEGDM)

Figure 12. Chemical Structures for Bis-GMA and TEGDMA: The chemicals represented above were investigated by Kong et.al. and by Orler et.al. These systems were crosslinked by thermal mechanisms using peroxide catalysts [25,29].

DSC temperature scans were done later to quantify transition behavior. The scans were run from -50 to 150°C at 10°C per minute. Sufficient for this discussion are the results of the 50/50 mixture, given in Fig. 13. The first scan shows a T_g for the partially reacted components at 40°C. The mobility of the system increases until, around 80°C, the exothermic reaction of trapped free radicals continues. This exothermic reaction reaches a maximum peak at 120°C. After heating to 150°C in the first scan and cooling to -50°C, the rescan shows none of the exothermic reaction shown by the first scan (Fig. 13). This indicates that further reaction occurs above T_g during the first scan depleting the reactive bonds. Very few unsaturated double bonds were left to react in the second scan.

The stress-strain and stress-relaxation data (all done on an Instron) basically showed that time after thermal cure is a significant factor in the bis-GMA/TEGDMA systems cured at ambient whereas no such effects are seen in material cured thermally at 160°C. The fact that time after cure affects the ambient-cured material supports the DSC findings that its cure is incomplete.

Orler et. al. [29] extended this work to include dynamic mechanical studies to investigate the products of this crosslinking reaction. The dynamic mechanical analyzer used in this study determined the relative modulus values which were termed relative rigidity. Samples were run over a temperature range from -150 to 150°C, and a rescan was run on each in a manner similar to the DSC. Scan rate was 5°C per minute. The resultant plots are given in Figs. 14 and 15 and the information they contain will be compared to the author's results presented later. The upper curves show the relative stiffness or modulus as a function of temperature, while the bottom curves give tan δ vs. temperature. Considering only the initial tan δ plot for the 87/13 mixture, two transitions are shown by the peaks at -110 and -60°C. These peaks generally exist due to local scale molecular mobility of side chains or possibly subgroups on the backbone. In addition, the T_g is indicated by the tan δ peak near 40°C. Similar plots for the rescan samples also show the low-temperature transitions, as well as the T_g value of 100°C. This is a 60°C increase in T_g over that obtained in the first scan. Again, the rescan

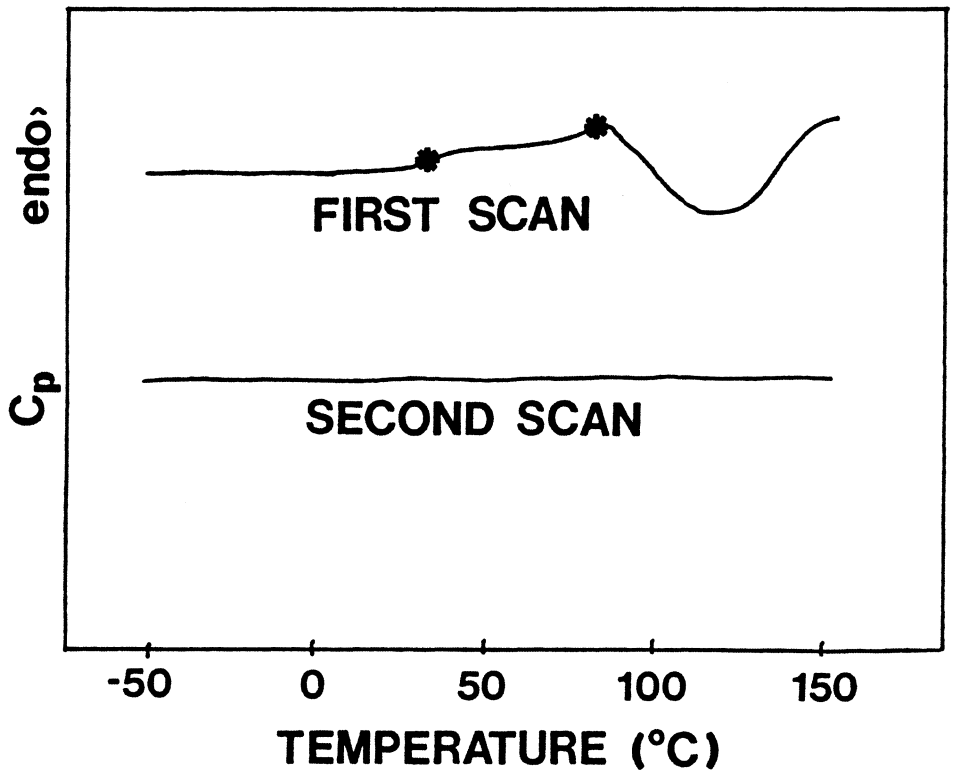

Figure 13. DSC Scan for a 50/50 Mixture of Bis-GMA and TEGDMA: The DSC scan shows the softening of the network at 40°C and the exothermic reaction which begins at 80°C. The rescan shows no exotherm, indicating that the reactive species were used in the first temperature scan [25].

shows the effect of further crosslinking at the higher temperatures achieved during the first thermal scan.

1.4.2 Effects of Temperature on Irradiation Curing

In light of the importance of the temperature of cure on physical properties in crosslinking systems, it is desired to know the temperature of cure in radiation processes such as in electron beam curing. This has been another subject of some uncertainty. One of the advantages often reported for the electron beam curing process is low temperature curing [2]. Degnan [31] has shown that there can be a significant temperature rise in reactive resin systems. A brief synopsis of the research relative to this subject follows for it is relevant to the author's own research presented in Chapter 3.

Some of the earlier work in this area led to the conclusion that the maximum temperature rise in polymers is about 5 to 10 K per Mrad. Both Davison [32] and Bailey [33] estimated this temperature rise by dividing the radiation energy absorbed per unit mass per Mrad (1 Mrad corresponds to 2.39 cal/gram) by the heat capacity (ca. 0.4 cal/g K in most polymers). This analysis is correct for non-reactive systems but can be misleading for resins which crosslink via exothermic reactions.

Milby [34] studied the exothermic reaction which crosslinks unsaturated polyester films. He found that energies up to 150 cal/gram can be generated, which can result in a temperature peak of 300 K. This work assumed no heat transfer out of the curing film, nor did it detail the effects of other system variables such as dose, electron beam intensity, or coating thickness.

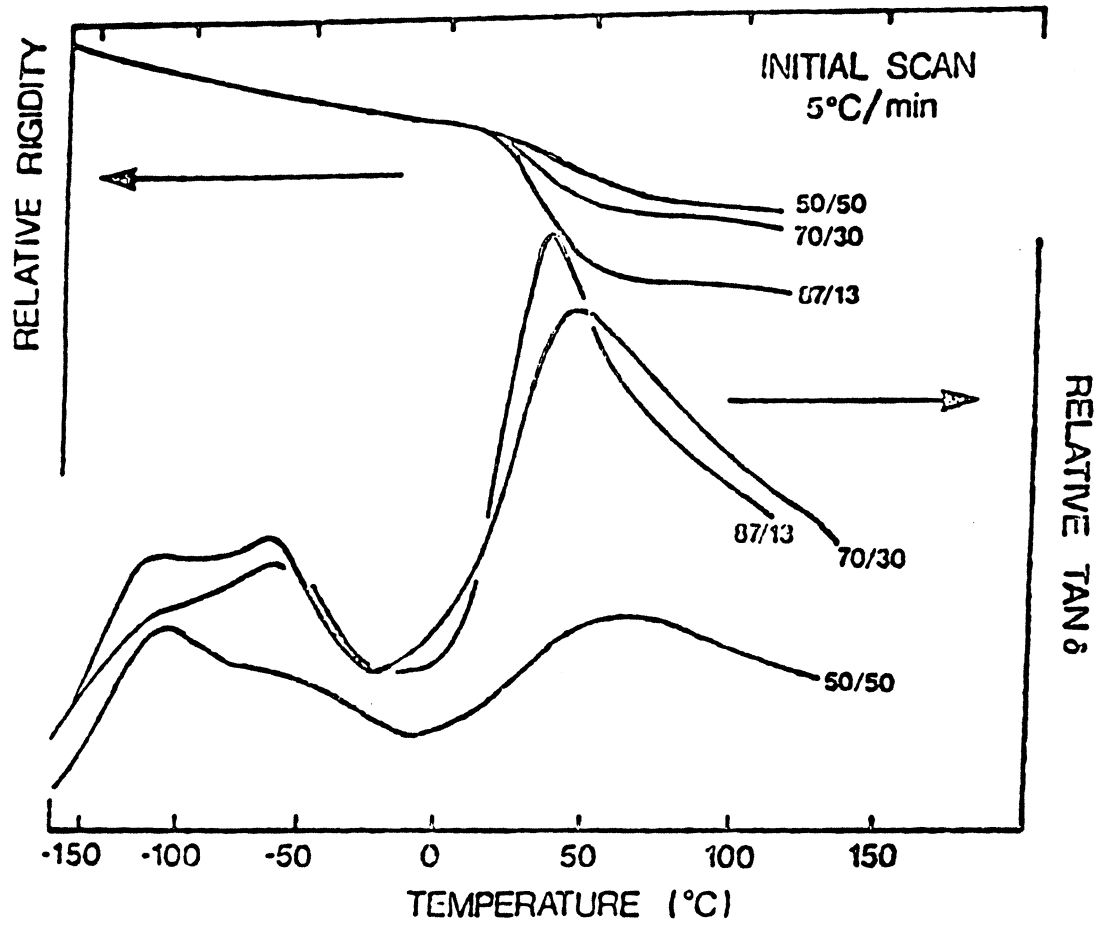

Figure 14. Dynamic Mechanical Results for Bis-GMA/TEGDMA Systems at Various Compositions.: Thermal curing was done using peroxide initiators (from Orler et.al., Ref. 29).

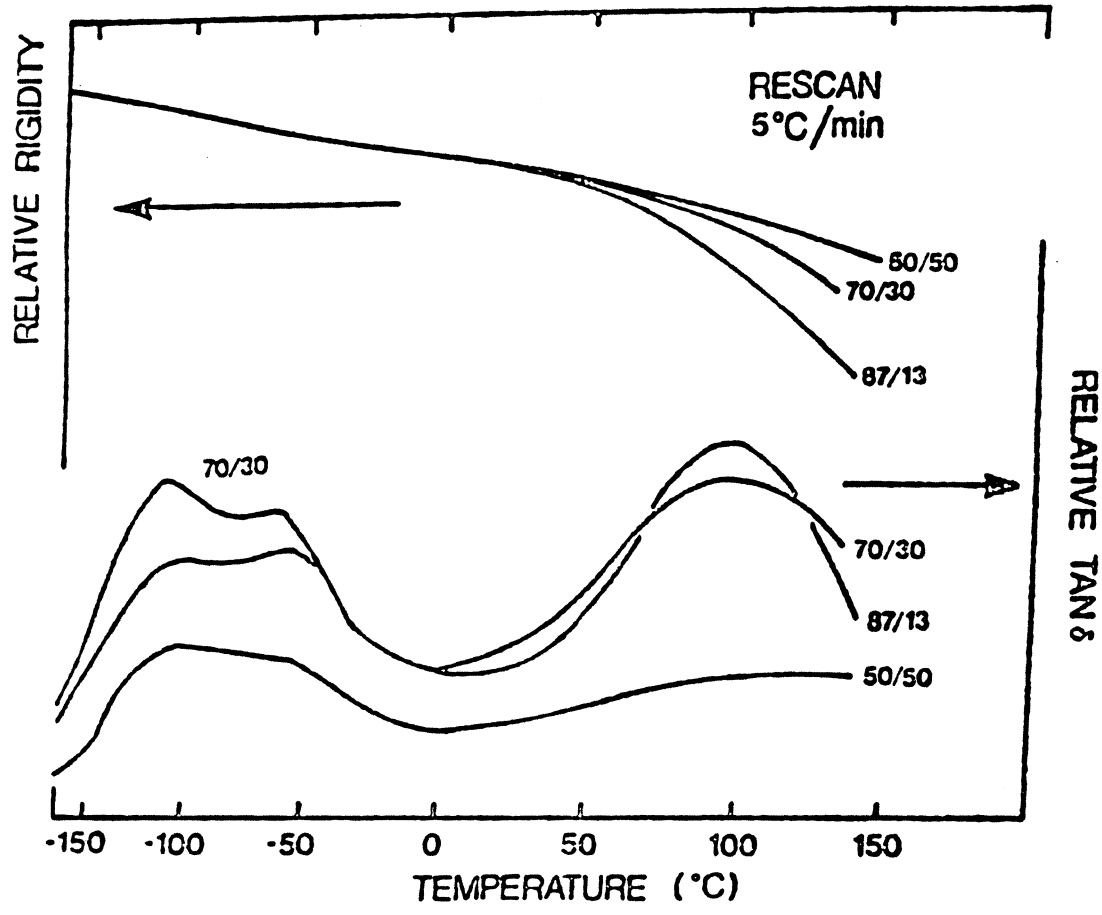

Figure 15. Rescans of Dynamic Mechanical Test for Bis-GMA/TEGDMA: Binary systems of bis-GMA and TEGDMA are tested at various compositions [29]. Scan rate was 5°C per minute.

Degnan's approach [31] was to look at a system of equations which included two-dimensional energy balances for both the coating and substrate, equations to describe the kinetics and heat generation in the coating, and the convective heat transfer to the inert gas. The model predicts a 50 K maximum temperature for an uncoated PET substrate irradiated at 10 Mrad, right in line with Davison and Bailey. Nitrogen flow rate was 850 liters per minute during this experiment. However, calculated temperatures of a Uvithane 783/trimethylopropane triacrylate (see Fig. 16) showed a surface temperature rise of 120 K at only 1 Mrad dose. The temperature rise is even higher within the coating. This temperature increase is ten times that predicted by Davison and Bailey.

Shown in Appendix A are calculations for the temperature rise in the bis-GMA material to be irradiated in this study. Presented first is a simplified model which only accounts for the exothermic heat of reaction from the opening of double bonds. Effects from heat transfer are not considered in these calculations, nor is any temperature rise from the energy of the electrons. A temperature rise of 73°C was calculated for the bis-GMA irradiated at 12 Mrads.

The temperature rise during electron beam curing is dependent on many factors such as dose, electron beam intensity, and even the flow rate of the inert gas which provides convective heat transfer. The most significant effect on temperature rise is determined by the chemical nature of the system. Non-exothermic systems incur a maximum temperature rise of only 5 to 10 K per Mrad. On the other hand, a highly exothermic system can experience a temperature increase of well over 100 K.

UVITHANE 783 (THIOKOL)

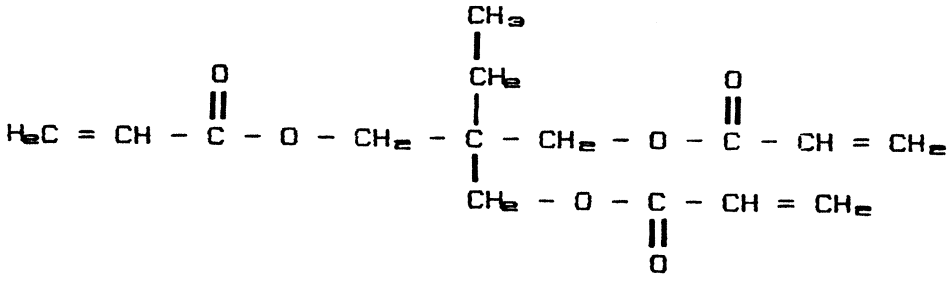

TRIMETHYLOLPROPANE TRIACRYLATE

(TMPTA, SARTOMER)

Figure 16. Chemical Structures for TMPTMA and Uvithane Used in Degnan's Temperature Rise Model: General structures for Uvithane 783 (Thiokol) and trimethylolpropane triacrylate (TMPTA, Sartomer) are given [31].

2.0 Materials, Instrumentation, and Experimental Methods

2.1 Materials

2.1.1 Bis-GMA

As mentioned in the earlier discussion of Kumar's work (sec. 1.3.2), 2,2 bis[4(2-hydroxy-3 methacryloyloxy-propyloxy)-phenyl]-propane, also known as bis-GMA, is a thermosetting acrylic resin. It is a highly viscous liquid at room temperature. It was purchased from Freeman Chemicals (NUPOL 46-4005). It is widely used in dental restorative compounds, and it offers excellent chemical and solvent resistance in coatings. It crosslinks to form a network which behaves as a brittle glass at ambient, but rubber modifiers can be added to provide flexibility in these coatings. The methacrylate groups on each end of the bis-GMA are reactive to thermal or radiation curing. This compound has been synthesized by Yilgor et. al. [35] by reacting Epon 825 with methacrylic acid. Characterization work also done by Yilgor et. al. shows bis-GMA offers higher glass transition temperatures and better stability at high temperatures (ca. 200°C) than the conventional diamine-cured epoxy networks.

2.1.2 Low Molecular Weight Modifiers

Triethylene glycol dimethacrylate (TEGDMA) was purchased from Alfa Chemicals. Its chemical structure, given in Fig. 12 (sec. 1.3.2), shows its methacrylate terminating groups. This material cures rapidly in thermally initiated bis-GMA/TEGDMA mixtures [25]. Higher concentrations of TEGDMA lower the viscosity, allowing more cure time (and as such, more cure) before vitrification. However, as will be discussed, TEGDMA does not cure to gelation when irradiated by an electron beam.

In order to explain this phenomenon, an analogous acrylate system was used. Polyethylene glycol diacrylate (PEGDA) has the chemical structure

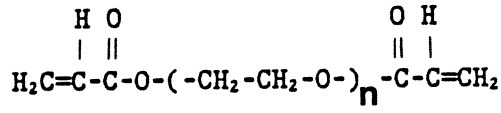

where n averages four. This material was kindly supplied by Sartomer (SR-268). Triethylene glycol diacrylate is not available because of its high toxicity. The acrylate group is generally more reactive than analogous methacrylates. One obvious reason is that the alkene on the methacrylate groups have more steric hindrance than similar acrylates. This is apparent from Miller's observations about crosslinking and scission for carbon backbone systems (one side group crosslinks, two side groups undergo chain scission) [12]. PEGDA crosslinks to form a soft solid at ambient with little physical strength upon deformation.

2.1.3 Higher Molecular Weight Rubbery Modifiers

Higher molecular weight rubbery modifiers end-capped with acrylate or methacrylate species were used with bis-GMA. These binary systems were irradiated, and tests were performed to determine if phase separation occurred. Separation of the rubbery phase from the glassy phase could provide rubber toughening of these glassy systems. If the phases do not sepa-

rate, some toughening may also be achieved, but a trade-off would occur from a lowering of the glass transition temperature.

Polytetramethylene oxide (PTMO) was end-capped with methacrylate groups by reacting methacryloyl chloride (MACl) with PTMO. The PTMO was Teracol-1000 supplied by DuPont. A ratio of 2 MACl to 1 PTMO was used to cap both ends of the diol chain. A sketch of this acid chloride reaction is given in Figure 17 on page 47. The reaction was done using a Dean-Stark apparatus. Toluene was the solvent chosen as a medium. Triethylamine was the base utilized to capture the HCl which is a product of the reaction. An inhibitor, phenothiazine, was used at a concentration of 100 ppm of oligomer to help prevent premature crosslinking of the methacrylate end groups. The methacryloyl chloride was added dropwise to the reactor flask containing a solution of the PTMO, inhibitor, triethylamine, and toluene. The reaction was stirred overnight at a temperature of 40°C. The salt product containing HCl and triethylamine was filtered out of the mixture using vacuum filtration. Toluene was evaporated using a rotary evaporator. This separation was not perfect, as some traces of toluene remained in the solution even after evaporation as shown by FTIR.

A similar reaction was used to end-cap the PTMO-1000 chains with acrylate groups. Acryloyl chloride replaced methacryloyl chloride in the reaction to give

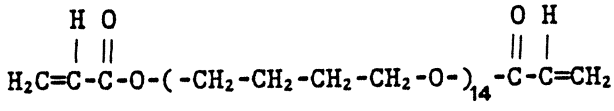

Other reaction conditions were the same as done in the methacrylate end-capping reaction discussed earlier.

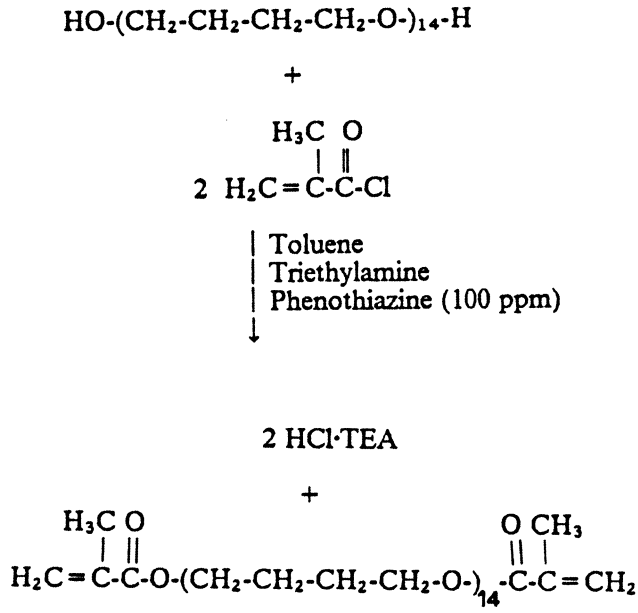

Figure 17. Reaction Scheme for the End-capping of Polytetramethylene Oxide

2.2 *Instrumentation*

2.2.1 Electron Beam Accelerator

The Electrocurtain CB/150/15/180 Laboratory Unit was used to irradiate the prepolymers mentioned above. The instrument was purchased from Energy Sciences, Inc. It operates at a voltage between 150 and 175 kilovolts (kV) with an electron beam current up to 10 mA. Penetration depths at these voltages limit sample thicknesses to 5 mils or below. A constant voltage of 170 kV was utilized throughout this study. A conveyor speed of 40 feet per minute was used for dosages up to 12 Mrad. Dosages of 15 and 20 Mrad were run at 20 feet per minute such that the current requirement (half the 40 fpm current) was within operating range. Dose rate experiments were run varying line speeds systematically from 20 to 100 fpm. Residence times under the electron beam at these line speeds range from 0.3 seconds at 100 fpm to 1.5 seconds at 20 fpm. The actual time of irradiation is therefore quite small. Operating parameters were set according to equation 1.1,

$$D = \frac{K\,I}{S} \qquad (1.1)$$

where K = 66.1 Mrad ft/mA/min. The coated PET films were placed on wood inserts in aluminum trays and run through the conveyor system of the electron beam instrument. The wood inserts were used to minimize the EB sample-to-window distance.

2.2.2 Sample Preparation for EB Curing

Binary mixtures were prepared using compositions on a weight basis. Bis-GMA was the featured component mixed with the acrylate (PEGDA or PTMO-ACI) or methacrylate (TEGDMA or PTMO-MACI) fillers. Slight heating was necessary to obtain good mixtures. The mixtures

were optically clear when irradiated. Temperatures were kept below 75°C during this heating. Since these systems contain no initiator, mild heating did not induce network formation.

The mixtures were coated onto polyethylene terephthalate film (4 mil Scotchpar) using a Bird Bar Wet Film Applicator (Gardner Company). A three-mil drawdown bar was used for coatings for physical property tests. As in the sample mixing, slight heating was necessary to reduce the viscosity of the pure bis-GMA samples to make the drawdowns. Since the samples were thin, the coatings quickly returned to ambient temperature before irradiation. Mixtures had lower viscosities such that drawdowns were made at ambient conditions. As coating thicknesses are dependent on the viscosity of the material, the lower viscosity mixtures (e.g., the 100% PEGDA or the 50% TEGDMA) coated to 1 or 2 mil thickness even with the 3 mil drawdown bar.

2.3 *Experimental Methods*

2.3.1 Percent Gel

Percent gel determinations were done on 30 to 100 milligram samples of the irradiated networks. Aging of these samples was at least 48 hours such that most of the trapped free radicals had dissipated with time (to be later discussed). Samples were weighed then immersed in 40 ml of acetone at room temperature for 24 hours. Next, these films were removed from the acetone and dried in a vacuum oven at room temperature for five days. Finally, the samples were weighed again. The ratio of final sample weight to initial weight was defined as the gel fraction. In this discussion, values are expressed on a percentage basis, hence the term percent gel. Acetone is a good solvent for bis-GMA, TEGDMA, and PEGDA, as it dissolves these monomers almost immediately. Since the networks were glassy at room temperature, there was some concern about the ability of the solvent to diffuse in and the ability

of the residual monomer and other sol molecules to diffuse out. The samples generated in this study were all thin films such that diffusion limitations were minimized.

In order to investigate the reliability of this test, percent gels were found for seven different bis-GMA samples irradiated at 5 Mrad. Results ranged from 91.0 to 97.6%, with a mean of 95.5 and standard deviation of 2.53%. This corresponds to a 90% confidence interval of about 7%. There is some experimental error in this test so it is best to consider only the trends.

Charlesby [15] has mentioned two potential problems with swelling tests of this type. First, the molecules in a swollen network have more freedom to move than do the molecules in the unswollen state. As such, free radicals trapped in the unswollen state could react when swollen thereby adding more crosslinks to the network. A second problem could easily occur as the solvent depresses the T_g of the polymer network. As expressed earlier in terms of the TTT diagram (Fig. 13), the T_g would fall below the cure temperature, maybe even low enough that the crosslinking reaction could continue if the radicals were still "alive". Increasing the temperature during this test could have an even greater effect by mobilizing the free radicals. It is for this reason that the familiar Soxhlet extractor was not utilized in this study. The search continues for more accurate tests to quantify the level of crosslinking in electron beam cured polymers.

2.3.2 Differential Scanning Calorimetry

The Perkin-Elmer DSC-4 was used to investigate heats of reactions and to obtain general trends of glass transition behavior. Samples were run from 20 to 200°C at a scan rate of 20°C per minute. Temperatures reported as T_g's from DSC test data are taken as the onset of the exothermic reaction (indicating that free radicals are thermally mobilized to continue the crosslinking reaction). The exothermic temperature (or exotherm) is defined as the peak temperature of the crosslinking reaction shown by the low point on the DSC temperature

scans. Rescans were run on a number of samples to see the effect of thermal curing from the previous heating cycle. In another study, the effects of time after cure were studied by running samples systematically at various times after EB cure.

2.3.3 Dynamic Mechanical Properties

The Autovibron Dynamic Viscoelastometer was used to measure the dynamic storage and loss moduli (E′ and E″) as well as tan δ (E″/E′) all as functions of temperature. This device allows investigation of thermal transitions which alter mechanical behavior. Many samples were run from 0 to 200°C to investigate T_g. Later samples, specifically those reacted with rubber modifier, were scanned from -150 to 200°C to also look at lower temperature responses. The scanning rate was 2°C per minute, and a frequency of 11 Hz is reported unless otherwise indicated. A frequency of 110 Hz was also investigated but a resonance tan δ peak was found in the lower temperature range. Thus, the 110 Hz results could not be reported in this case.

The temperature referred to as T_g from the Autovibron results was the peak of the log tan δ vs. temperature curve. These T_g values are somewhat complicated because the crosslinking reaction can continue during the Autovibron test as free radicals gain mobility above the initial T_{g0}. The slow temperature scan rate as compared to the DSC test (20°C per minute) leads to competition between thermal softening and chemical crosslinking. The continued crosslinking can lead to a broad tan δ peak or even a second apparent T_g at a higher temperature. Hence, the T_g by this method is accurate at best to within a few degrees. It is realized that there can be a distribution of temperatures over which molecules gain mobility. As such, reductions in modulus that occur at temperatures below the tan δ peak can affect the physical properties of the network. However, for much of this discussion this author will follow the literature and report T_g as the peak from the tan δ vs. temperature curve. Another parameter which will be periodically discussed is a "softening temperature", where the storage modulus begins to

decline with heating. For this analysis, the softening point is defined as the temperature where the storage modulus reaches a value of 5×10^9 dynes/cm^2. Although this definition is somewhat arbitrary, it will provide a comparison for results obtained during this study.

2.3.4 FTIR -- Residual Double Bond Content

The Nicolet 5DXB was used to quantify double bond content in irradiated networks. Peaks corresponding to unsaturated carbons in crosslinked materials were compared to the similar peaks in unirradiated prepolymer samples. The peaks were normalized to an invariant peak to account for variations such as sample thickness. Similar studies have been done for thermally cured systems by Wu and Fanconi [36] and served as a guide to procedures utilized in this study.

Three peaks were needed to quantify double bond content in these polymer samples. First, the alkene (-CH=CH-) peak exists around 1638 cm^{-1}. The disappearance of this peak indicates the reaction of double bonds. Next, the phenyl ring peak, which occurs at 1583 cm^{-1}, is used to normalize the unsaturation peak in systems containing the aromatic bis-GMA. The aromatic group is inert to radiation due to its ability to form resonance structures. Third, the methyl peak at 1369 cm^{-1} was used to normalize the alkene peak in the absence of aromatic groups (e.g. pure PEGDA or TEGDMA systems). The methyl group is more reactive to EB than the phenyl ring, but it contains many more contributors in these long chain materials, so changes do not alter the peak significantly.

The percent double bond content was found by determining the peak heights after subtracting the baselines, dividing the alkene peak height by the normalization peak height (phenyl or methyl) and comparing the results to similar calculations for unirradiated samples. The baseline points were determined by averaging the ordinate values found on each side of the peaks. This analysis is shown by a sample calculation in Appendix B. The reliability of this

test was investigated by finding double bond content for five bis-GMA samples irradiated at 5 Mrad. Percent double bonds ranged from 44.4 to 50.2%, with a mean value of 46.5% and a standard deviation of 2.3%.

2.3.5 Scanning Electron Microscopy

Scanning electron microscopy was done using the International Scientific Instruments, Super III-A electron microscope. Photomicrographs were taken of fractured surfaces of irradiated coatings at 500x and 3000x magnification. The coatings contain bis-GMA and either the acrylate or methacrylate-capped PTMO. The molecular weight of the PTMO was 1000 g/mol, and the end-capped material was added to bis-GMA at a composition of 15% by weight. Irradiation was done at 2 and 20 Mrads to test the two extremes. Samples were fractured at ambient and at liquid nitrogen temperatures. In addition, some samples were immersed in THF to remove any extractables (i.e., the rubbery phase or bis-GMA soluble component) before electron microscopy was run. The purpose of this study was to look for phase separation of the rubbery component from the glass which would give a "rubber toughening" effect on physical properties and give two T_g's as a result of dynamic mechanical tests.

3.0 Bis-GMA Coatings Cured by Electron Beam Irradiation

3.1 Introduction

The matrix of experiments discussed in this chapter characterizes electron beam cured systems containing bis-GMA referred to in Chapter 2. Three-mil drawdowns were coated onto polyethylene terephthalate film and irradiated with an electron beam curtain. Characterization was done first to quantify the crosslinking reaction by percent gel and residual double bond tests. DSC and dynamic mechanical tests were performed to investigate thermal and mechanical transition temperatures.

A number of parameters have been varied systematically in these studies. Radiation dose is an important variable because there is an optimum dose for sufficient cure and minimum energy consumption. In addition, the effects of time after cure and thermal annealing on physical properties will be discussed. Another variable which is investigated for bis-GMA systems is the effect of dose rate on cure and physical properties.

3.2 *Crosslinking Reaction*

To quantify the crosslinking reaction, percent gels were determined for bis-GMA films irradiated at different dosages. Percent gel content increased with dose, ranging from 58% gel content at 0.5 megarads to 100% at 20 megarads. Although the percent gel content was found to be essentially 100% by the solvent swelling test, this does not mean that all of the double bonds have been utilized to form crosslinks. It simply indicates that a sufficient gel was formed to entrap any remaining monomer or oligomer. Percent gel content is plotted vs. irradiation dose in Figure 18 on page 56. The figure shows a leveling off near 100% gels at high dosage, suggesting a "diminishing returns" relationship between the two parameters. The bis-GMA showed a broad range in percent gel over the dosages used in this study. The percent gel curve levels off above 10 Mrad.

A related test was done to characterize the crosslinking reaction in terms of the swelling ratio. The swelling ratio (q) was defined by Flory [36] as the swollen volume divided by the initial (unswollen) volume for a polymer network. The assumption necessary for this work is that swelling occurs as the solvent diffuses into the network, such that the weight of the network will increase due to the weight of the solvent as does the volume. Thus, q as defined for this set of experiments is simply the swollen weight divided by the unswollen weight. The degree of swelling is inversely proportional to the degree of crosslinking in the network. So, the swelling ratio should confirm or negate the claims made above from the percent gel data. Since irradiated samples may contain some sol components, extraction in acetone was done and the films were dried prior to the swelling ratio experiments.

Data for the equilibrium swelling ratio of bis-GMA in acetone is plotted in Figure 19 on page 57for the irradiation dosages tested. The equilibrium swelling ratio does in fact decrease as dosage increases. Since the crosslink density in all of these networks is high relative to other networks such as an elastomer or lightly crosslinked polyethylene, the swelling ratios are all

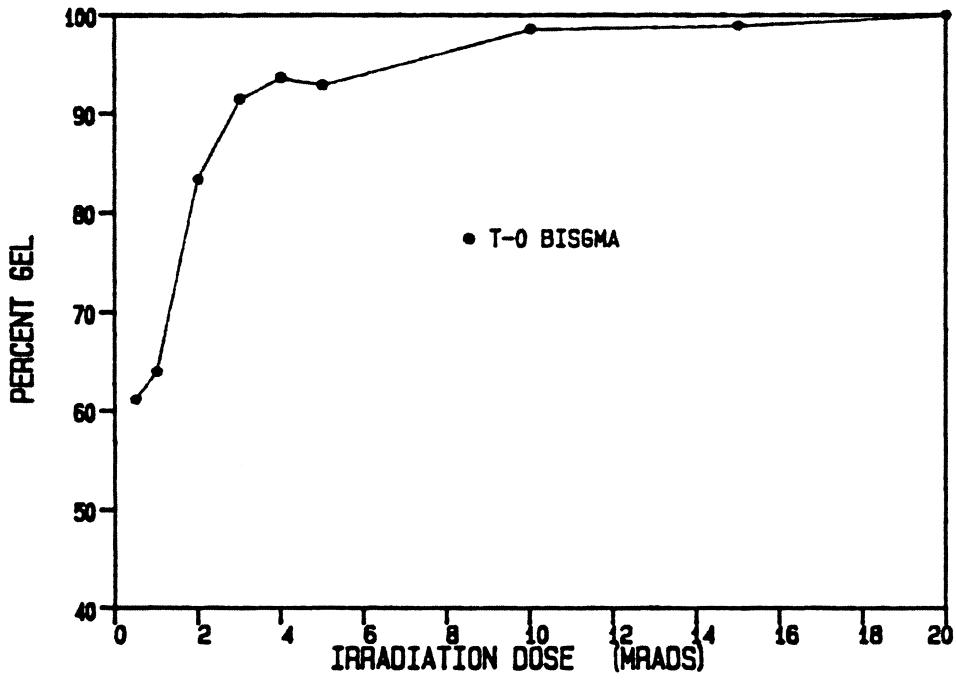

Figure 18. Percent Gel vs Irradiation Dose for Bis-GMA at 0.5 to 20 Megarads: This experiment was done by swelling the irradiated films in acetone for 24 hours, then removing the films and transferring them to a vacuum oven for five days.

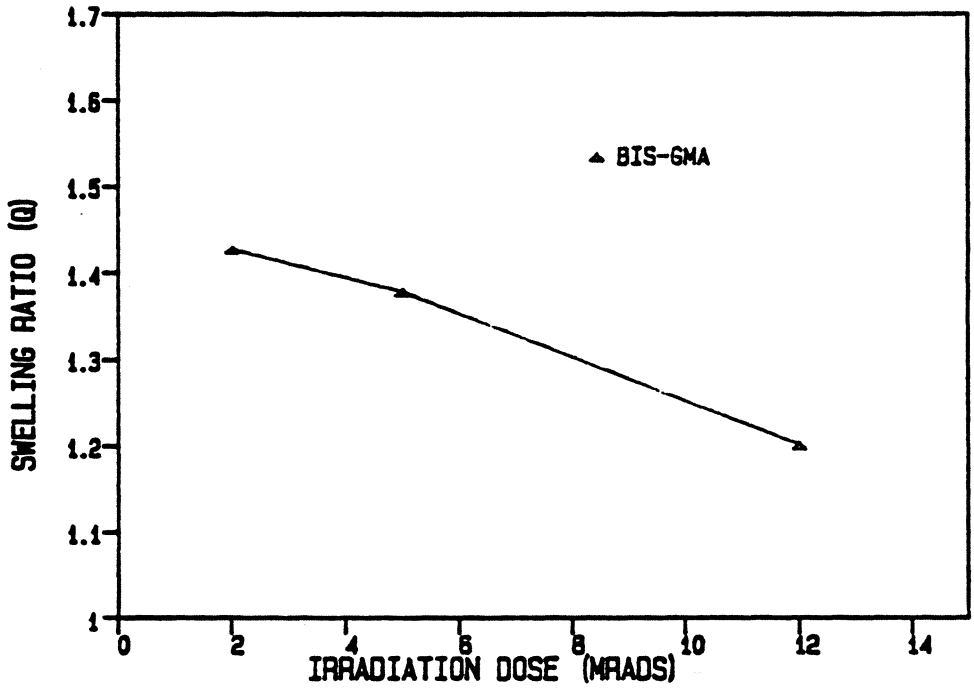

Figure 19. Swelling Ratios at Equilibrium vs. Dosage for Bis-GMA Samples: Irradiated film samples were extracted in acetone. Swollen films were dried in a vacuum oven for five days. Then, samples were returned to the acetone and swelling ratios were calculated.

low (below 1.5). The 12 Mrad film had an equilibrium swelling ratio of 1.20, lower than the value of 1.38 for the 5 Mrad sample and the value of 1.43 for the 2 Mrad film. As expected, these data suggest that the crosslink density is higher for the 12 Mrad film than for the lower dosage samples.

Residual double bonds were quantified by FTIR. As expected from the percent gel data and previous discussion about the crosslinking reaction which takes place by addition across the double bond, residual double bond content decreased as dosage increased, indicating more crosslinking takes place at higher dosage. The percentage of residual double bonds is plotted vs. irradiation dose in Figure 20 on page 59.

From Fig. 20 it is seen that percent residual double bonds can be as high as 55% at 2 Mrad. It should be remembered that this data point corresponds to a percent gel value of 80%. These percent double bond values seem rather high relative to the percent gel data, suggesting the radiation leaves a number of double bonds unreacted. This seems somewhat reasonable in light of the fact that the bis-GMA chains can join the network by a crosslinking reaction at only one end of the chain. The other chain could retain its double bond, remaining unattached to the network. One reacted double bond and one unreacted double bond would be seen in the FTIR test, a 50% residual double bond content. Another possibility, as mentioned above, is that a short-chain oligomer could form by the crosslinking of only a few bis-GMA molecules with no links to the main network. The oligomer could be trapped into the network by diffusion limitations such that it is not removed by solvent extraction.

3.3 Physical Properties

3.3.1 Effects of Dose

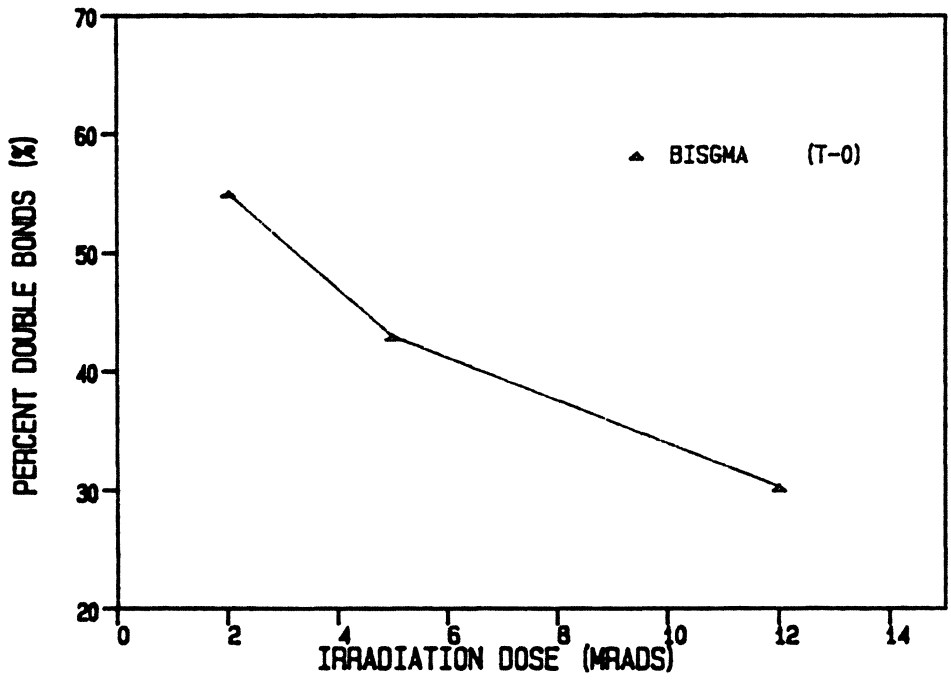

Figure 20. Percent Residual Double Bonds for Irradiated Bis-GMA Coatings at Various Dosages.: FTIR was done 1 hour after electron beam cure to determine the residual double bond content.

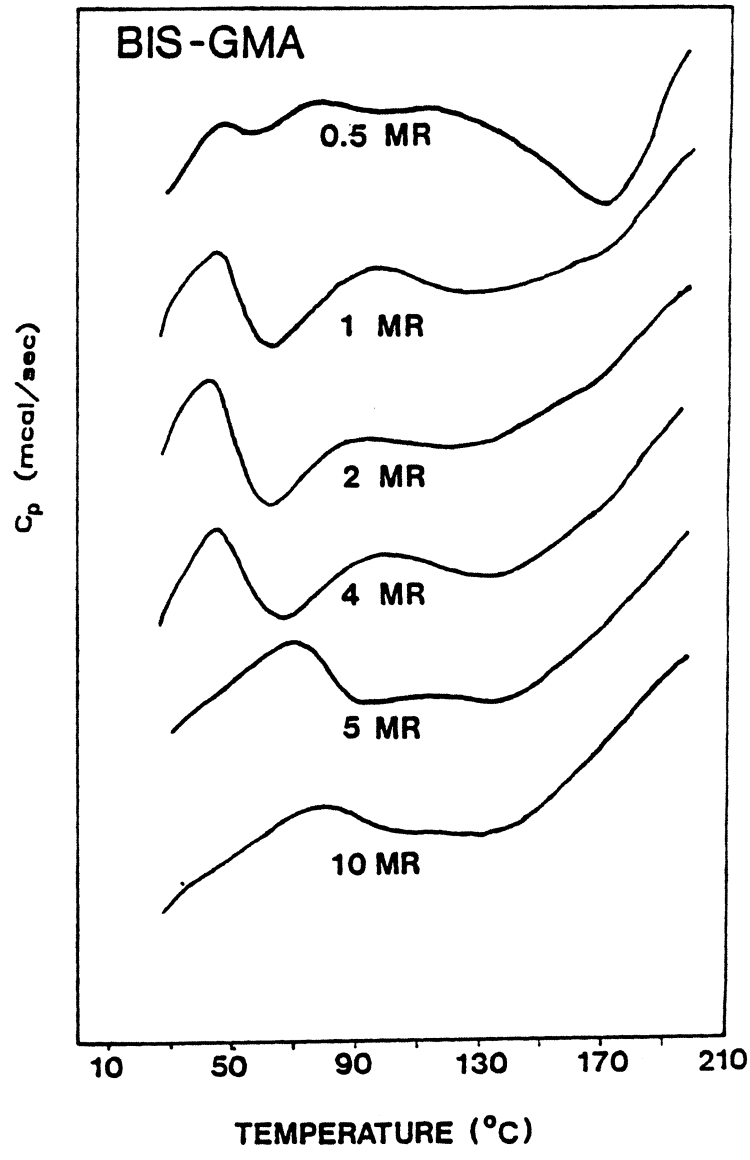

Figure 21. Differential Scanning Calorimetry for Bis-GMA Irradiated at Various Dosages.: The DSC curves show the exothermic crosslinking reaction which occurs as trapped free radicals are thermally mobilized. Aging time was one hour after cure. Distance between tick marks is 0.04 mcal/sec.

Figure 21 displays the DSC thermograms for bis-GMA systems irradiated at dosages of 0.5 to 10 Mrads. All samples were aged at room conditions for one hour prior to the DSC test. As previously mentioned, the initial T_g (or onset of T_g) is indicated by the exothermic reaction which takes place as free radicals are thermally mobilized. Samples with less than 5 Mrad dose display this onset of T_g between 40 and 50°C. The exotherm reaches a maximum near 70°C. The 0.5 Mrad dose sample is an exception. Although it, too, has an exothermic peak which begins near 50°C, its exothermic peak is small. This suggests that only a few free radicals were generated during irradiation. The 5 Mrad curve shows the T_g is shifted to a temperature near 70°C. The T_g at 10 Mrads is even higher at 86°C. Another stage of this exothermic reaction exists for all dosages between 130 and 150°C and is discussed below.

Although Fig. 21 gives a good picture of the effects of radiation dose on the physical properties, it does not differentiate between crosslinks that occur from free radicals formed during irradiation and those from thermal opening of the double bonds during the DSC test. In order to distinguish the two, a sample of unirradiated bis-GMA (liquid) was put in a pressure cell. The DSC temperature scan was run from 20 to 250°C. The results are presented in Figure 22 on page 62. An exothermic reaction is initiated at about 130°C, reaches a first minimum specific heat at 150°C, then the exothermic reaction continues to its peak at 198°C. This exothermic peak resembles the one from the 0.5 Mrad bis-GMA sample shown in Figure 21 on page 60. This reaction is clearly due to the breaking of double bonds by thermal mechanisms. It is apparent that the higher temperature exotherms occur from the reaction of residual double bonds (i.e., those remaining after EB cure).

Dynamic mechanical tests were also run for bis-GMA samples cured at 2, 5, and 12 Mrads. The resulting plots of storage modulus (E′), loss modulus (E″), and log tan δ vs. temperature are presented in Figs. 23, 24, and 25. From Fig. 23, the 2 Mrad sample showed an initial glass transition at 53°C. Another T_g (log tan δ peak) exists at 161°C. This new T_g is the result of the experiment, as the crosslinking reaction continues above the initial T_g. The storage modulus curve (E′) gives more detail about the "softening" of the bis-GMA film. A slight decline of the

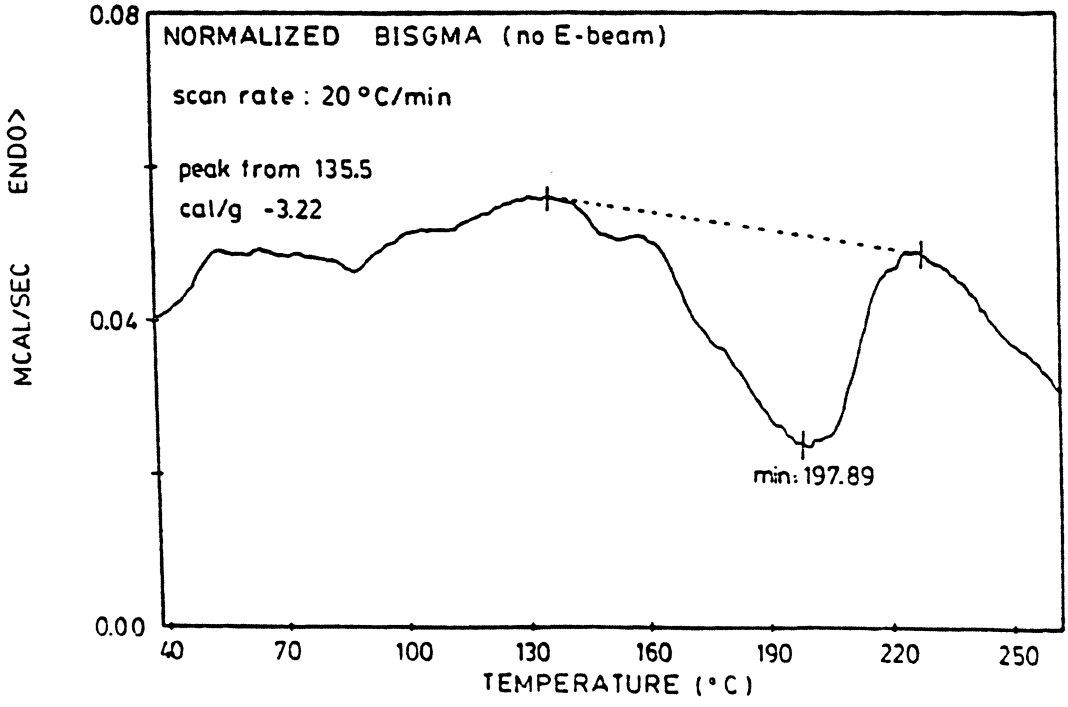

Figure 22. Differential Scanning Calorimetry Temperature Plot for Liquid Bis-GMA.: The DSC curve shows the exothermic crosslinking reaction which occurs above 130°C due to the thermal opening of double bonds.

E′ vs. temperature curve exists at 35°C, indicating the initial softening that is also shown by the rising tan δ curve. Above 35°C the storage modulus levels off until a sharper decline begins around 115°C.

The temperature defined earlier in Chapter 2 as the softening point temperature (where E′ = 5×10^9 dynes/cm^2) exists at 135°C.

The 5 Mrad sample, shown in Fig. 24, also had an initial T_g at 53°C. In addition, it showed signs of a higher T_g when it physically failed at 150°C. This sample had a slight decline in storage modulus around 35°C as did the 2 Mrad sample. This indicates some mobility is gained in the bis-GMA chains. The DSC scan shows that the exothermic reaction of crosslinking begins above this temperature for the 2 Mrad sample, and above 70°C for the 5 Mrad sample. The softening point was not reached because of the sample failure, but it obviously exists above 150°C, higher than the value of 135°C at 2 Mrads.

The dynamic mechanical temperature plot for the bis-GMA irradiated at 12 Mrads is given in Fig. 25. The initial T_g is shown by a broad tan δ peak which exists at 84°C. Another tan δ peak exists at 198°C. An interesting point is shown by the storage modulus vs. temperature curve, which does not decline until well over 100°C. The softening point for comparison with the other dosages occurs at 187°C.

The results from DSC and dynamic mechanical tests clearly demonstrate that the amount of cure in bis-GMA films is proportional to the radiation dosage. Differences in T_g values between the DSC and dynamic mechanical tests can be attributed to scan rate. The DSC scan rate was 20°C per minute, ten times that of the Autovibron (2°C per minute). Since bis-GMA can continue crosslinking as it is thermally mobilized, the scan rate makes a significant difference. The glass transition as determined by the two instruments are physically quite different. The DSC test gives T_g as the temperature where thermal mobility is high enough that previously trapped radicals can react to continue crosslinking. It is the exothermic chemical

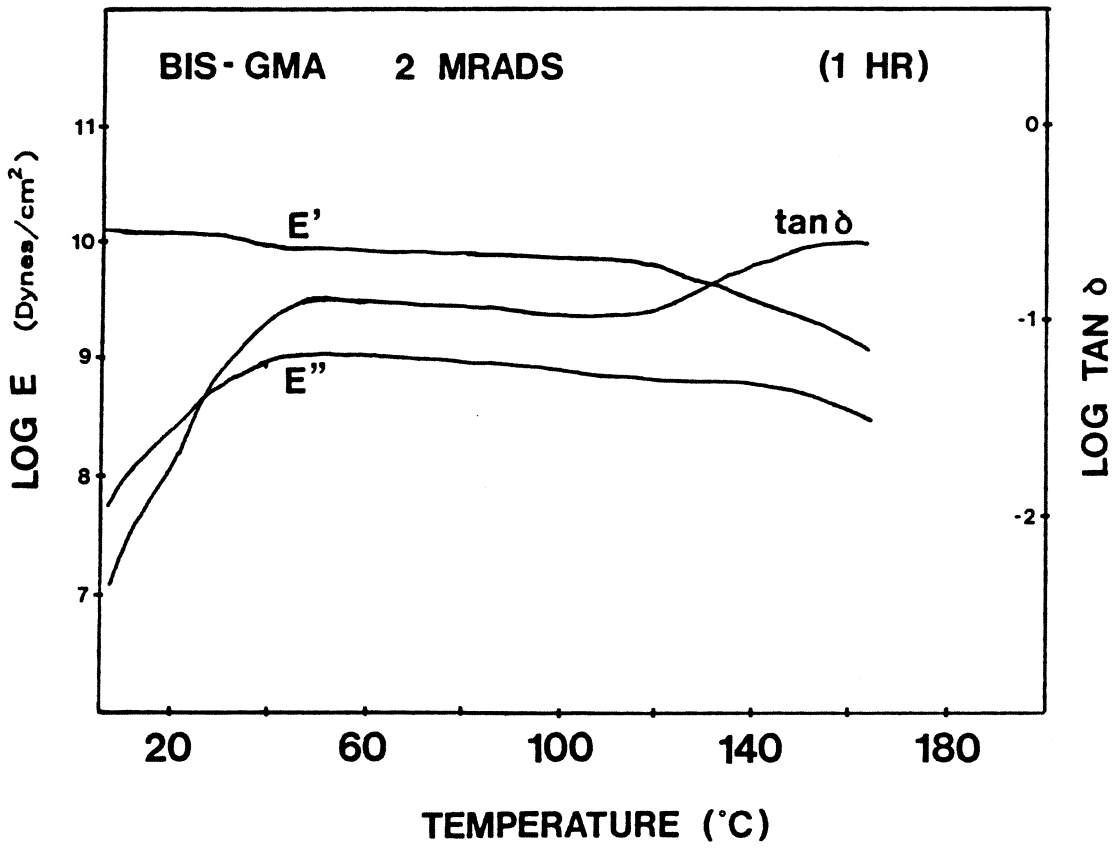

Figure 23. Dynamic Mechanical Temperature Scan for Bis-GMA Irradiated at 2 Mrads.: The temperature scan was run one hour after EB cure. Scan rate was 2°C per minute, and the frequency is 11 Hz for the results shown.

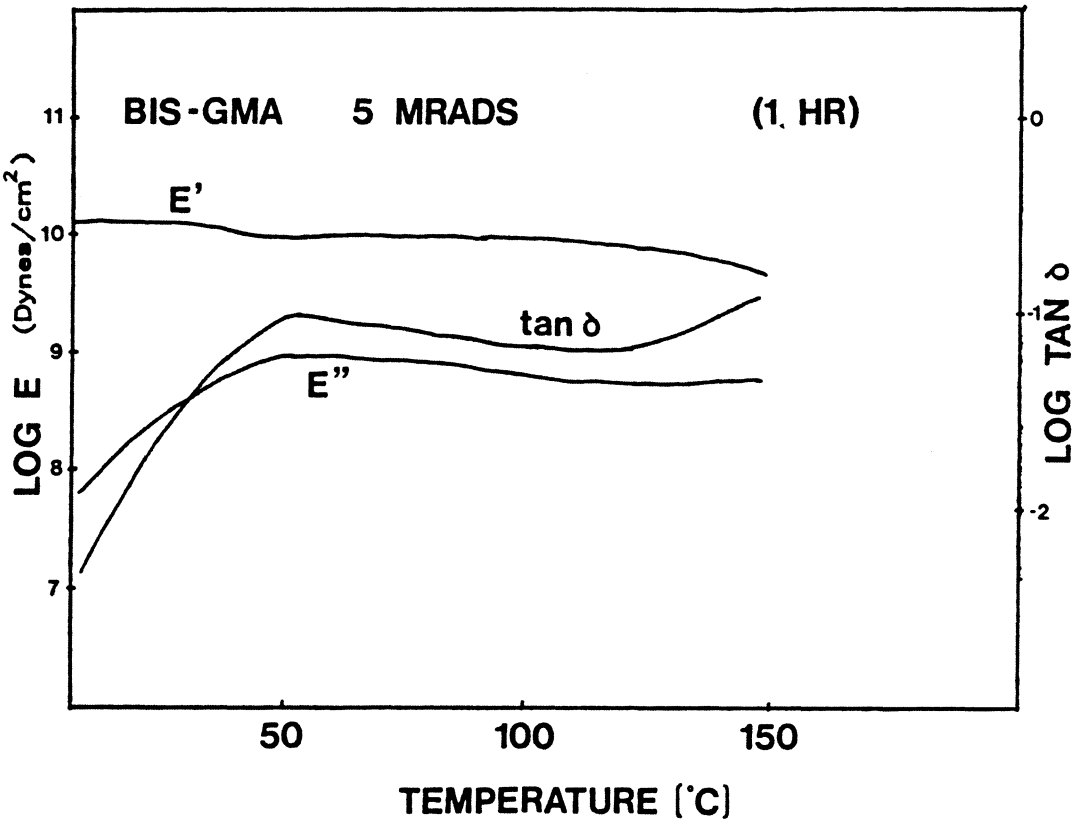

Figure 24. Dynamic Mechanical Scan for Bis-GMA Irradiated at 5 Mrads.: The temperature scan was run one hour after EB cure.

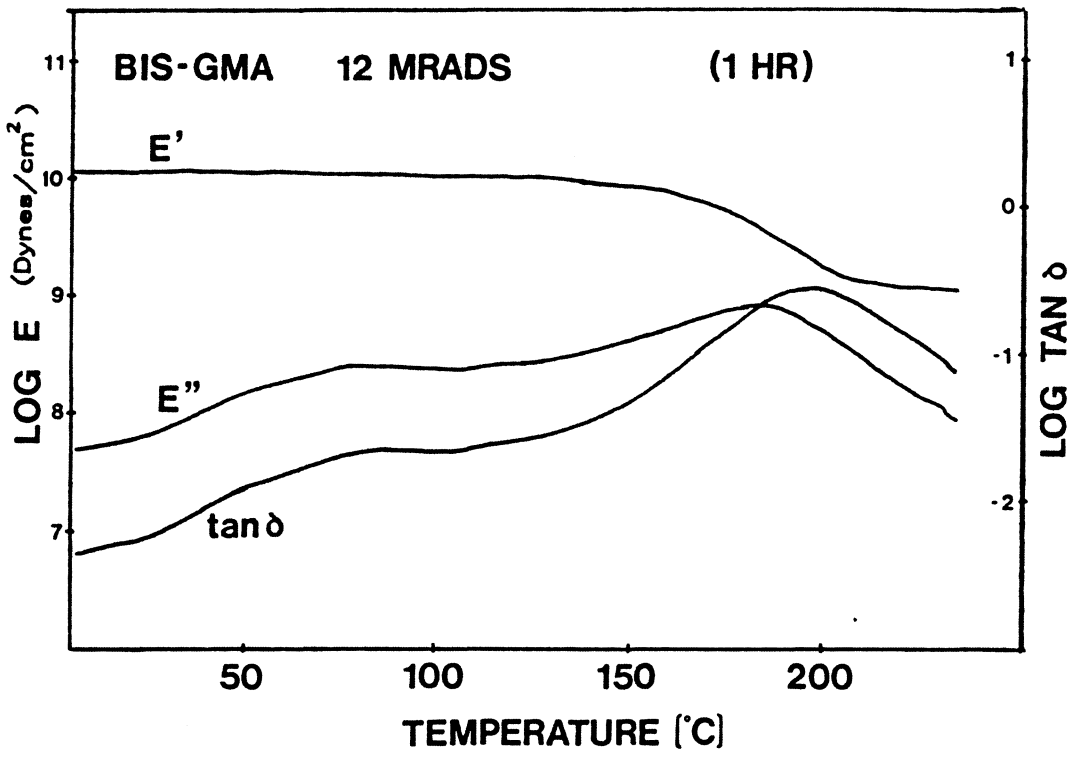

Figure 25. Dynamic Mechanical Temperature Scan for Bis-GMA Irradiated at 12 Mrads.: The temperature scan was run one hour after EB cure. Scan rate was 2°C per minute, and the frequency shown is 11 Hz.

reaction that is monitored. The Autovibron test shows the temperature where the film physically softens. This is somewhat complicated because the crosslinking reaction can continue if reactive species remain in the matrix. At a temperature scan rate of only 2°C per minute, the two phenomena (thermal softening vs. chemical crosslinking) actually compete. In terms of the Time-Temperature-Transformation diagram (see Figure 11 on page 34), as the temperature scan proceeds in the DSC or Autovibron tests, the cure temperature from the radiation process is surpassed. At this point the material softens and the chains acquire mobility such that activated species can continue the crosslinking reaction. From the TTT diagram, the material temperature goes above that of vitrification, and the gelled rubber region is again reached. With time, further crosslinking occurs to increase T_g until the material reaches the glassy state. A summary of these results is presented in Table 3, giving percent gel, residual double bonds, and glass transition temperatures from DSC and dynamic mechanical testing.

3.3.2 Effects of Time after Cure

Another variable investigated by DSC and dynamic mechanical experiments is the effect of ambient aging after irradiation. Aging was done in dry air (in a dessicator) at room temperature.

Figure 26 shows the DSC results for bis-GMA aged 120 hours after electron beam cure. Dosages of 2, 3, 4, 5, and 15 Mrads were tested. The onset of T_g for the 2 Mrad sample is shifted well past 90°C, compared to a T_g near 50°C at only 1 hour after cure (see Fig. 22). The 3 and 4 Mrad samples display an onset of T_g near 90°C. these samples also have peaks at 55°C, which could result from physical aging. Also as shown earlier for the one-hour aged samples, an exotherm exists at 130°C from the breaking of double bonds by thermal mechanisms. Another exotherm is evident near 170°C. The 5 Mrad sample shows the same trends, with the exception of the onset of T_g which is slightly higher than the low dosage samples

Table 3. Physical Properties for Bis-GMA at Various Dosages

DOSE *(Mrads)*	% GELS *(%)*	RESID. DB *(%)*	Tg (DSC) *(°C)*	Tg (VIBRON) *(°C)*
2	81.3	55.1	42	53
5	95.5	43.0	71	53
12	98.6	30.2	86	84

(105°C). The 15 Mrad sample does not show the magnitude of exothermic reaction that the other samples display. However, there is a peak near 60°C and an exotherm at 130°C.

DSC temperature scans for bis-GMA irradiated at 2 Mrad dosage taken at various times after cure are presented in Fig. 27. Samples were tested at 1, 6, 13, 28, 37, 53, and 77 hours after cure. As time after cure increases, the temperature for the onset of reaction also increases. The first peak essentially disappears after 77 hours. At 77 hours the T_g from the DSC measurement is 90°C.

The general trend from this data suggests that the glass transition temperature as indicated by the thermal mobility of reactive groups (DSC test) increases as time after cure increases. In addition, the magnitude of the exothermic peaks at 130 and 170°C tend to increase with time after irradiation. This is because there are fewer radicals to continue the crosslinking, so more of the double bonds are opened via thermal mechanisms at the higher temperatures.

Percent residual double bond content was also determined for bis-GMA irradiated at 2, 5, and 12 Mrads at different times after EB cure. Figure 28 presents the residual double bond contents plotted vs. time after cure. There appears to be a slight drop within the first 24 hours, then the double bond values remain fairly constant. Even this initial drop is within experimental error, but the fact that it occurs for all three samples suggests it is real.

Dynamic mechanical tests were also performed for bis-GMA cured at 2 and 12 Mrads aged 48 and 120 hours after cure. The four resulting plots are given in Figs. 29 through 32. These plots can be compared to those done one hour after cure, given in Figs. 23 and 25. As mentioned in Chapter 2, the frequency of 11 Hz was chosen for all discussion.

Figure 29 gives the E′, E″, and tan δ curves for a temperature scan of the 2 Mrad sample aged 48 hours in dry, ambient air. This sample has tan δ peaks at 73 and 134°C. The storage modulus (E′) begins to decline soon after start-up, and the softening point temperature exists

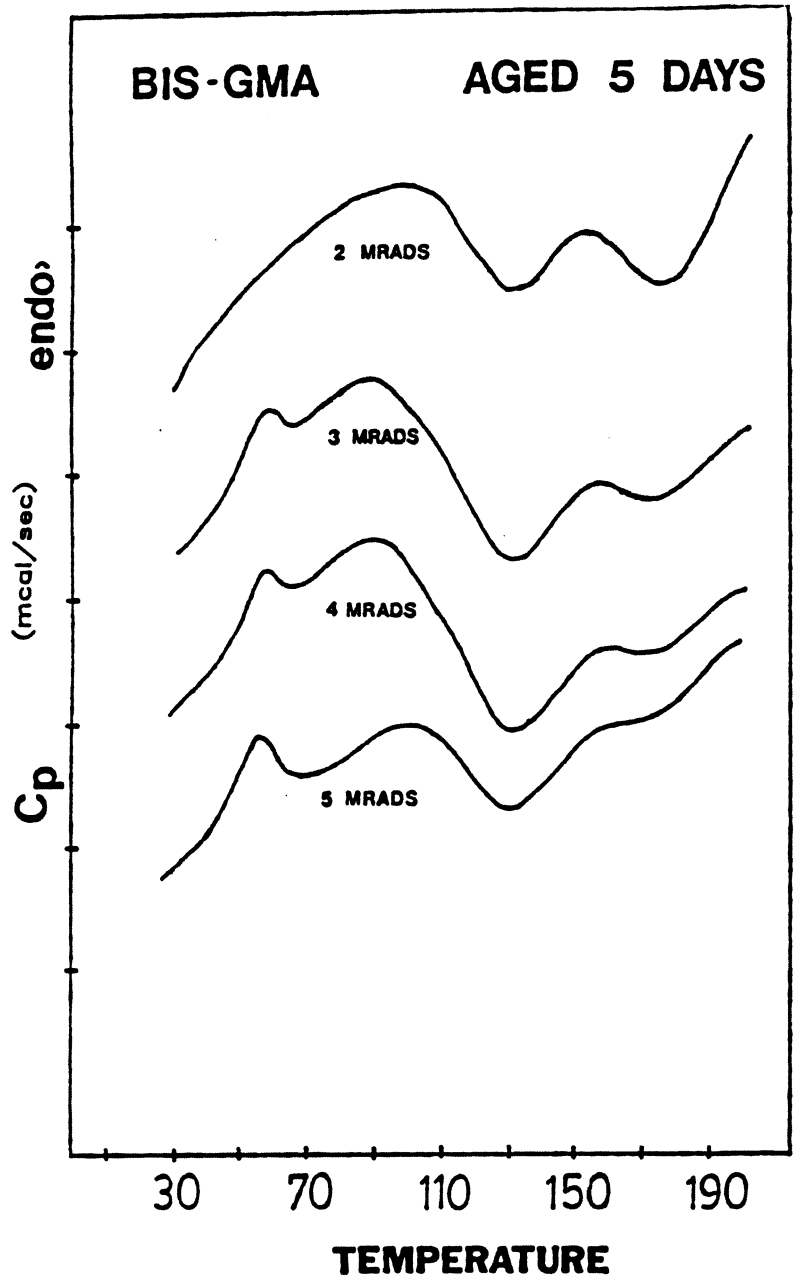

Figure 26. DSC Temperature Plots for Bis-GMA Irradiated at Various Dosages Aged 120 Hours after EB Cure.: Dosages were 2,3,4,5, and 15 megarads. Aging time was five days (120 hours at ambient temperature in dry air.

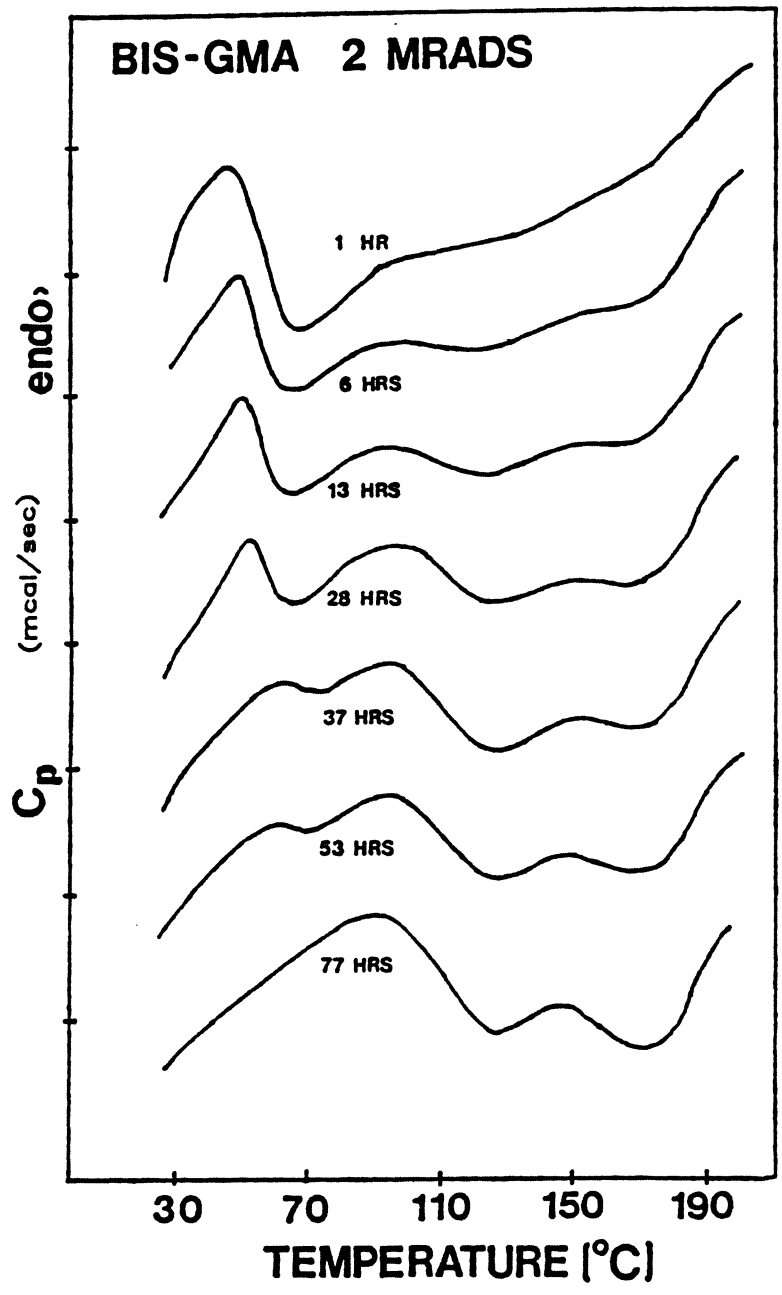

Figure 27. DSC Temperature Scans for Bis-GMA Irradiated at 2 Mrads at Various Times after Cure.: Bis-GMA was irradiated at 2 Mrads and aged for the following times; 1,6,13,28,37,53, and 77 hours. Scan rate was 20°C per minute.

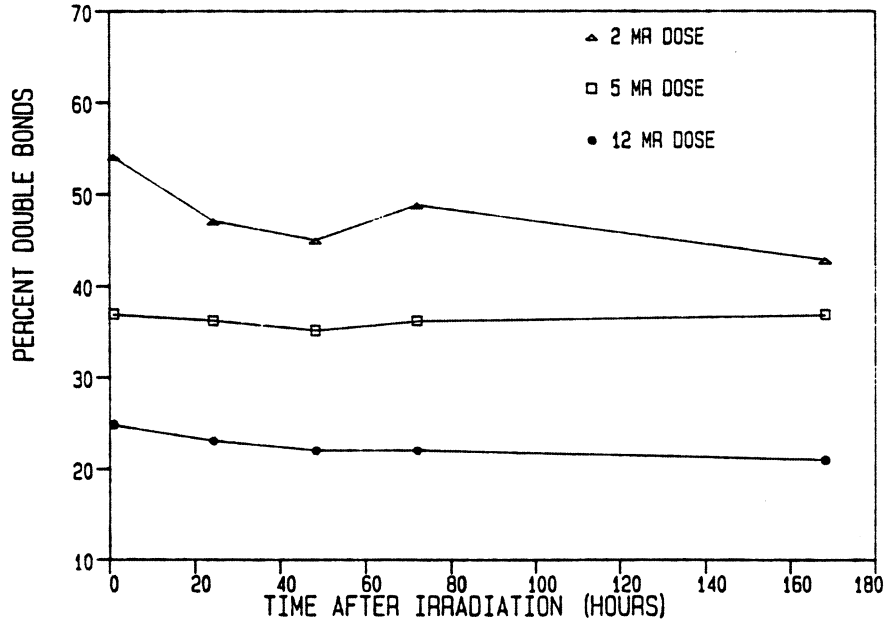

Figure 28. Residual Double Bond Content vs. Time after Irradiation for Bis-GMA.: Irradiation dosages were 2, 5, and 12 Mrads. Aging times ranged from 1 to 168 hours.

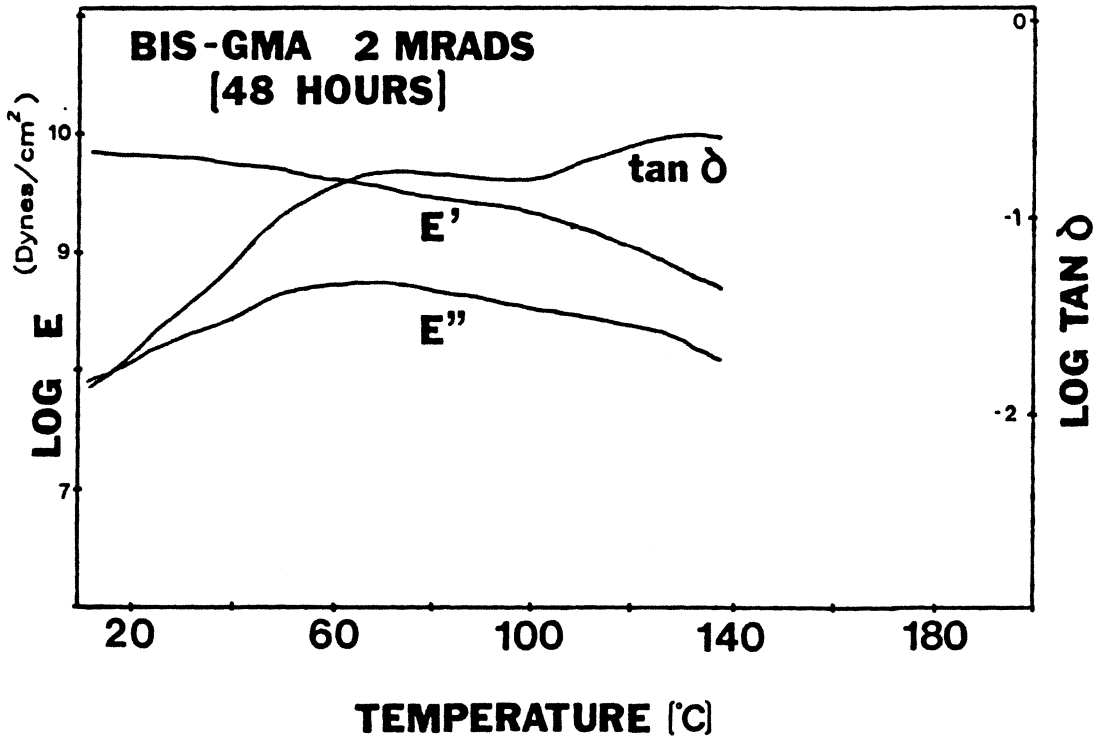

Figure 29. **Dynamic Mechanical Temperature Scan for Bis-GMA Irradiated at 2 Mrads and Aged 48 Hours after Cure.:** The scan rate was 2°C per minute, and 11 Hz is the frequency given in the data. Curves for storage modulus (E'), loss modulus (E"), and tan δ are given.

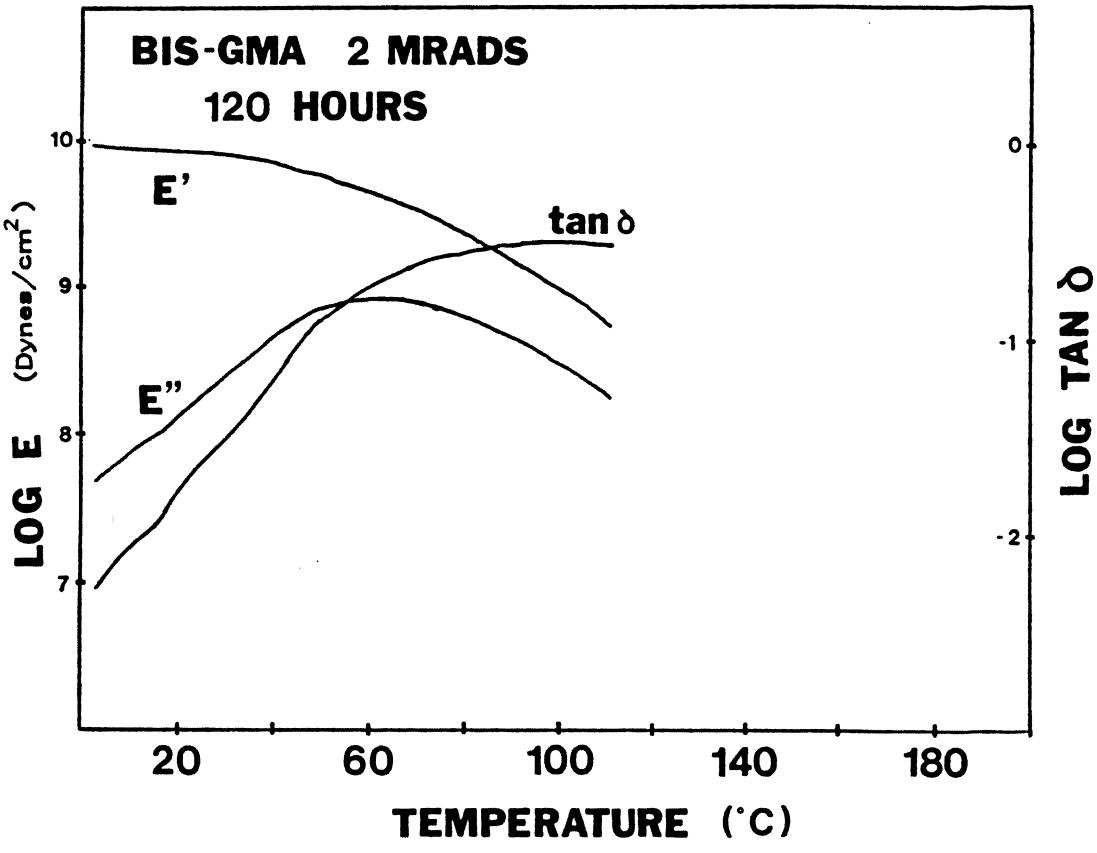

Figure 30. Dynamic Mechanical Temperature Scan for Bis-GMA Irradiated at 2 Mrads and Aged 120 Hours after Cure.: Curves for storage modulus (E'), loss modulus (E"), and tan δ are given. The scan rate was 2°C per minute, and frequency is 11 Hz.

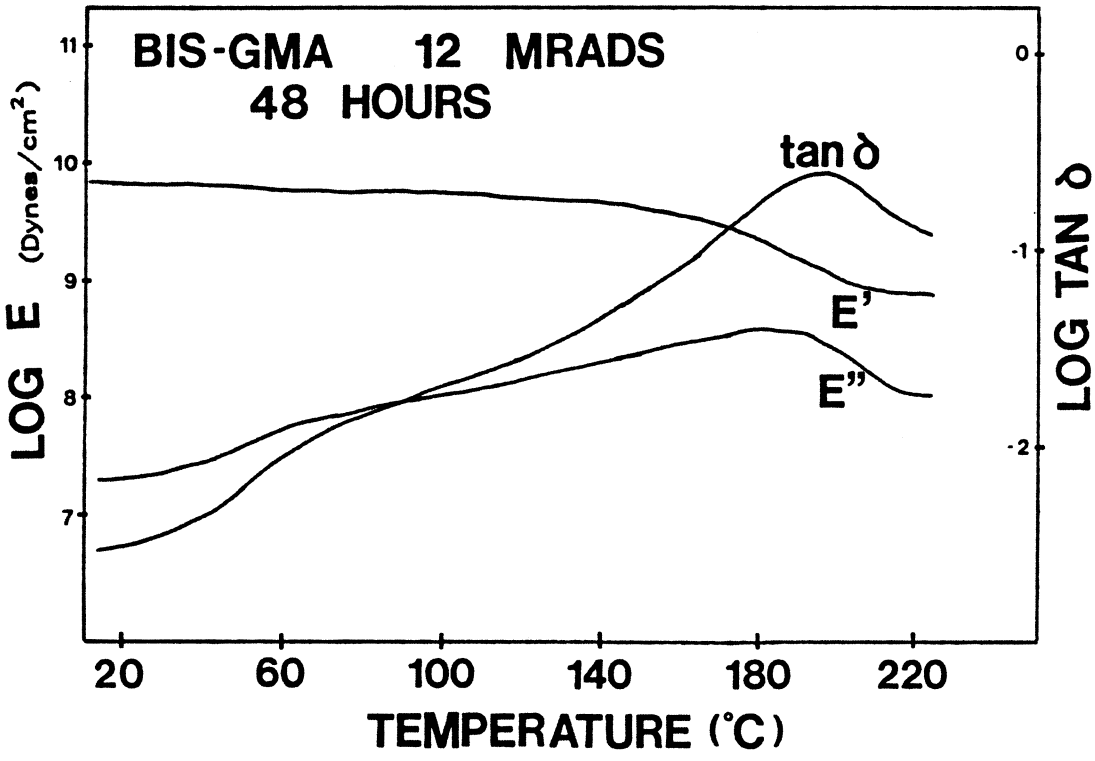

Figure 31. Dynamic Mechanical Temperature Scan for Bis-GMA Irradiated at 12 Mrads and Aged 48 Hours after Cure.: Curves for storage modulus (E'), loss modulus (E"), and tan δ are given. Frequency is 11 Hz and temperature scan rate is 2° C per minute.

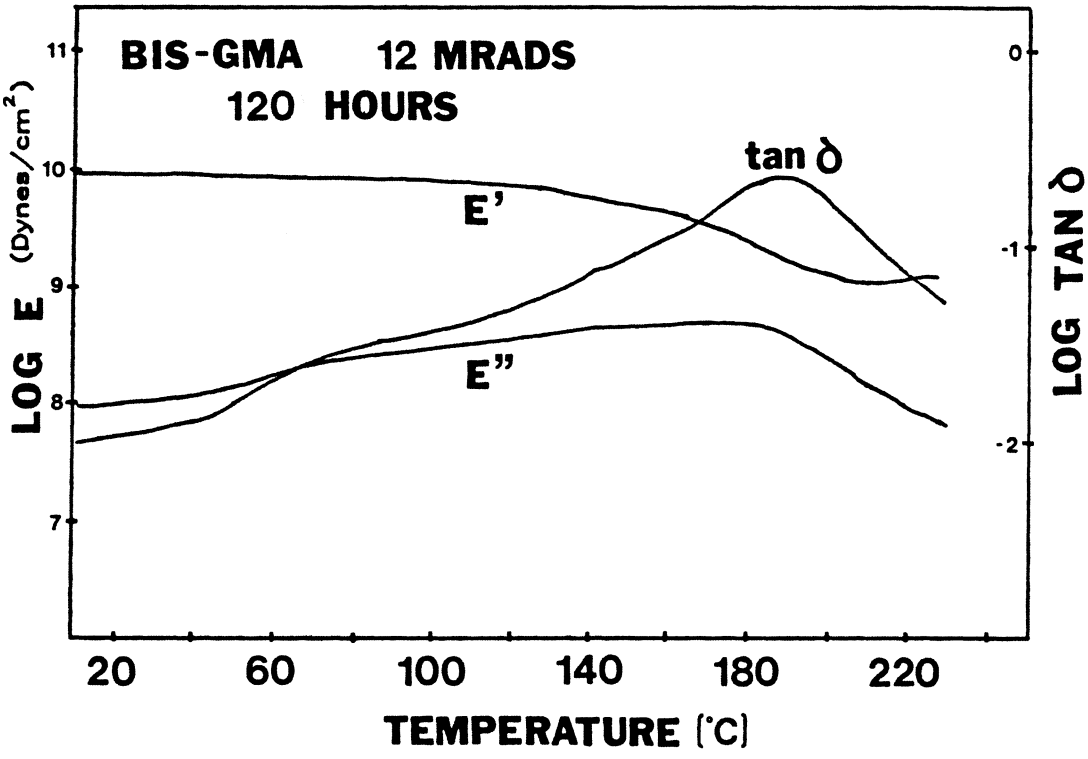

Figure 32. Dynamic Mechanical Temperature Scan for Bis-GMA Irradiated at 12 Mrads and Aged 120 Hours after Cure.: Curves for storage modulus (E'), loss modulus (E"), and tan δ are given. Frequency is 11 Hz and temperature scan rate is 2°C per minute.

at 69°C. The softening point for the a one-hour aged 2 Mrad sample occurs at 135°C (see Fig. 23). After an aging time of 120 hours, as shown in Fig. 30, the softening point exists at 72°C. The T_g as indicated by the tan δ peak occurs at 105°C. This sample physically failed at 110°C, below the normal temperature of a second T_g. For this low dose bis-GMA sample, the softening temperature decreases as aging time after cure increases. In contrast, the glass transition from the tan δ peak increases with time after cure.

The dynamic mechanical results for bis-GMA irradiated at 12 Mrad and aged for 1, 48, and 120 hours are presented in Figs. 25, 31, and 32. Figure 25, previously discussed, gives results for the one-hour aged bis-GMA film. This sample is characterized by T_g's (the tan δ peaks) at 84 and 198°C, with a softening temperature (where $E' = 5 \times 10^9$ dynes/cm^2) of 188°C. The results for the 48 hour aged sample (Fig. 31) show a T_g of 195°C and softening of the modulus at 169°C. The dynamic mechanical plot for the 12 Mrad bis-GMA sample aged 120 hours is given in Fig. 32. It is characterized by a T_g at 191°C and a thermal softening at 173°C. So, the low temperature T_g from dynamic mechanical data at 12 Mrads disappears with aging time, and the high temperature T_g remains fairly constant. However, the softening temperature of the storage modulus decreases with time but the 48 and 120 hour samples are very nearly the same.

Glass transition temperature data are presented in Table 4 for the various aging times. The data can be explained by the idea of a finite lifetime for free radicals in the system. With an aging time of only one hour, many free radicals are present. These radicals may crosslink with other molecules when thermally mobilized, adding more crosslinks and as such, more strength to the coating. With time the radicals recombine or are captured by oxygen, such that there is not as much crosslinking in the system. Thus, the material softens at lower temperatures at long times after cure.

Table 4. Glass Transitions for Bis-GMA at Various Aging Times (Vibron)

AGING TIME *(HOURS)*	GLASS TRANSITION TEMP. *2 Mrad*	*12 Mrad*
1	53	84
48	73	195
120	107	190

3.3.3 Effects of Thermal Annealing

Another variable studied in the DSC experiments with pure bis-GMA systems was annealing temperature. First, a simple rescan of a DSC sample was done. During the first scan, the temperature of the sample was raised from 20 to 200°C at 20°C per minute, then quickly cooled back to 20°C. This scan, along with the rescans for bis-GMA irradiated at 2 and 5 Mrads is shown in Fig. 33. The rescan results are relatively flat, showing none of the exotherms of the first scan. These plots are rather unexciting but are quite helpful in describing the reactions involved. The plots suggest the crosslinking reaction continued above the initial T_g, driving the new T_g near the final temperature of 200°C. Previously unreacted free radicals were cross-linked above the initial T_g (53°C) and above 130°C double bonds were opened by thermal mechanisms.

Another DSC experiment was done to illustrate this point. A bis-GMA film irradiated at 2 Mrad was aged at ambient conditions for two hours. A DSC sample was cut, placed in the instrument, and the following temperature cycle was run:

	Scan range	Onset of T_g
Step 1	20 - 70 °C	42 °C
Step 2	20 - 140 °C	66 °C
Step 3	20 - 200 °C	125 °C

The first cycle is well below the 130°C mark where double bonds are broken by thermal energies (see Fig. 22). As shown in the results of Fig. 34, T_g was found at 42°C during the first scan with an exotherm at 66°C. Also in Fig. 34 is the second DSC scan, which shows an onset of T_g at 66°C. The peak of the exothermic reaction occurs near 90°C. The curve then returned to its linear shape until it reached 140°C. The third DSC scan showed no exotherm until the onset of T_g is reached at 125°C. This peak is broad in comparison to the others. The exotherm

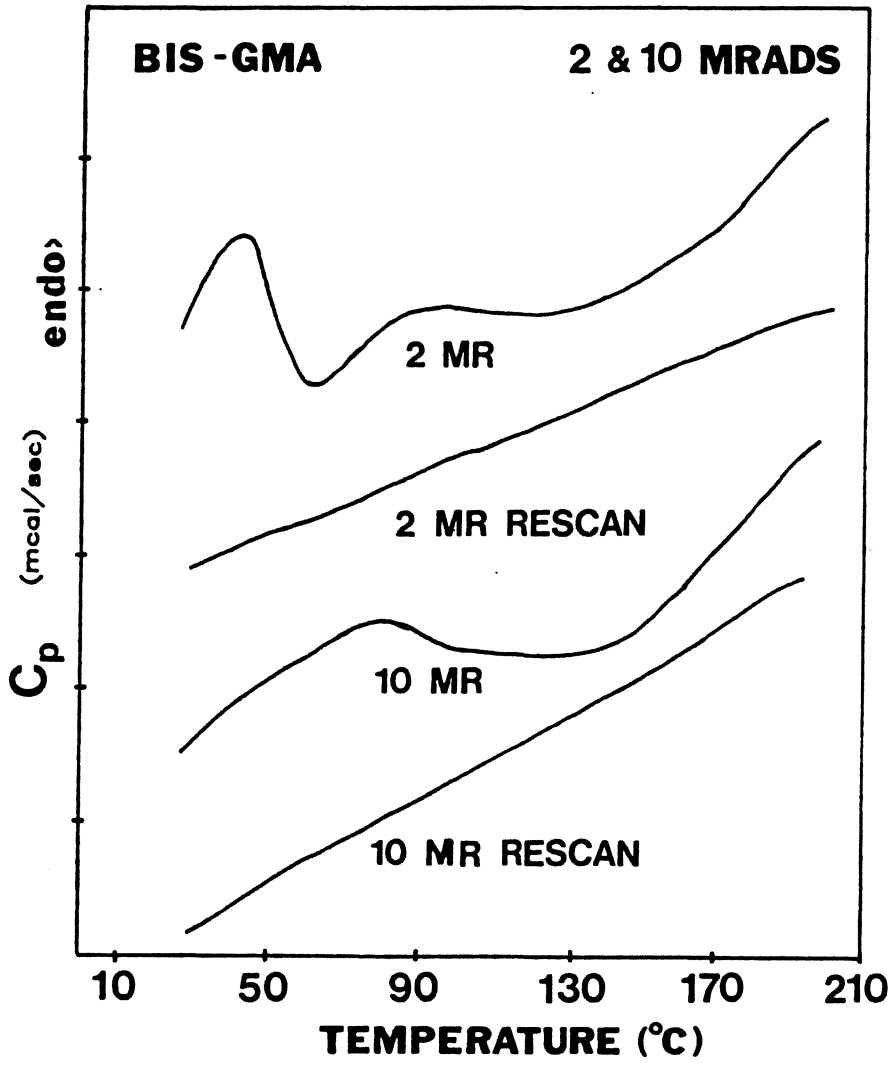

Figure 33. DSC Temperature Scans and Rescans for Bis-GMA Irradiated at 2 and 10 Mrads.: The first scans show an exothermic reaction as the bis-GMA network softens such than reactive species gain mobility and continue the crosslinking reaction. Rescans do not show these exotherms.

reaches a maximum at 160°C. The temperature during the third scan is high enough to open any residual double bonds to essentially complete the crosslinking reaction. Although the transitions do not correspond exactly to the highest temperature from the previous step (70 and 140°C), the trends clearly confirm the continued crosslinking reaction at temperatures above the previous T_{cure}.

In order to verify these trends, a similar experiment using FTIR was done to look at residual double bonds for annealed samples of irradiated films. Coatings of bis-GMA were irradiated at a dosage of 2 Mrads. Annealing was done for 5 minutes at temperatures of 70, 140, and 200°C, in hopes of repeating the DSC annealing as closely as possible. Results are tabulated in Table 5. As predicted by the exothermic reactions in the DSC experiment (Fig. 34), percent double bonds are reduced by the annealing at higher temperatures.

An attempt was made to correlate the heat of reaction data with the residual double bond data. Heats of reaction were determined from the areas of the exothermic reaction shown on the DSC curves. The heat of reaction was also calculated from the residual double bond data by determining the number of double bonds reacted per unit volume, and multiplying this by the heat of reaction for a methacrylate group (13 kcal/mol). This method is discussed in Chapter 1 and sample calculations are given in Appendix A. Heat of reaction values are given in Table 6. Although the values for the first two temperature ranges do not correlate well, the 20-200°C scan gives 14.2 and 17.2 cal/g for the DSC and calculated values respectively. This correlation is quite good. The DSC values from the lower temperature studies were too low because the crosslinking reaction in the bis-GMA can continue even after the 70 or 140°C temperature is reached. The DSC curve stops exactly at 70 and 140°C in the two steps, and the area under the curve is taken only to that point. In contrast, the residual double bond test is done after the reaction such that only double bonds remaining after the crosslinking reaction are considered to be residual double bonds. This test also assumes all opened double bonds react in the crosslinking reaction, which could yield ΔH values that are slightly high. In the 20-200°C scan, almost all of the double bonds were opened to participate in the cross-

Table 5. Percent Residual Double Bonds for Annealed Bis-GMA

SAMPLE	ANNEALING (°C)	PERCENT DOUBLE BONDS
bis-GMA 2 MR	none	42.9%
bis-GMA 2 MR	70°C, 5 min	17.0%
bis-GMA 2 MR	140°C, 5 min	10.0%
bis-GMA 2 MR	200°C, 5 min	9.1%

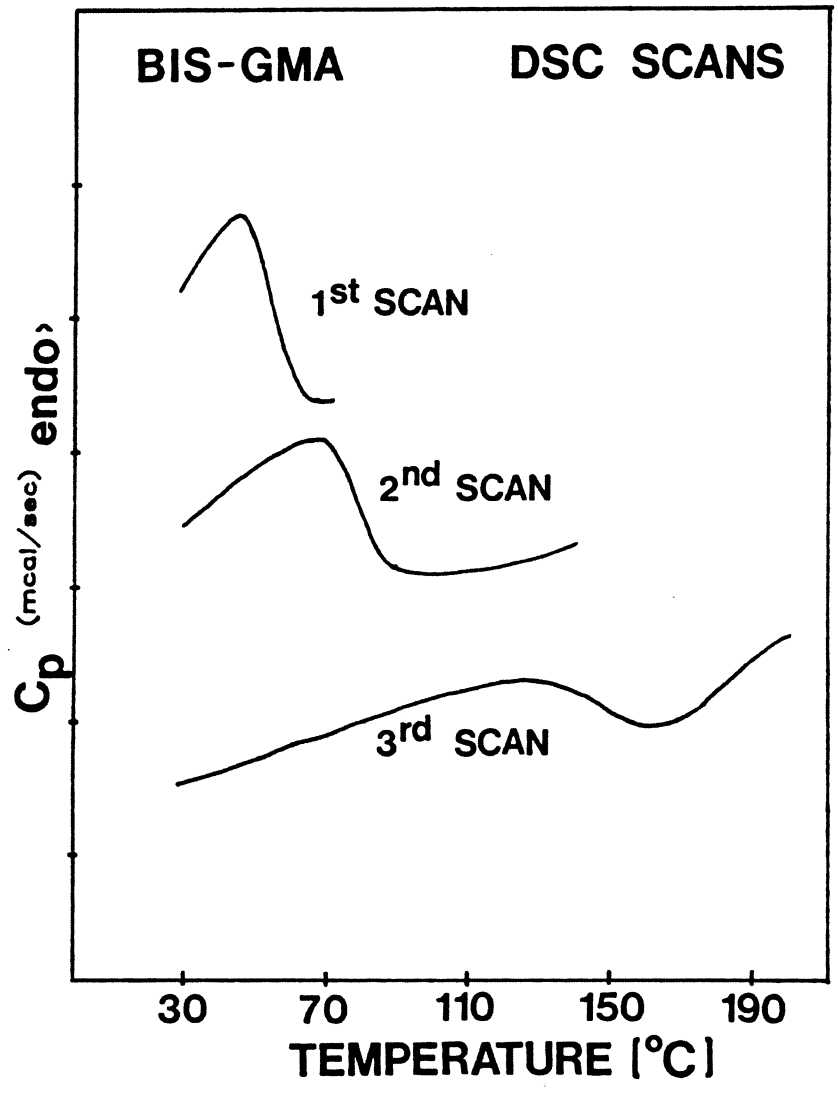

Figure 34. DSC Temperature Cycle Run on Bis-GMA Irradiated at 2 Mrads.: The bis-GMA sample was aged one hour after cure. The following temperature cycle was run; 20-70°C, 20-140°C, 20-200°C. The DSC scan rate was 20°C per minute, and cooling rate was 320° C per minute.

linking reaction, so there were very few reactions after the 200°C temperature was reached. This is the reason for the much better agreement with the ΔH value calculated from residual double bond content.

Dynamic mechanical tests were also run to study the effects of thermal annealing on irradiated bis-GMA networks. Figure 35 shows the results of a 2 Mrad sample annealed at 150°C for 30 minutes. The storage modulus (E′) is linear until it reaches the annealing temperature of 150°C, where a sharp decline occurs. The log tan δ curve has a rather curious peak at 115°C, followed by a more characteristic peak at 194°C. These T_g's are quite a bit higher than those from Fig. 23 for 2 Mrad cure with no annealing (53 and 161°C). As shown here and by the DSC results just discussed, the thermal annealing raises the temperature of the bis-GMA film sample above T_g such that the chains are mobilized and the crosslinking reaction continues.

3.3.4 Effects of Dose Rate vs. Dose per Pass

A final set of experiments was done to look at varying dose rate and dose per pass. Dose rate was varied by changing the line speed and electron beam current proportionally to give the same total dosage. Line speeds run were 20, 40, 60, 80, and 100 feet per minute. Current was varied from 1.2 mA at 20 fpm to 7.5 mA at 100 fpm to keep total dosage constant at 5 Mrad. The dose per pass experiment was done for 5 Mrad total dose. One sample was run five passes at one Mrad per pass, compared to a one-pass sample radiated at 5 Mrads. Each pass takes about 10 seconds to run, such that the five pass process was done over a time period of almost one minute.

Table 7 lists the results of residual double bond tests and glass transitions from DSC for the dose rate experiments. Percent double bonds from FTIR experiments ranged from 46 to 50%, well within experimental error. The DSC thermograms for the five line speeds are sketched

Table 6. Heats of Reaction for Bis-GMA (2, 5, and 12 Mrad)

ANNEALING TEMPERATURE	ΔH (DSC) (cal/g)	ΔH (CALC) (cal/g)
20-70°C	2.5	13.2
20-140°C	5.8	16.7
20-200°C	14.2	17.2

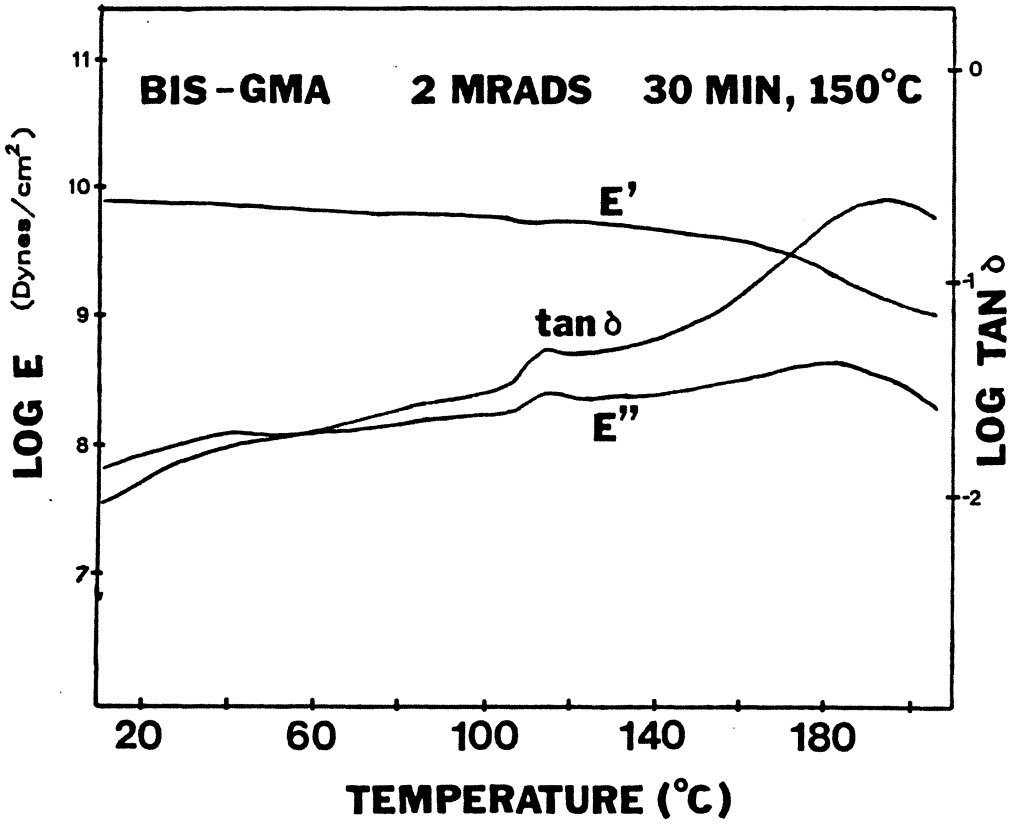

Figure 35. Dynamic Mechanical Temperature Scan for Bis-GMA Irradiated at 2 Mrads and Annealed 30 Min. at 150°C.: The sample was irradiated, then placed in an oven for 30 minutes at 150°C. The frequency of the vibron shown is 11 Hz, and the temperature scan rate is 2°C per minute.

in Fig. 36. The glass transition temperatures ranged from 47 to 50°C, again showing no differences. The T_g's here are lower than the values for pure bis-GMA given earlier. This was due to a higher oxygen concentration (near 3000 ppm) than in earlier runs, inhibiting the crosslinking reaction, especially on the surface. The previous runs had oxygen concentrations below 1100 ppm. Dose rate seems to have little effect on crosslinking, as the data show no significant trends.

Table 8 lists the residual double bonds and T_g values for the dose per pass experiments. In contrast to the dose rate tests, the differences are quite pronounced. First, the five-pass sample had 6.5% higher residual double bond content than the one-pass film. This suggests less crosslinking occurred when irradiation is done in a multi-pass process. The corresponding onset of T_g from the DSC experiment was 26°C lower for the five-pass sample, supporting the results from FTIR tests. The two DSC scans are plotted in Fig. 37. The difference in T_g's from the dynamic mechanical tests was only 5°C, but it showed the same trend. Figure 38 gives the Vibron temperature scan for a 5 pass process, which may be compared to the one-pass film in Fig. 24.

The difference in the variables of dose rate and dose per pass can be explained in terms of the temperature rise during cure discussed in Chapter 1. A one-pass process receives all the electron energy in a short time interval, such that the maximum cure temperature is higher than achieved in a multi-pass process. This leads to a higher glass transition temperature and more crosslinking can occur before diffusion limitations are reached. However, the dose rate experiments do not show these differences. Since all of the experiments were done in one pass, the heat of crosslinking was experienced at one time. The times under the electron beam were different, but only by a factor of 5 (20 fpm to 100 fpm). At 100 fpm, the residence time under the electron beam was 0.3 seconds. At 20 fpm the residence time was 1.5 seconds. Since the polymer network is organic, it is a poor heat transfer agent. So, the heat from the reaction remains in the material long enough that the differences in residence time are not important.

Table 7. Residual Double Bonds and Tg for Bis-GMA at Varying Dose Rates

SPEED (fpm)	DOSE RATE (Mrad/sec)	% DB --FTIR (%)	T_g (DSC) (°C)
20	3.3	50.0	48
40	6.7	46.5	48
60	10	·	50
80	13.2	47.4	47
100	16.7	45.1	50

Table 8. Double Bonds and Tg for Bis-GMA at Various Dose per Pass

PASSES	% DB	Tg (DSC)	Tg (Vibron)
5 passes 1 MR	57	42	48
1 pass 5 MR	51	68	53

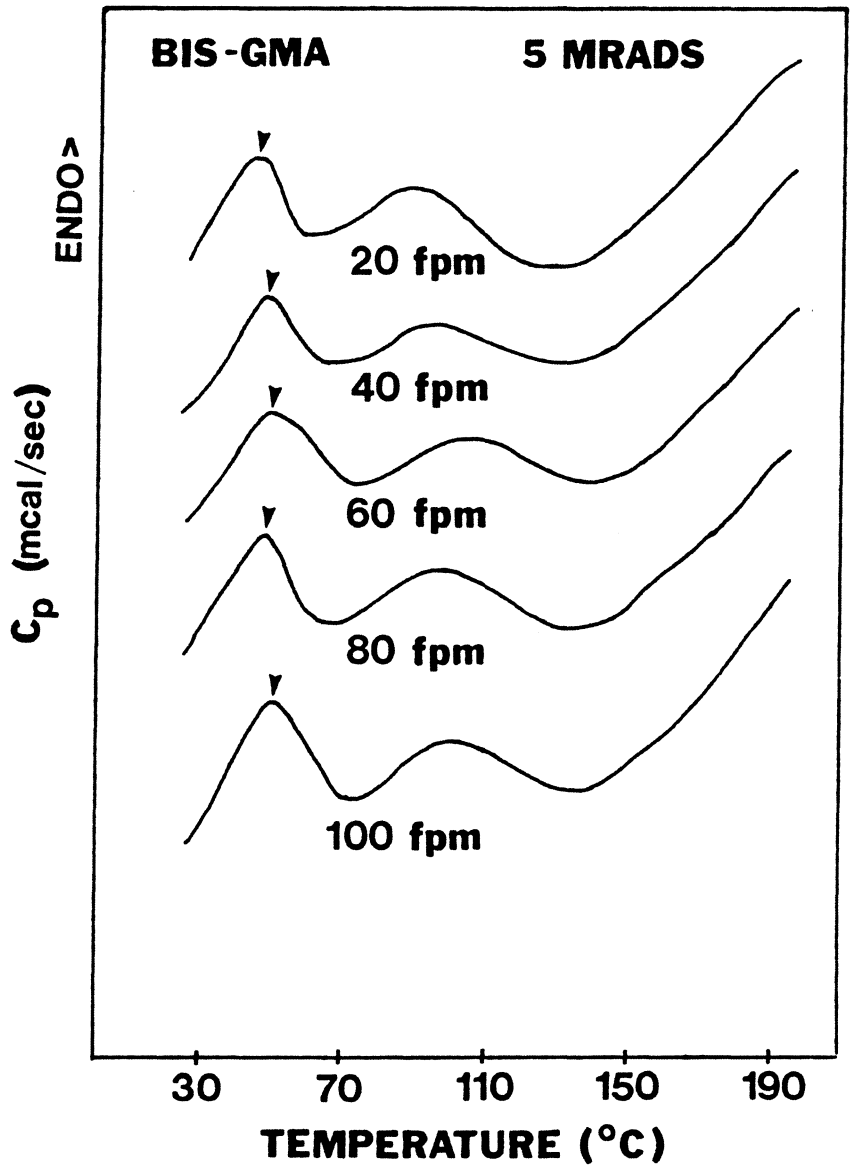

Figure 36. DSC Scans for Bis-GMA Irradiated at Various Dose Rates, with Total Dosage Being 5 Mrads.: Line speeds and electron beam intensity were varied proportionally to give a constant total dosage at different dose rates. Line speeds are listed above, and the DSC scan rate is 20° per minute.

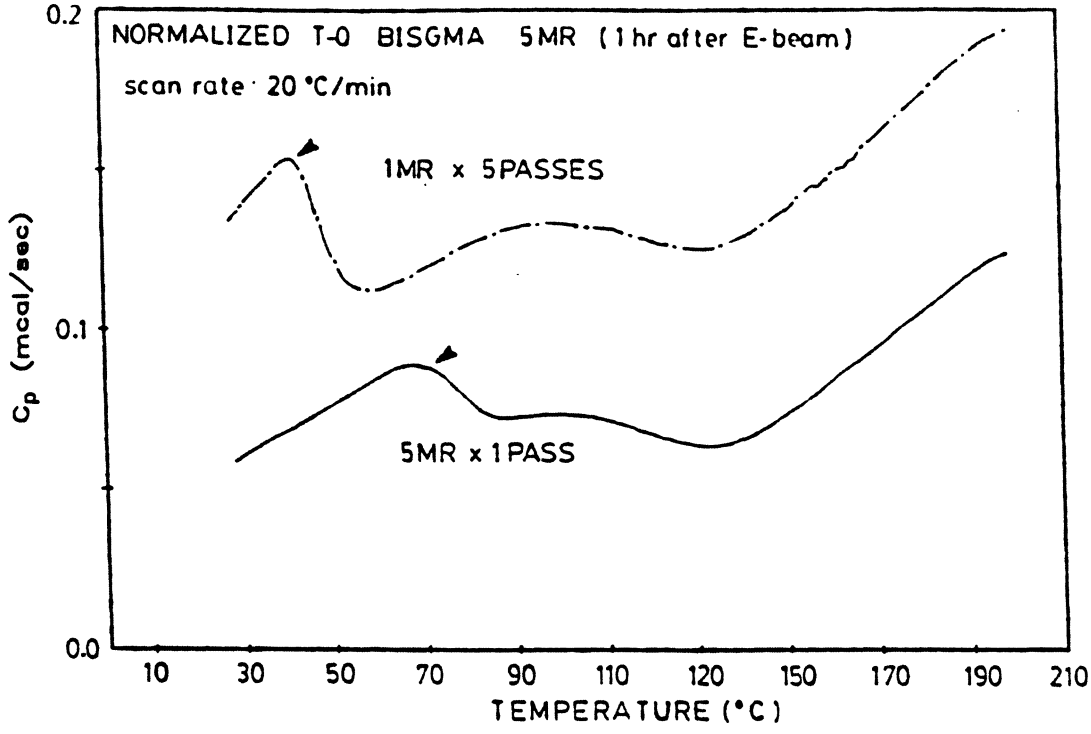

Figure 37. DSC Scans for Bis-GMA Irradiated at 5 Mrads Total Dose (One-pass vs. Five-pass Process).: DSC temperature scans are presented for bis-GMA samples irradiated 5 Mrads (one pass) and five passes at one Mrad per pass. Scan rate in the DSC is 20°C per minute.

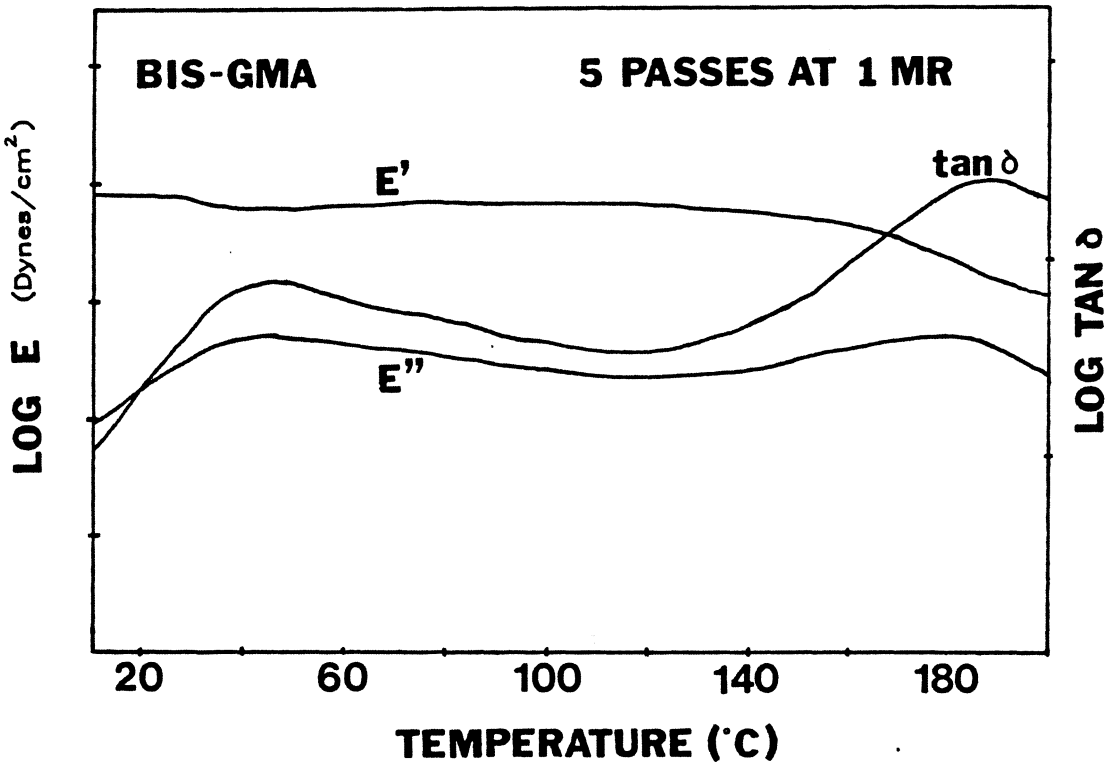

Figure 38. Dynamic Mechanical Temperature Scan for Bis-GMA Irradiated Five Passes at 1 Mrad per Pass.: The data from the curves may be compared to the one-pass process given in Fig. 24. Scan rate is 2°C per minute.

3.4 *Conclusions from the Bis-GMA Studies*

A number of conclusions can be made concerning the bis-GMA systems. First, as shown by Charlesby [15] and others [37,38] for other polymeric systems, the degree of crosslinking increases with dose up to some critical dose. This was determined by percent gels, which increased as dosage increased, and residual double bond content, which decreased as dosage increased. Swelling ratio was also investigated, in a manner similar to the percent gels test. The decrease in swelling ratio as dosage increases indicates a higher crosslink density occurs at higher dosage. In addition to the degree of crosslinking, the glass transition temperature tends to increase with dose. As explained before in terms of the TTT diagram (see Fig. 11) T_g depends on the curing temperature, which undergoes a thermal spike upon irradiation. The temperature increase is due to the heat of the exothermic crosslinking reaction and energy transfer from the source electrons. A higher irradiation dose gives more energy to the coating which adds more to the temperature increase. This effect is compounded by the fact that more free radicals are formed which leads to increased crosslinking.

Time after cure is another important variable in these radiation cured bis-GMA systems. Free radicals which are trapped in the glassy matrix have a finite lifetime, so the physical properties can change quite dramatically as these radicals are deactivated. Since many of the radicals are depleted by oxygen scavengers (from the dry air in the dessicator) or find a lower energy state in the molecules, they are no longer available to contribute to crosslinking if thermally mobilized (as in the DSC or dynamic mechanical experiments discussed earlier).

A third variable studied in this work is that of annealing at higher temperatures after EB cure. At relatively short aging times after cure, annealing at higher temperatures can thermally mobilize free radicals which can continue the crosslinking reaction. More crosslinking increases T_g, eventually driving T_g up to the temperature of annealing. This was shown from the DSC and dynamic mechanical data. If the annealing temperature is above 130°C, additional crosslinking takes place as remaining double bonds are opened by thermal energy.

The final variable studied in this matrix of experiments is the effect of dose rate on the crosslinking reaction. For the range of dose rates investigated here, dose rate does not greatly affect the physical properties of irradiated bis-GMA, provided all other factors are constant. However, a multi-pass process can yield a less crosslinked material than a single pass process of the same total dosage. The difference is due to the higher thermal spike which occurs during the one-pass process.

4.0 Bis-GMA/TEGDMA and Bis-GMA/PEGDA Mixtures

4.1 Introduction

The purpose of this chapter is to discuss the effect of adding flexible modifiers to the bis-GMA to form binary systems. The binary systems were coated onto PET and irradiated by electron beam just as the bis-GMA was done as previously discussed. The mixtures were homogeneous, as a clear, one-phase solution was maintained for weeks at room temperature. The components making up these mixtures were not stored at room temperature, but were kept in a refrigerator at about 5°C. New mixtures were made for subsequent EB crosslinking experiments from these components. Many of the same tests were performed on these systems as were previously described in Chapter 3 for pure bis-GMA systems (percent gel, residual double bonds, DSC, and dynamic mechanical). Most of the effort has gone to quantify the extent of crosslinking through the percent gels and FTIR tests. The effects on T_g as seen through DSC and dynamic mechanical measurements are shown for selected compositions only.

This discussion will key on three parameters. First is the irradiation dosage, already shown to be important from the work with bis-GMA. Second, composition will be varied systematically to investigate its effects on bis-GMA. Finally, an acrylate-capped material as well as a methacrylate- capped modifier will be compared. Triethylene glycol dimethacrylate (TEGDMA) is the methacrylate-capped species which will be mixed with bis-GMA. It has a viscosity of 7.5 centipoises (cp) at 25°C. The acrylate is polyethylene glycol diacrylate (PEGDA), which has a viscosity of 50 cps at 25°C. Since bis-GMA is the featured material in

this study, most of this author's effort will be directed to relatively small weight fractions of the modifier materials.

4.2 Extent of Crosslinking Reaction

4.2.1 Percent Gels

Percent gel tests were run for a number of the binary mixtures. Figure 39 is a plot of percent gels vs. irradiation dose for bis-GMA/TEGDMA mixtures containing 15, 30, and 50 percent TEGDMA. From Fig. 39 it can be seen that percent gel increases as dose increases until an upper limit is reached. The 15 and 30% TEGDMA resemble the results for pure bis-GMA. That is not surprising since bis-GMA is the main component in these systems. However, the 50% TEGDMA only reaches 60% gel content even at 12 Mrads dosage. Coatings of 100% TEGDMA (no bis-GMA) did not form a solid gel at all after irradiation, but remained in the liquid state even at dosages up to 30 Mrads (a multiple pass process). The data suggests that TEGDMA does not crosslink sufficiently to form a solid via electron beam irradiation. This seems a bit peculiar, especially in light of the ease of crosslinking in thermally initiated systems which contain bis-GMA and TEGDMA detailed in references 22, 26, and 27. More discussion will be given later in an effort to explain this phenomenon. Percent gels are plotted vs. irradiation dose in Fig. 40 for the bis-GMA/PEGDA systems. The 15 and 100% PEGDA systems have nearly 90% gels with dosages as low as 2 Mrads. The 50% PEGDA reached 90% gels at 5 Mrads dose. There does not seem to be a significant pattern to this data for the matrix of compositions. In any event, it is evident that all of the PEGDA/bis-GMA systems crosslink readily with radiation to form a solid gel.

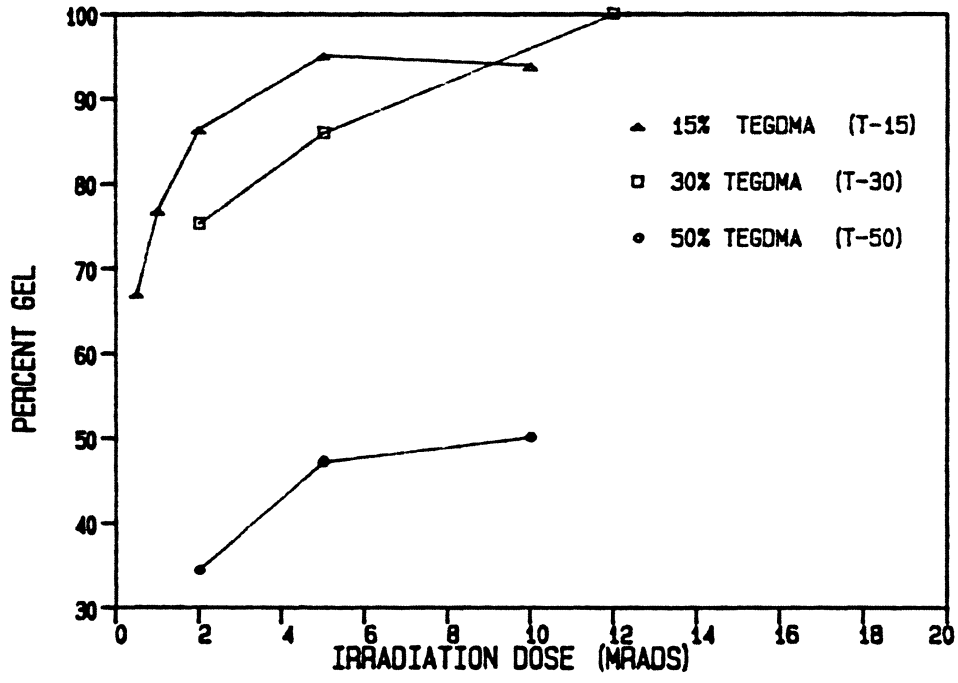

Figure 39. Percent Gel vs. Irradiation Dose for Bis-GMA/TEGDMA Mixtures.: Percent gel content is given for 15, 30, and 50% TEGDMA mixtures, at dosages from 0.5 to 12 Mrads.

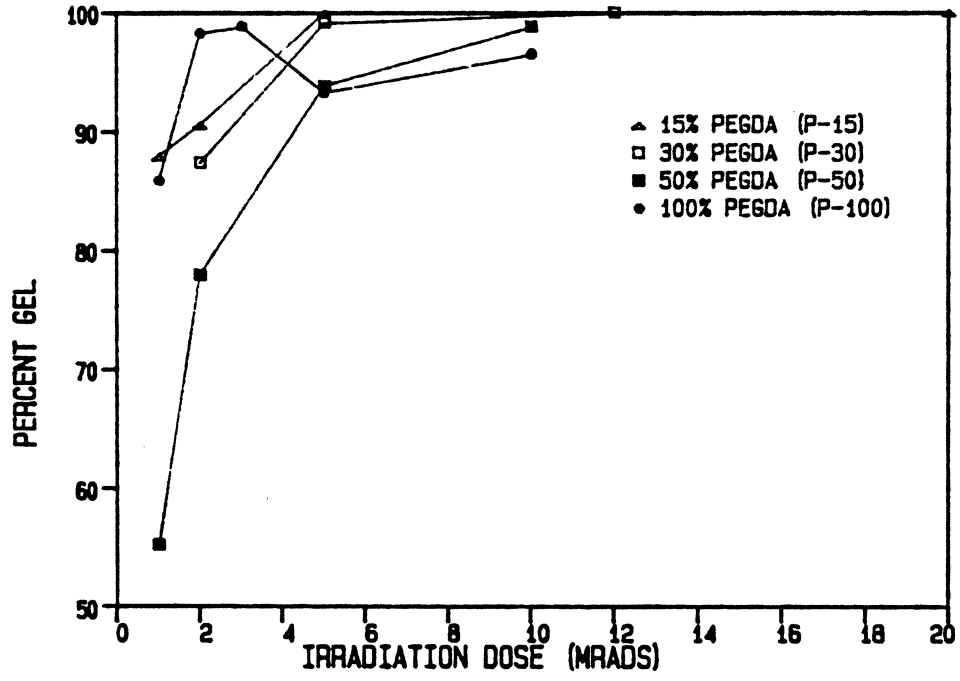

Figure 40. Percent Gel vs. Irradiation Dosage for Bis-GMA/PEGDA Mixtures.: Percent gel is determined from swelling in acetone for 15, 30, 50, and 100% PEGDA mixtures. Dosages range from 1 to 20 Mrads.

4.2.2 FTIR--Residual Double Bond Content

Residual double bond content was also determined for the various binary mixtures. Table 9 lists the percent residual double bonds for the different compositions at 2, 5, and 12 Mrad irradiation. For the most part, percent double bonds decrease as dosage increases. These values are plotted in Figs. 41 and 42 for the different compositions of TEGDMA and PEGDA mixtures respectively. For the TEGDMA/bis-GMA mixtures (Fig. 41), the 15 and 30% TEGDMA have lower double bond content than pure bis-GMA. This difference is mainly due to the lower viscosity provided by the TEGDMA component. More reactions can occur before diffusion limitations are reached. At 50 and 100% TEGDMA, double bond content is higher than for pure bis-GMA, as the poor reactivity of the TEGDMA component dominates. It appears there is an optimum concentration for the lowest residual double bond content at a composition between 15 and 30 weight percent TEGDMA. At this percentage of TEGDMA, the viscosity is lowered so that diffusional limitations are not reached as quickly, yet not enough that many more crosslinking reactions are necessary to form a gel from the TEGDMA component.

Figure 42 gives residual double bond content for bis-GMA/PEGDA mixtures. Compositions of 0, 15, 30, and 100% PEGDA by weight are shown. Looking at the 15 and 30% PEGDA mixtures (P-15 and P-30), double bond content was found to be lower than that for pure bis-GMA, and slightly lower than the 15 and 30% TEGDMA mixtures from Fig. 41. The 100% PEGDA did not totally follow the pattern set by the lower percentage PEGDA irradiated films. Since the pure PEGDA contains no aromatic groups, the FTIR data could not be normalized by the phenyl ring peak. Thus, a methyl group peak (1369 cm^{-1}) was used for normalization of this sample.

Some comparison of the percent gel and residual double bond data is in order. First, the TEGDMA/bis-GMA data will be investigated. At low dosage (2 Mrads) the percent gel values for the 0, 15, and 30% TEGDMA mixtures is in the range of 75 to 86% gels. Residual double

Table 9. Residual Double Bonds for Binary Mixtures at 2,5,and 12 Mrads

SAMPLE	RESIDUAL DOUBLE BONDS --FTIR(%)		
	2 MR	5 MR	12 MR
bis-GMA	55.1	43.0	30.2
T-15	48.5	39.9	21.6
P-15	50.2	26.3	19.8
T-30	50.6	37.6	21.7
P-30	47.7	19.3	6.6
T-50	60.2	79.1	50.0
P-50	50.9	18.6	4.7
T-100	97.3	99.8	95.3
P-100	34.9	12.3	10.6

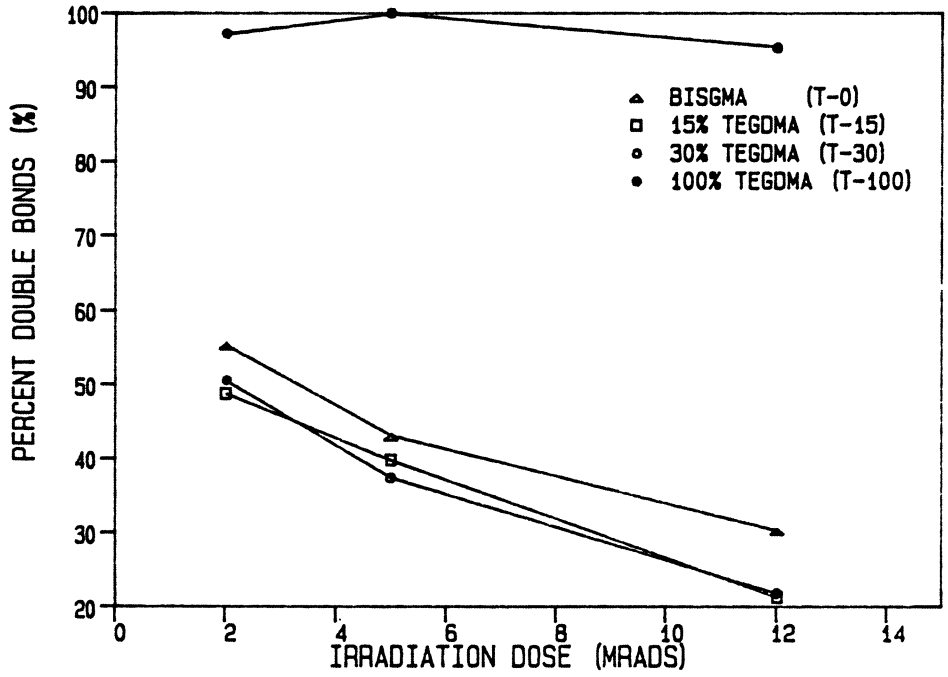

Figure 41. Percent Residual Double Bond Content for Bis-GMA/TEGDMA Mixtures at Different Irradiation Dosages.: Residual double bond content is shown for bis-GMA as well as 15, 30, 50, and 100% mixtures with TEGDMA.

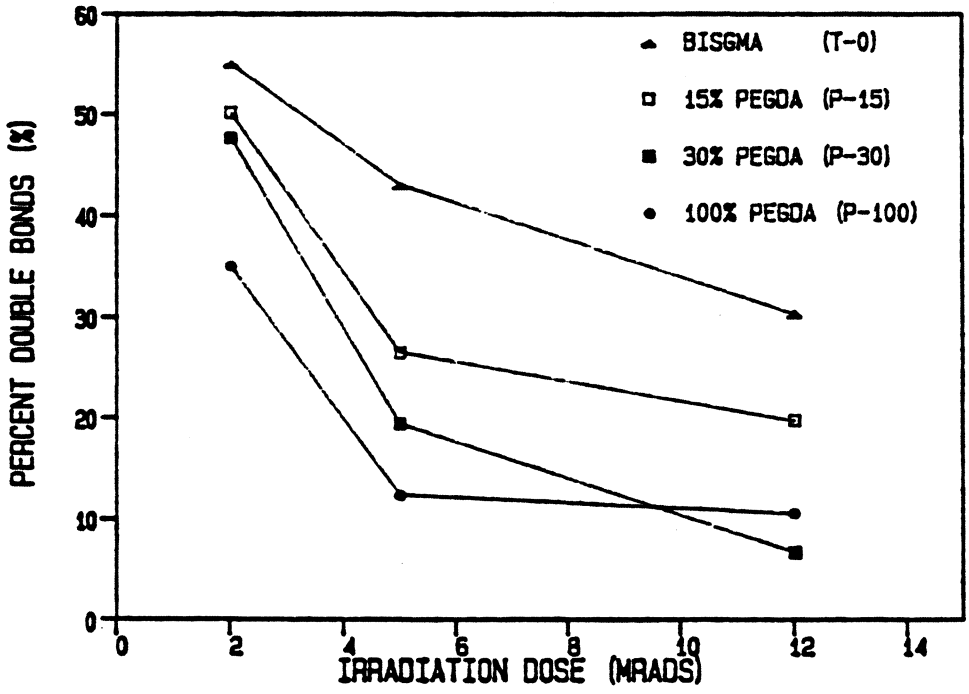

Figure 42. Percent Residual Double Bond Content for Bis-GMA/PEGDA Mixtures at Different Irradiation Dosages.: Residual double bond content is shown for bis-GMA as well as 15, 30, and 100% PEGDA mixtures.

bond content ranges from 48 to 55% for these samples. Specifically the values are as follows for the 2 Mrad samples

	Percent Gels	Residual Double Bonds
bis-GMA	82%	55%
15% TEGDMA	86%	48%
30% TEGDMA	75%	50%

It is expected that the highest percent gel value should correspond to the lowest residual double bond content, and the sample with the lowest gel value should have the highest residual double bond content. This is confirmed for the former case (15% TEGDMA) but not for the latter case (30% TEGDMA). Although the trends are not totally confirmed, the values seem reasonable in light of the experimental error of each test (up to 7% error for each test). A complicating factor which could be quite real is that crosslinks could occur in places other than at the double bond end groups. This could help explain the seemingly high values for double bond content.

At the high dosage (12 Mrads) the following data are found for the bis-GMA and TEGDMA/bis-GMA samples

	Percent Gels	Residual Double Bonds
bis-GMA	95%	43%
15% TEGDMA	94%	40%
30% TEGDMA	87%	37%

Again the 30% TEGDMA has a lower percent gel value and a lower double bond content. This inconsistency suggests that chain scission could be occurring during irradiation in the TEGDMA.

In order to confirm or refute this speculation of chain scission, intrinsic viscosity was run on a pure TEGDMA liquid irradiated at 10 Mrads and a control TEGDMA which was not irradiated. Viscosity for the 10 Mrad sample at 28°C was 0.029 centipoise (cp), three times the 0.008 cp value for the control sample. These results suggest that crosslinking takes place in the TEGDMA samples, but it is not sufficient to form a gel. This does not rule out the occurrence of chain scission, but does indicate that more crosslinking reactions occur than chain scissions. Gel permeation chromatography (GPC) was also performed on these two samples, but results were inconclusive because the molecular weight of TEGDMA (286 g/mol) was too close to the solvent (THF at 68 g/mol).

From the PEGDA/bis-GMA systems discussed in Figs. 40 and 42, the comparisons for the percent gel and percent residual double bonds can be made. At an irradiation dosage of 2 Mrads percent gels ranged from 84 to 97%. Residual double bonds for these samples ranged from 34 to 51%. These values correlate well, as the 97% gel for pure PEGDA corresponds to the lowest double bond content at 34%. Similarly, the lowest percent gel sample (50% PEGDA at 84% gels had the highest residual double bond content (51%). The composition variable does not seem to follow any general trends at high concentrations of PEGDA. In general, the PEGDA component facilitates the crosslinking reactions because it reduces the system viscosity and it provides a higher density of double bonds. In addition, these double bonds are acrylate species rather than the methacrylate species from TEGMDA. The acrylates are more reactive in these EB cured systems than similar methacrylates. Moreover, the heat of polymerization is higher for the acrylate species than the methacrylate groups. Flory [39] gives the heat of polymerization as 18.7 kcal/mol for methyl acrylate, but only 13 kcal/mol for methyl methacrylate. Since these end groups are attached to a long chain rather than a methyl group, these figures may not be precise but they would certainly be relative. It is worth

mentioning here that the irradiated PEGDA films were quite hot to the touch when removing the samples from the electron beam chamber (approximately 5 seconds after EB cure). The TEGDMA/bis-GMA systems did not feel nearly as warm as PEGDA. This is due to the higher reactivity and higher heat of polymerization of the acrylate groups. The percent gel values for the bis-GMA/PEGDA systems are all in the 80 to 100% range. There is more variability (at least from a percentages standpoint) in the residual double bond data. The trend at low concentrations of PEGDA is that more crosslinking occurs as PEGDA content increases. At higher concentrations, the trends are a bit more difficult to distinguish. From the FTIR data (Fig. 42) the 100% PEGDA has residual double bond values between the higher values at 50% PEGDA and the very low values at 90% PEGDA.

4.3 Glass Transition Behavior via DSC

DSC temperature scans were run for 15% TEGDMA/85% bis-GMA and 15% PEGDA/85% bis-GMA by weight. Figure 43 gives the temperature scans from DSC for the TEGDMA/bis-GMA systems irradiated at 1, 2, 5, and 15 Mrads. These plots follow many of the same trends as shown earlier for pure bis-GMA in section 3.1.2 (see Fig. 21). The 1 and 2 Mrad samples each have onsets of T_g at 45 and 49°C respectively, followed by another exothermic reaction beginning at 90°C. The 5 and 15 Mrad scans display onset of T_g at 85 and 95°C, quite a bit higher than the pure bis-GMA results of Fig. 21. The exotherm at 130°C appears for all samples. As shown in Chapter 3 for pure bis-GMA, this peak is the result of free radicals that must be highly mobilized to find other reactive species and thermal opening of double bonds. The magnitude of this exothermic peak tends to increase with dose.

Figure 44 shows the PEGDA/bis-GMA DSC results. The values for onset of T_g for the 2, 5, 10, and 12 Mrad samples are 96, 97, 98, and 98°C respectively. Taking scan rate and experimental error into account, it is difficult to call these differences in T_g significant. However, it is sig-

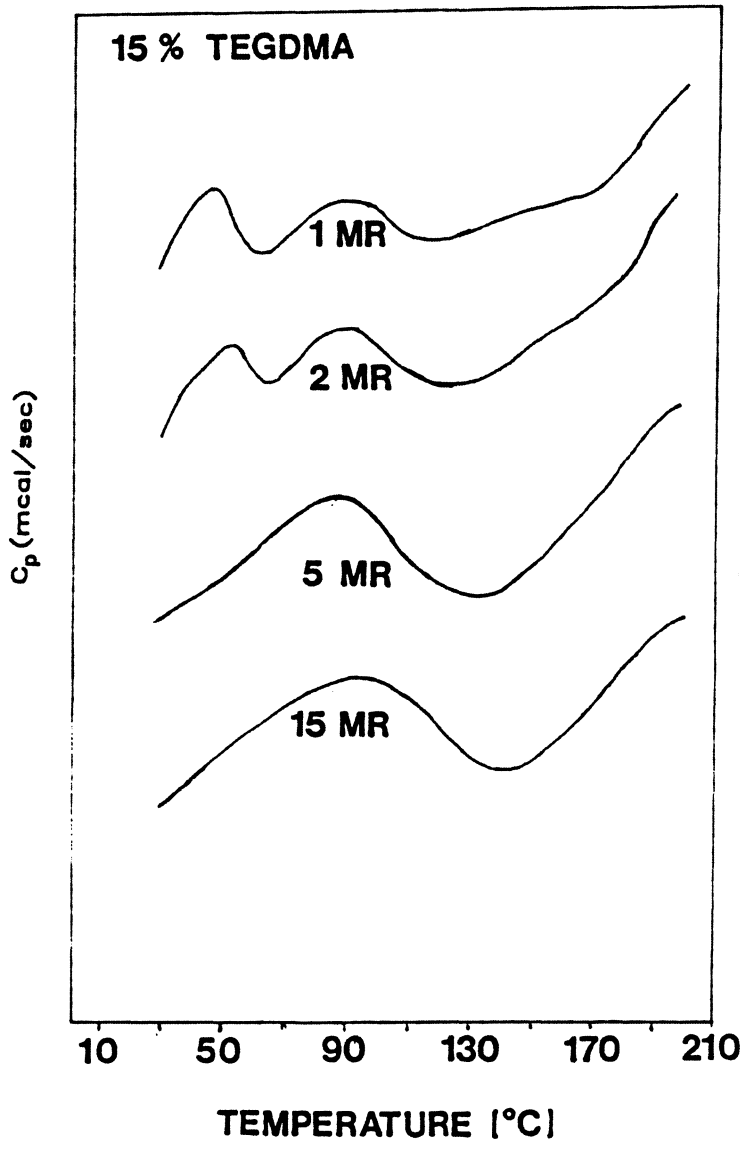

Figure 43. DSC Temperature Scans for 15% TEGDMA/ 85% Bis-GMA Irradiated at 1,2,5, and 15 Mrads.: The DSC scan rate was 20°C per minute and aging time was one hour after cure.

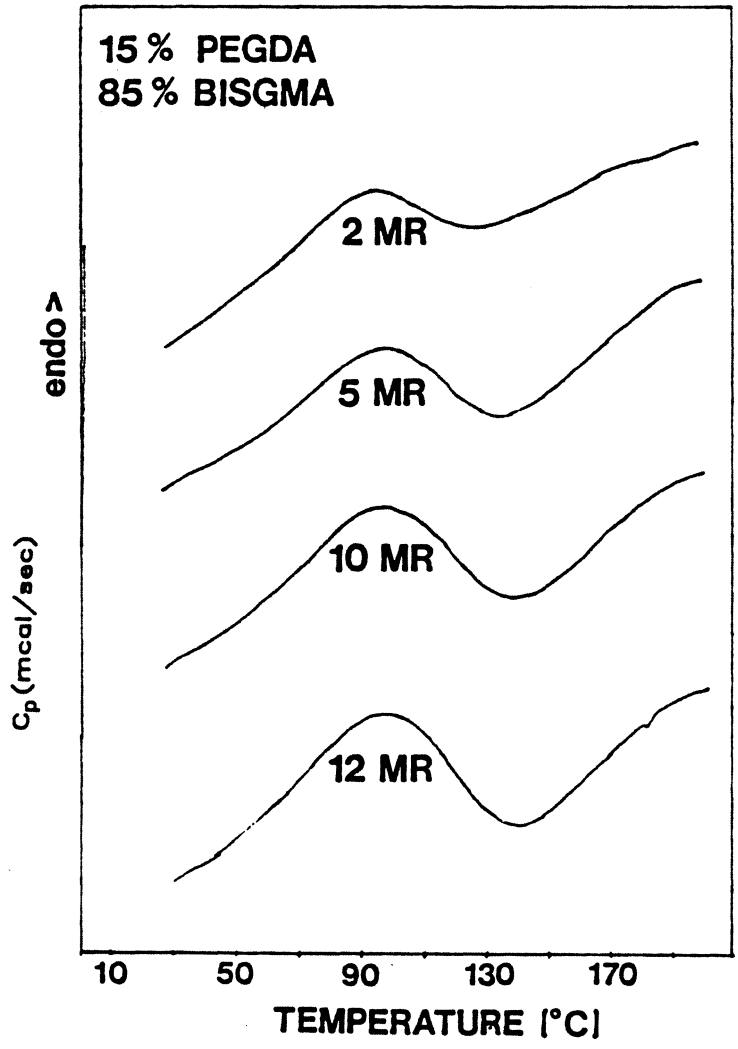

Figure 44. DSC Temperature Scans for 15% PEGDA/ 85% Bis-GMA Mixtures Irradiated at 2, 5, 10, and 12 Mrads.: DSC scan rate was 20°C per minute and aging time was one hour after cure.

nificant that these scans are quite different than those for the TEGDMA/bis-GMA system (Fig. 42). The 2 and 5 Mrad samples do not contain the T_g at 40-50°C present in the TEGDMA/bis-GMA sample results. This data confirms the earlier finding that acrylate groups are more reactive than the analogous methacrylate groups. One reason for this fact is the methyl group extending from the double bond prevents the crosslinking reaction due to steric hindrances (i.e., the radicals are less likely to find the appropriate double bond or other free radicals). Another factor that makes the PEGDA (as well as TEGDMA) reactive is its short chain length compared to bis-GMA, which gives these two species a higher density of double bonds than bis-GMA. The crosslinking reaction is essentially a chain reaction (a radical bonds with a double bond to form a crosslink and another free radical which reacts further). In addition, the PEGDA performs a similar function to TEGDMA in that it reduces the viscosity of the system with bis-GMA. Also mentioned before in this chapter is the higher exothermic heat of reaction of acrylates than analogous methacrylates. From all of the influences mentioned above, the PEGDA is reactive enough that it continues the crosslinking reaction once it is initiated. In this manner, the crosslinking reaction is not as dependent on dosage as the TEGDMA/bis-GMA mixture.

4.4 Conclusions from Low Molecular Weight Modification Studies

A number of conclusions were made for the binary systems containing bis-GMA and TEGDMA or PEGDA. They can be summarized as follows:

1. Percent gels increase with dose up to a critical dose. A dosage of 5 to 10 Mrad seems sufficient to crosslink the systems mentioned thus far. This is similar to the results for bis-GMA discussed in Chapter 3.

2. Percent residual double bonds decrease as dosage increases. An exception to this was found for the 100% TEGDMA system which did not crosslink to form solids. Residual double bonds were in the 90 to 100% range for all dosages of the 100% TEGDMA samples.

3. Glass transition temperature (from DSC measurement) increases with dose for 15% TEGDMA/ 85% bis-GMA and is relatively constant for the 15% PEGDA/85% bis-GMA systems. This increase shown in the TEGDMA is less pronounced for the mixtures than for pure bis-GMA systems. The PEGDA samples have T_g's at higher temperatures than the pure bis-GMA films irradiated at equivalent dosages.

4. Rescans of DSC samples containing 15% modifier show no exothermic reactions, indicating the crosslinking reaction continues to open nearly all of the double bonds. This suggests the TEGDMA crosslinks via thermal mechanisms even though it showed little reactivity in electron beam cured systems.

5. Acrylate modifiers are more reactive to EB cure than methacrylate-capped modifiers in these systems. They also generate more heat due to the exothermic reaction which is higher than that of analogous methacrylates.

The binary mixtures have rather complex results because several variables arise. First, the TEGDMA and PEGDA both lower the viscosity of the bis-GMA. Since the crosslinking systems begin with lower viscosities, more crosslinking reactions occur before diffusion limitations intervene. A similar variable concerns the length of the chains. The bis-GMA has a molecular weight of 512 g/mol. The short chain TEGDMA and PEGDA materials have molecular weights of 286 and 302 g/mol respectively. As such, there are more chain ends, and in this case, double bonds per unit volume (a higher double bond density) in the TEGDMA and PEGDA systems than in the bis-GMA. Since the double bonds are much closer to each other, it is easier for the radicals to find reactive species and continue the crosslinking reaction. This factor also explains the higher T_g values given for the low percent modified mixtures (15 and 30% TEGDMA or PEGDA). Another possibility for either TEGDMA or PEGDA is the formation of cyclic monomer or oligomer species because the molecular weight of the prepolymer is relatively low as compared to bis-GMA and the chains are more flexible. The final factor concerns the reactivity of the acrylate vs. methacrylate capped modifier. The PEGDA material crosslinks readily, while the TEGDMA mixtures only crosslink partially when irradiated. In high concentrations, the TEGDMA does not crosslink sufficiently to form a gel. The methyl group

on the methacrylate seems to retard the crosslinking reaction due to steric hindrances. At first thought, it seems puzzling that a single methyl group would cause such a significant difference in physical behavior. However, the actual network formation is not a single reaction, but consists of a series of reactions. So, the hindrance of one reaction can make quite a difference in the network, in that many crosslinks do not occur that would have otherwise. Obviously, this is the case with TEGDMA.

The double bond density and viscosity variables mentioned above represent the trade-off in prepolymer coatings for radiation crosslinking. Higher molecular weight materials have the advantage that only a few crosslinks are needed to form a gel. Their disadvantage, especially with vinyl-terminated prepolymers, is that activated groups may not be able to find other reactive groups. This leads to a significant number of residual double bonds and even trapped free radicals in the irradiated coatings. The lower molecular weight prepolymers or monomers have just the opposite trade-off; the reactive species can find the other species but a greater level of crosslinking is required for gelation to occur. Radiation crosslinkable prepolymers give best results when these two effects are optimized.

The above phenomena can help explain some of the results discussed in Chapter 4 from the percent gel and residual double bond data. Although many of the double bonds are unreacted even after radiation, there is more of a tendency for molecules to become trapped in the matrix due to diffusion limitations if the molecular weight is greater. In addition, the residual double bond test is done on a molar basis while the gel test is by weight.

Another way to look at the comparison of the two tests is to consider an irradiated film where 80% of the reactive groups (e.g., the methacrylates) have reacted as detected by FTIR. P(DB) is defined as the probability that a randomly selected double bond has been opened by the irradiation process. Similarly, P(chain) is the probability that both double bonds on a randomly selected chain have been opened by the crosslinking process. Finally, P(0) is the probability that neither of the double bonds on a randomly selected chain has been opened

after irradiation. Looking at the respective probabilities, and assuming that the double-bond opening reaction occurs randomly:

$$P(DB) = 0.80$$

$$P(Chain) = 0.8^2 = 0.64$$

$$P(0) = (1 - 0.8)^2 = 0.04$$

From this hypothetical situation, the sol content would be the fraction of molecules where neither double bond was opened, four percent in this case. The percent gel test would give a result of 96% gel even though only 80% of the double bonds are opened. If only 70% of the double bonds are opened, similar probabilities show:

$$P(DB) = 0.7$$

$$P(Chain) = 0.7^2 = 0.49$$

$$P(0) = (1 - 0.7)^2 = 0.09$$

The sol component, where neither double bond of a molecule has been opened is only 0.09, corresponding to a gel content of 91%. The percent residual double bond content is 30%, since 70% of the double bonds have reacted. So, the double bond content on a percentage can be quite a bit higher than the analogous sol fraction (where sol fraction is 1 - gel fraction). This helps explain the discrepancies in the data from the two tests.

5.0 Bis-GMA and Rubbery Modifiers

In Chapter 4, the binary systems of bis-GMA and low molecular weight flexible species (molecular weight ca. 300 g/mol) were discussed. Longer chain rubbery modifiers consisting of polytetramethylene oxide (PTMO) end-capped with acrylate or methacrylate species were also mixed with bis-GMA, coated in a similar manner, and irradiated by EB. The end-capping reaction for synthesizing these materials is discussed in detail in Chapter 2. Experimental results which explain the extent of crosslinking and glass transitions of these irradiated coating systems comprise the bulk of this chapter.

The purpose of introducing a higher molecular weight material to the bis-GMA was in hopes of providing rubber toughening to the glassy network in order to reduce its brittleness. If, for example, the soft material could undergo phase separation from the glassy matrix during the crosslinking reaction, a classical rubber toughening effect would occur. Should this morphology be achieved, the material could be characterized by the existence of two separate glass transition temperatures, one for each phase. If phase separation does not occur, one T_g would be expected between the T_g's of the separate phases, the exact value of which would depend on the composition ratio and the degree of crosslinking. In this latter case of no phase separation, the T_g of the bis-GMA would be decreased by mixing, and the material properties at higher temperatures may well be compromised. However, rubber toughening can take place even though the phases do not separate.

As in the case of the low molecular weight modifiers described earlier, acrylate as well as methacrylate end-capped systems were investigated. The PTMO chains had an average molecular weight of 1000. Percent gel and FTIR (residual double bond content) tests were done for many compositions of the methacrylate-capped system (PTMO-MA/bis-GMA) as well as for

the acrylate-capped system (PTMO-A/bis-GMA). The trends of the crosslinking reaction with dose and composition can be discussed from these data. DSC and dynamic mechanical tests were carried out only for lower concentrations of the PTMO-MA and PTMO-A, since this author was interested in rubber-toughened glassy materials.

A bit should be mentioned about the bis-GMA/PTMO-MA and bis-GMA/PTMO-A liquid mixtures obtained. Mixing was sufficient to give clear solutions in the liquid state. Irradiation was done at that time. Within a few days time, phase separation occurred in the liquid state, especially in the 30 and 50% mixtures.

In addition to the experimental tests mentioned above, scanning electron microscopy was done on fractured samples of irradiated coatings. The purpose of this series of experiments was to observe any actual phase separation that might have occurred.

5.1 Extent of Crosslinking Reactions

5.1.1 Percent Gel Results

Percent gel tests were run on a number of PTMO-MA/bis-GMA systems. Dosage and composition were the parameters which were systematically varied. Samples were irradiated at dosages of 2, 5, and 12 Mrads in a one-pass process at a line speed of 40 feet per minute. Compositions of 15, 30, and 50 weight percent PTMO-MA were tested. Percent gels for the three compositions ranged from 82 to 100%, increasing as the total irradiation dose increased, consistent with the results detailed in Chapters 3 and 4. A plot of percent gel vs. irradiation dose is presented in Fig. 45. The percent gel decreases at increasing rubber modifier com-

positions for the 5 and 12 Mrad dosages; that is, the 30% modified bis-GMA has percent gel values lower than those of the 15% modified material. In a similar manner to the TEGDMA discussed in Chapter 4, coatings of 100% PTMO-MA did not form solid gel materials. Dosage and composition were the parameters of interest as in Chapter 4 for the low molecular weight materials.

The percent gel values for the bis-GMA/acrylate-capped PTMO systems have been plotted vs. irradiation dose in Fig. 46. Again, percent gel content increased as dosage increased, and it decreased as the composition of the acrylate component increased. The pure PTMO-A formed a solid network, but it had lower values for percent gels than the bis-GMA/PTMO-A mixtures. The pure PTMO-A yielded only 49% gels when irradiated at 2 Mrads. Although the acrylate species is more reactive to EB curing than the methacrylate species, the EB process does not generate more crosslinks in PTMO to form a complete network than in bis-GMA/PTMO-A mixtures or pure bis-GMA. One significant factor is the molecular weight of the PTMO-A which is about 1100 g/mol. As such, the chains are twice as long as bis-GMA (molecular weight = 512 g/mol). It is more difficult for the activated groups (radicals) to find other reactive groups to continue the crosslinking reaction. There is a trade-off here in that the higher molecular weight material has more mobility due to the nature of the PTMO chains. So, one might expect to find more trapped free radicals in the PTMO-A matrix. Another factor relates to the exothermic heat of reaction. Since there are less acrylate double bonds per unit volume in PTMO-A than methacrylate groups per volume in bis-GMA, the heat of reaction on a volume basis is less for PTMO-A than for the bis-GMA. However, the heat of reaction is greater for the acrylate than methacrylate species, as has been discussed in Chapter 4. One final possibility could be the occurrence of chain scission along the PTMO chains.

In order to test the validity of this chain scission speculation, gel permeation chromatography (GPC) was run on two samples of PTMO-MA (MW = 1000). One sample had been coated onto PET, irradiated at 10 megarads under the electron beam, and collected into a sample vial. It remained in the liquid state even after irradiation. The other sample was unirradiated

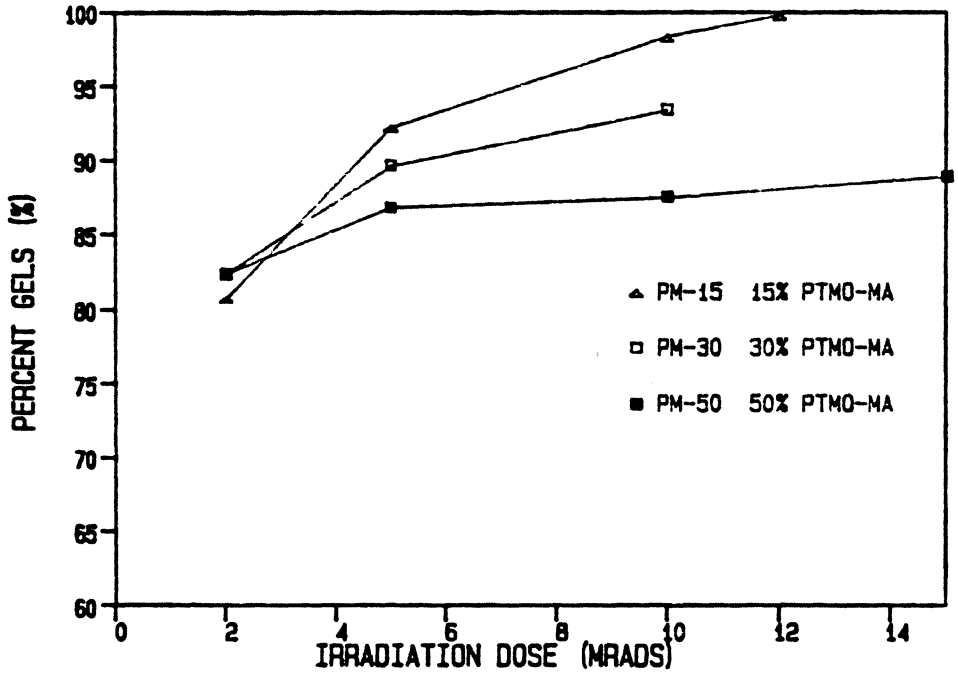

Figure 45. Percent Gels vs. Irradiation Dose for Bis-GMA/ PTMO-MA Mixtures.: The binary mixtures contain 15, 30, and 50% of the methacrylate- capped PTMO component. Irradiation dosages were 2, 5, and 12 Mrads.

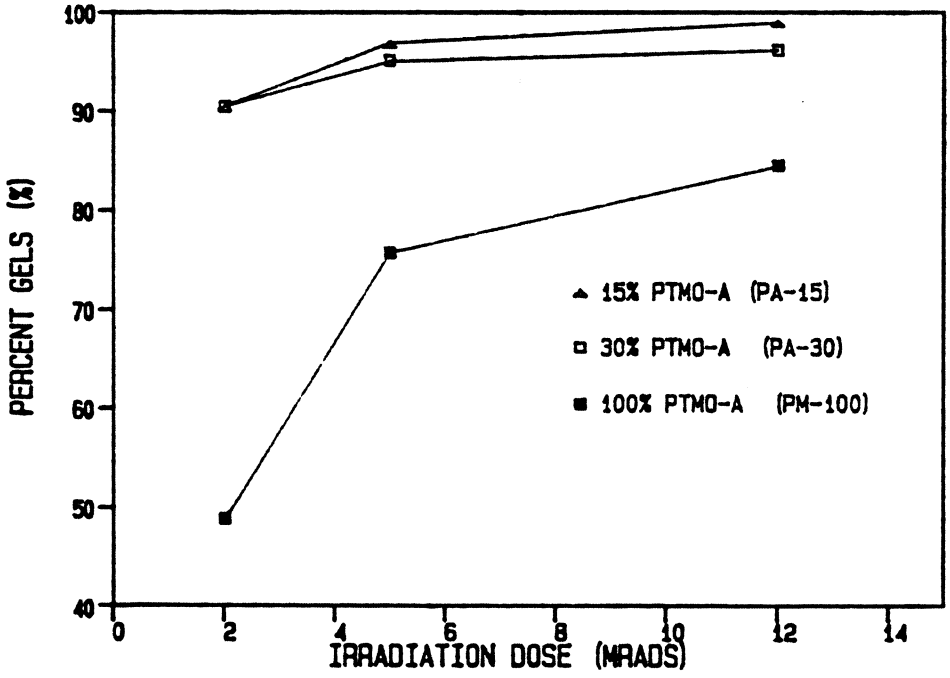

Figure 46. Percent Gels vs. Irradiation Dosage for Bis-GMA/PTMO-A Mixtures.: Percent gel data is given for 15, 30, and 100% PTMO-A materials. Irradiation dosages are 2, 5, and 12 Mrads.

PTMO-MA used as a control. Tetrahydrofuran was the solvent used for the test. The irradiated sample had a peak in elution volume corresponding to a higher molecular weight than the control, suggesting that some crosslinking did occur with radiation. However, there also appeared to be more PTMO-MA molecules corresponding to lower molecular weights, such that the 10 Mrad electron beam cure widened the molecular weight distribution through both crosslinking and scission reactions. The THF peak was strong at very low molecular weights (below 100 g/mol), such that small products of chain scission (e.g., a methyl group) would not be detected by this method.

5.1.2 Percent Residual Double Bonds

Residual double bond content was determined using Fourier Transform Infrared Spectroscopy. The details of the experimental methods are given in Chapter 2 and Appendix A. Dosage and composition were the parameters of interest as in Chapter 4 for the low molecular weight modifiers.

Values for percent residual double bonds are plotted vs. irradiation dosage in Figure 47 on page 118 for the bis-GMA/PTMO-MA mixtures. Percent residual double bonds decrease as radiation dose increases, consistent with the discussions of Chapters 3 and 4. For example, the 50% PTMO-MA sample has residual double bond contents of 36, 26, and 17% at dosages of 2, 5, and 10 Mrad respectively. The composition variable also shows a consistent trend in this matrix of experiments. The residual double bonds tend to decrease as the weight fraction of PTMO-MA component increases up to 30% PTMO-MA. This is due to the viscosity lowering effect of the PTMO-MA component. The 50 and 100% PTMO-MA samples have higher residual double bond content. The 100% PTMO-MA did not form a solid film at any dosage. Residual double bonds for this sample were 5% higher at 5 Mrad than at 2 Mrad. This data is not

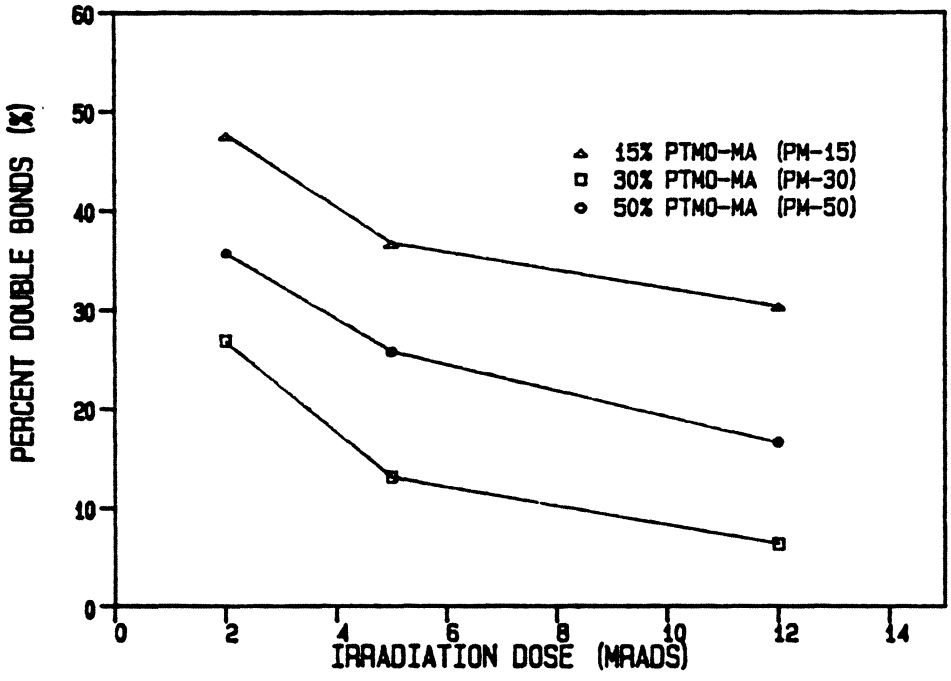

Figure 47. Percent Residual Double Bonds vs. Dose in PTMO-MA/Bis-GMA Irradiated at Various Dosages.: Percent residual double bonds decreases as dosage increases, indicating more crosslinking occurs at higher dosages.

consistent with the trends shown earlier that percent double bonds decreases at higher dosage, but could possibly be due to the error of experiment (a 7% range as discussed in Chapter 2).

Similar residual double bond data for the bis-GMA/PTMO-A mixtures are presented in Figure 48 on page 120. Again, the residual double bond content decreases as the weight fraction of PTMO-A increases up to the 30% PTMO-A mixture. Residual double bond values for the 30% PTMO-A mixtures were 23% at 2 Mrads, 18% at 5 Mrads, and 9% at 12 Mrads. The 50% PTMO-A mixture gives values which are close to the 30% values with the exception of the 2 Mrad film. In contrast to the PTMO-MA discussed above, a coating of 100% PTMO-A did crosslink to form a network at only 2 Mrads as well as at higher dosages. Residual double bond percentages are 30, 24, and 15% for the pure PTMO-A samples irradiated at 2, 5, and 12 Mrads respectively. It is evident that the PTMO-A crosslinking reaction proceeds much further than the PTMO-MA reaction at high concentrations (i.e., the 50 and 100% modifier mixtures). In addition, the heat generated in the reaction is higher in the acrylate-capped material in light of the differences in the heat of polymerization discussed earlier (18.7 kcal/mole for the acrylates vs. 13 kcal/mole for the methacrylates).

Some difficulty arises in correlating the residual double bond data to the percent gel data. First, the data for the methacrylate capped rubber modifier (Figs. 45 and 47) will be compared. At 2 Mrad, the percent gel values for the 15, 30, and 50% PTMO-MA mixtures are all between 80 and 83%. The percent residual double bonds for these materials are 48, 29, and 36%, much more variable than the percent gel data. Another point of concern deals with the high dosage materials. The 30 and 50% PTMO-MA films irradiated at 10 Mrads have lower percent gel values than the 15% PTMO-MA film. The residual double bond content is also lower for the 30 and 50% PTMO-MA than for the 15% modifier material. This suggests the double bonds are being opened at high radiation dosages but not all of the reactions lead to cross-linking. Since there are less PTMO-MA chain ends per volume than are present in bis-GMA, the chances are greater that diffusion may limit the reaction even above the T_g of the network.

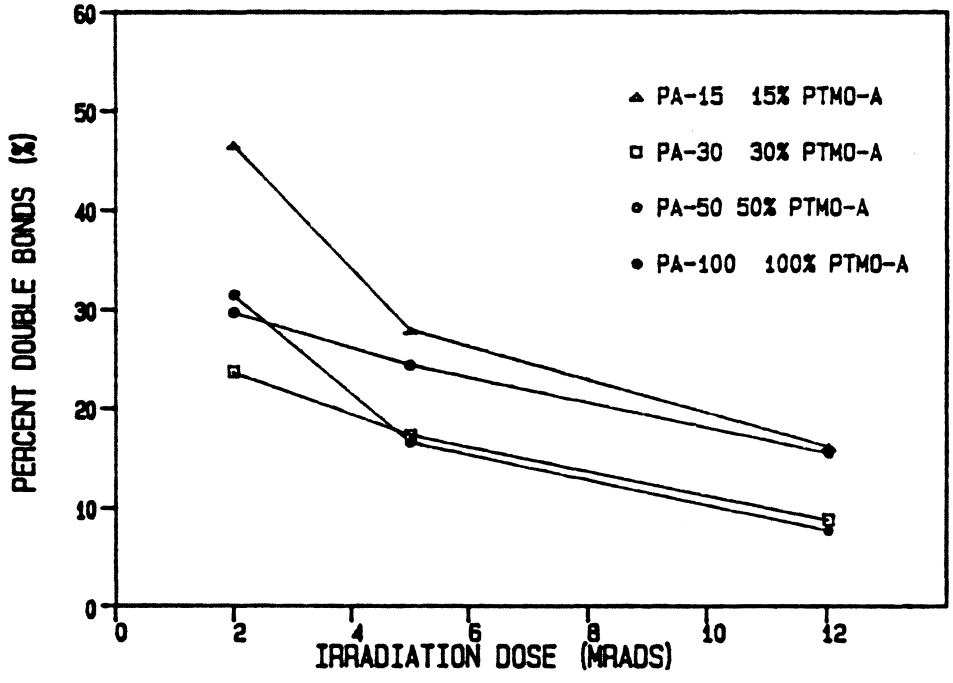

Figure 48. Residual Double Bonds vs. Irradiation Dosage for Bis-GMA/PTMO-A Mixtures: The FTIR test was done for 15, 30, 50, and 100% PTMO-A mixtures. Aging time was one hour after cure.

Turning to the PTMO-A mixtures (Figs. 46 and 48), the same trends are present. Percent gels are 90 and 91% for the 2 Mrad irradiated films with 15 and 30% PTMO-A respectively. However, the 15% PTMO-A film has a 22% higher residual double bond content than the 15% PTMO-A. In addition, at high dosage again the 15% PTMO-A had higher percent gel and higher double bond content than the 30% PTMO-A. Another trend is seen with the acrylates by looking at the pure PTMO-A irradiated at 2 Mrads. The data reveals 70% of the double bonds were opened (30% residual double bond content), while only 49% gel was found for the same sample. This suggests that again the double bonds are opened but not all contribute to formation of a gel. The radicals in the higher molecular weight materials are less likely to find the proper reactive species for the crosslinking reaction.

5.2 Physical Properties of Irradiated Networks

5.2.1 DSC Temperature Scans

In order to describe the glass transition effects in these rubber modified mixtures, DSC and dynamic mechanical tests were run. DSC was run for several samples, varying both composition and dose. Dynamic mechanical was only run for the 15% rubber modified mixtures for both the acrylate and methacrylate modifiers with bis-GMA. The samples were irradiated at 12 Mrads. All tests were carried out 1 hour after irradiation.

Figures 49 and 50 give the DSC scans for 15 and 30% PTMO-MA mixtures in binary systems with bis-GMA. In Fig. 49, the samples resemble the bis-GMA data discussed in Chapter 3. The T_g's are 40°C at 2 Mrads, 66°C at 5 Mrads, and 81°C at 12 Mrads. The exotherm at 130°C is present here as it has been throughout the previous studies. The 30% PTMO-MA, as shown in Fig. 50, is characterized by a less obvious T_g. The tan δ peak is broad, suggesting a distribution of temperatures exists where the chains gain mobility. The 2 Mrad cured film has its

T_g at 93°C. There is a significant exothermic reaction above this temperature, which peaks at the familiar 130°C. The 5 Mrad sample shows very little exothermic behavior but a thermal softening is present at 76°C. The 12 Mrad sample more closely resembles that of pure bis-GMA, with an onset of T_g at 74°C. A significant exotherm follows which peaks around 110°C. From the data, and remembering the soft PTMO-MA at 30% contributes significantly by lowering the viscosity of the system, it appears that the low dosage films did not reach diffusion limitations as quickly. The 12 Mrad dose was enough to generate many radicals such that sufficient crosslinking occurred to reach diffusion limitations as well as trap radicals in the glassy matrix.

Figures 51, 52, and 53 give the DSC scans for the 15, 30 and 100 % compositions of the acrylate-capped modifier. Figure 51 details the 15% PTMO-A/85% bis-GMA mixture irradiated at 2, 5, and 12 Mrad. The 2 Mrad sample has an onset of T_g at 61°C, followed by another exotherm at 85°C. The exotherm which follows has great magnitude, not reaching its maximum until 170°C. The 5 Mrad sample has its T_g at 88°C, and the 12 Mrad film has an onset of T_g at 90°C. Looking at the 30% PTMO-A DSC scans shown in Fig. 52, T_g's for the 2, 5, and 12 Mrad films exist at 76, 87, and 80°C respectively.

DSC was also performed for the 100% PTMO-A irradiated at 2, 5, and 12 Mrads. The 2 Mrad film shown in Fig. 53 has T_g at 83°C, followed by an exotherm that peaks around 150°C. The 5 and 12 Mrad coatings have T_g's at 93 and 97°C, with an exotherm at 160°C. The high temperature exotherms are quite large. The heat capacity does not increase at high temperatures as it does for the bis-GMA component, again showing the more exothermic nature of the crosslinking reaction of the acrylates.

Although the DSC curves are not as clear-cut as some of the earlier data, a few points concerning the functional end groups are apparent. Most of these have been discussed in Chapter 4 so only a few brief remarks are necessary here. First, the acrylates are more reactive than the methacrylates. Thus, the T_g's of the methacrylate modified coatings are more

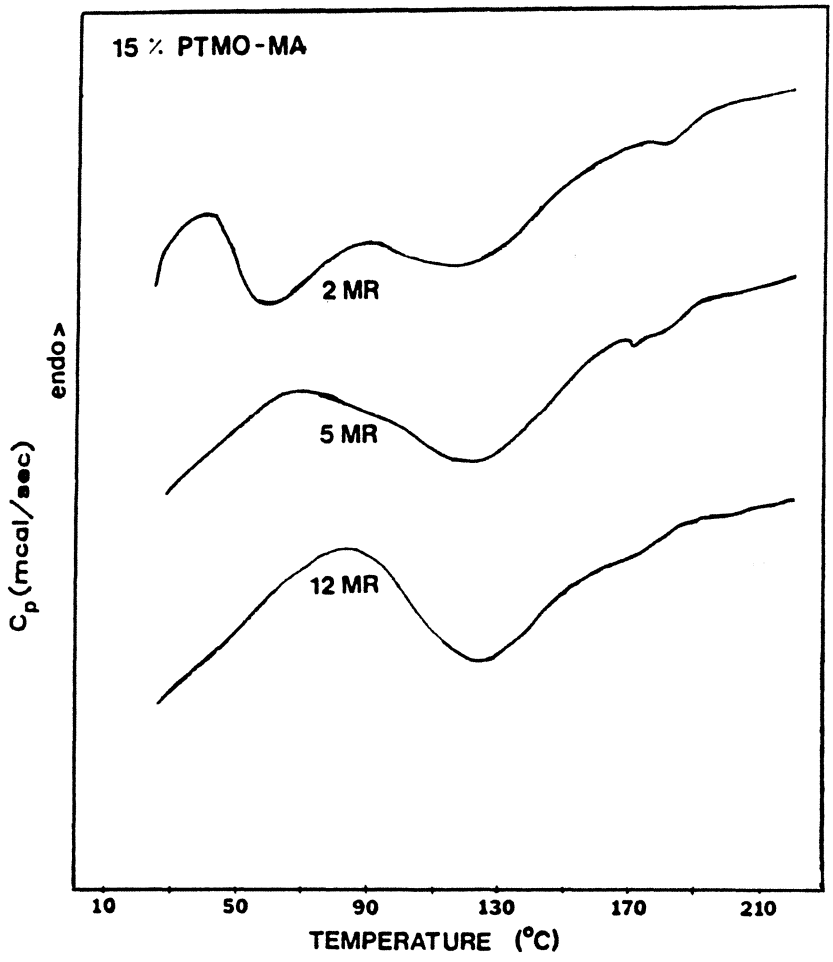

Figure 49. DSC Temperature Scans for 15% PTMO-MA/85% Bis-GMA Mixture at Different Irradiation Dosages.: Dosages were 2, 5, and 12 Mrads. Aging time after cure was one hour, and the DSC scans were done at 20°C per minute.

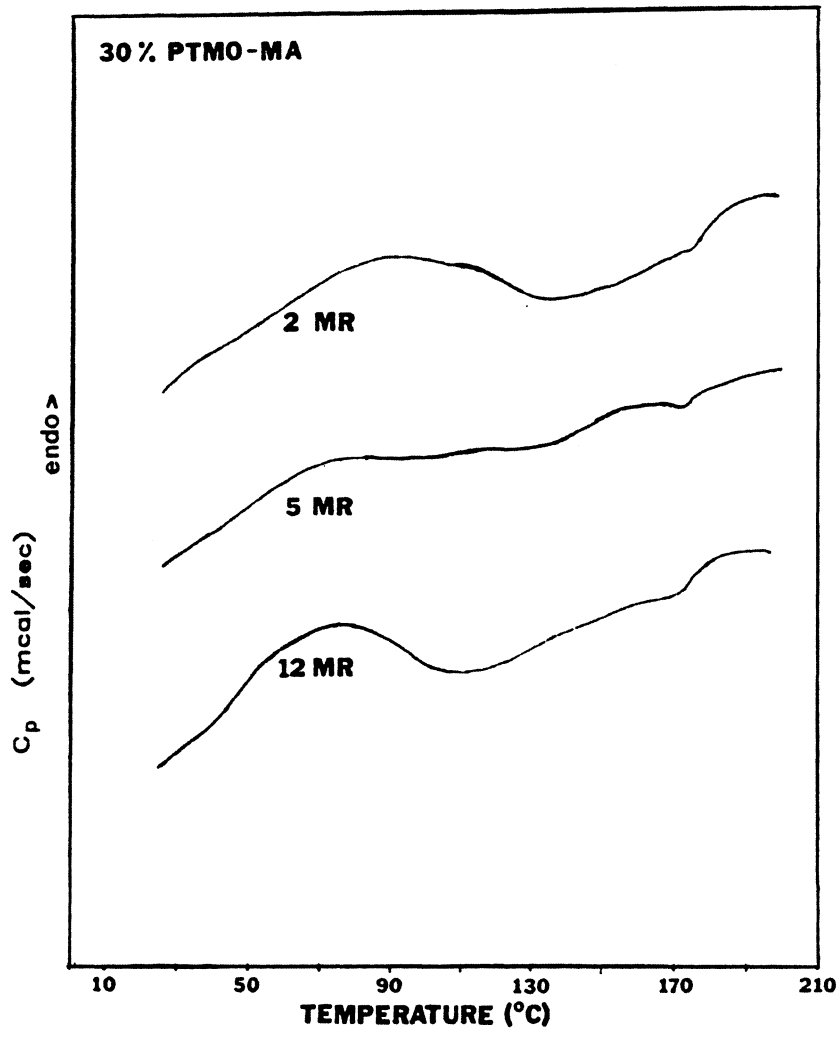

Figure 50. DSC Temperature Scans for 30% PTMO-MA/ 70% Bis-GMA Mixtures at Different Irradiation Dosages.: Dosages were 2, 5, and 12 Mrads. Aging time after cure was one hour, and the DSC scans were done at 20°C per minute.

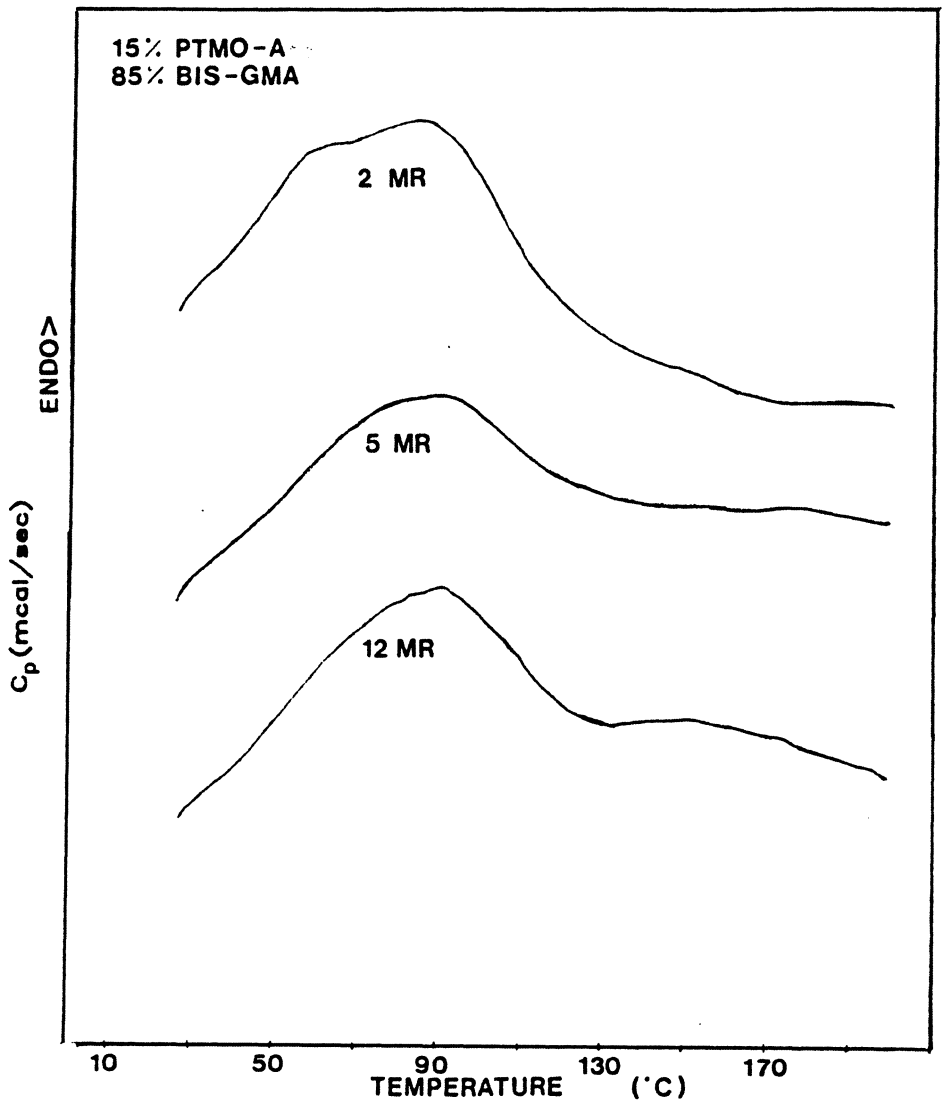

Figure 51. DSC Temperature Scan for 15% PTMO-A/ 85% Bis-GMA at Different Irradiation Dosages.: Dosages were 2, 5, and 12 Mrads. Aging time after cure was one hour, and the DSC scan rate was 20°C per minute.

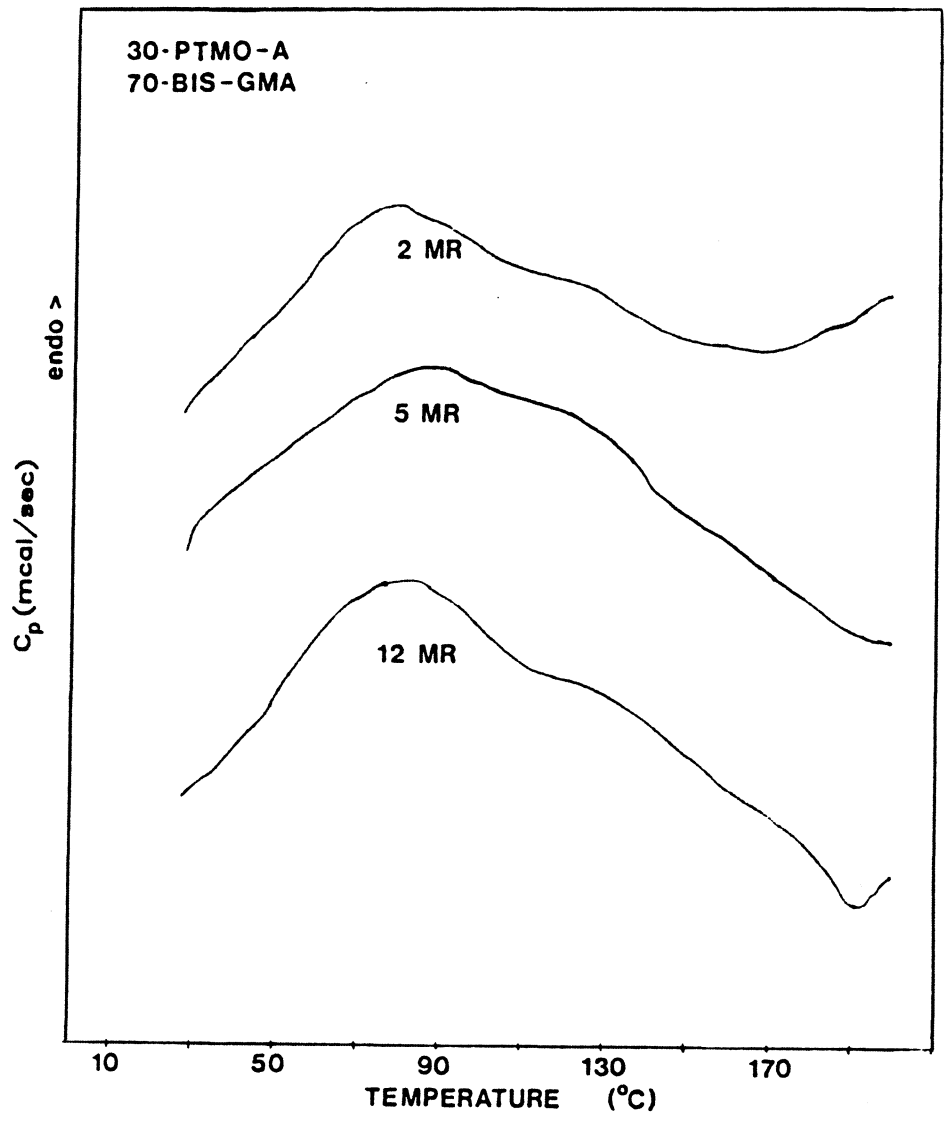

Figure 52. DSC Temperature Scan for 30% PTMO-A/ 70% Bis-GMA at Different Irradiation Dosages.: Dosages were 2, 5, and 12 Mrads. Aging time after cure was one hour and temperature scan rate was 20°C per minute.

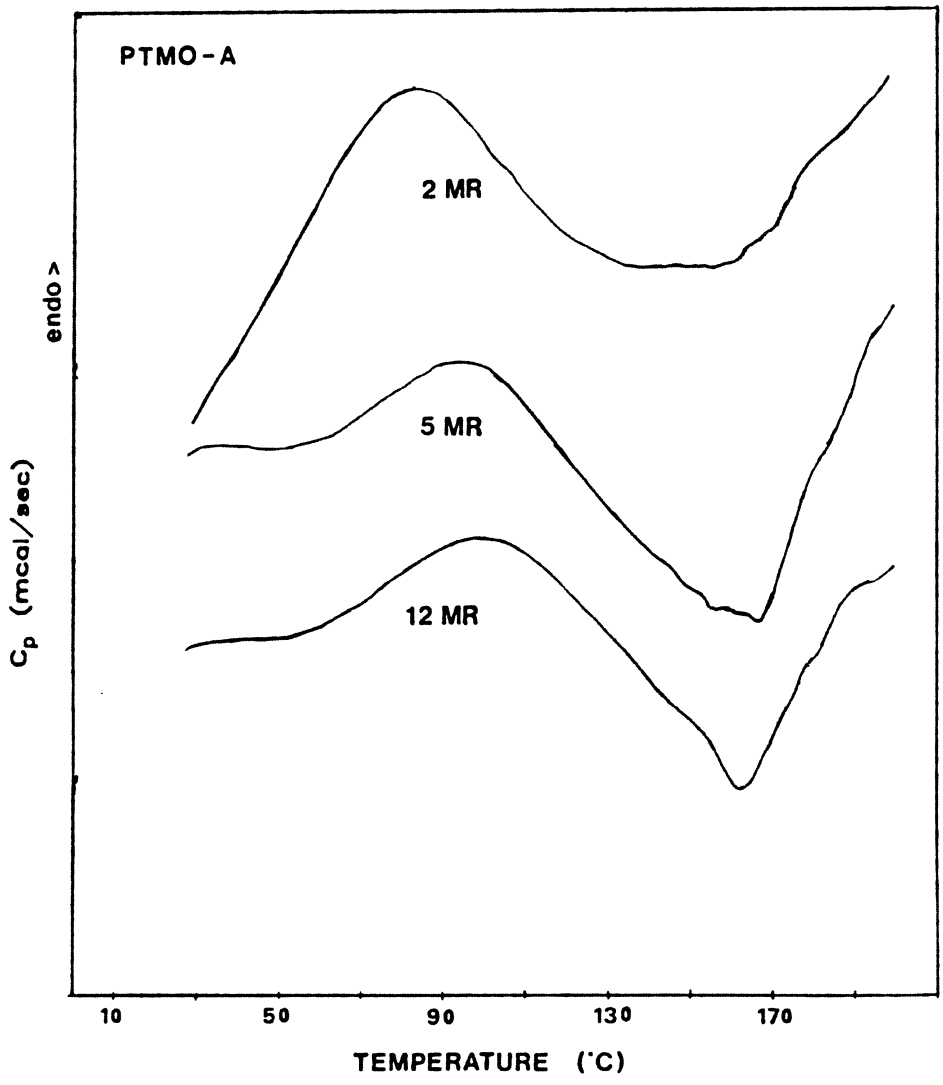

Figure 53. DSC Temperature Scans for 100% PTMO-A at Different Dosages.: Dosages were 2, 5, and 12 Mrads. Aging time after cure was one hour and temperature scan rate was 20°C per minute.

dependent on dosage, because the acrylates continue their crosslinking reaction once initiated. In addition, the heat of polymerization is higher for the acrylate species than for the methacrylate species. This leads to a higher temperature spike for the acrylates during irradiation such that the temperature at which T_g "runs into" the reaction temperature is higher, as discussed earlier in terms of the TTT diagram (Fig. 11). The high exothermic reaction is also apparent from the DSC tests just discussed. As residual double bonds are opened in the PTMO-A systems, the magnitude of the resulting exotherm is quite large, assuming there are a number of double bonds left to react. As a result, the heat capacity in many of the curves does not increase again at the high temperatures as it does in the pure bis-GMA systems (Fig. 21).

5.2.2 Glass Transitions from Dynamic Mechanical Spectroscopy

Dynamic mechanical spectra were obtained for the 15% mixtures of the acrylate and methacrylate species with bis-GMA. The irradiation dosage was 12 megarads for each sample. These results will be compared to each other as well as to bis-GMA (see Fig. 25). Temperatures were run from -150 to 200°C.

The plot of E′, E″, and tan δ vs. temperature for the 15% PTMO-MA /85% bis-GMA sample is presented in Fig. 54. This plot is characterized by a slow, gradual softening of the modulus. Its softening point temperature, where $E' = 5 \times 10^9$ dynes/cm^2 exists at 157°C. The tan δ curve is flat until the glass transition temperature is reached at 168°C. As mentioned earlier and shown in Fig. 45, the percent gel content at 12 Mrads is 98% for the 15% PTMO-MA, indicating the system is almost fully crosslinked.

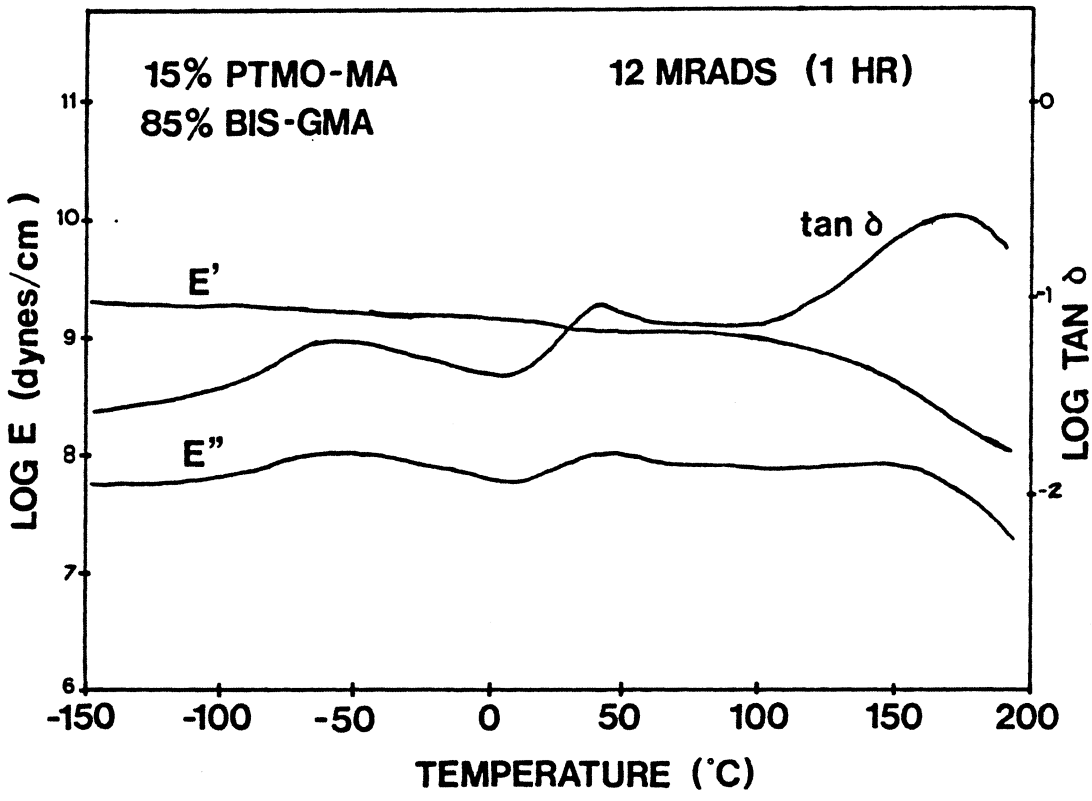

Figure 54. Dynamic Mechanical Temperature Scan for 15% PTMO-MA/ 85% Bis-GMA Irradiated at 12 Mrads.

The Autovibron plot for the 15% PTMO-A /85% bis-GMA coating is given in Fig. 55. Again, the storage modulus (E′) undergoes a gradual decline as temperature is increased. Above 100°C the decline becomes sharper. The softening point temperature is reached at 174°C. The log tan δ curve contains a number of features. First, the low temperature data is quite scattered, but a substantial tan δ peak occurs at -70°C. This peak is due to the movement of a side chain or subgroup of the backbone. Another tan δ peak exists at 40°C. This is analogous to the initial T_g peaks shown in earlier dynamic mechanical scans (Figs. 23, 24, and 25). A third tan δ peak occurs at 180°C, which is much larger than the other two peaks. This temperature corresponds to the temperature on the general TTT diagram (Fig. 11) called $T_{g\infty}$.

These data can be compared to the bis-GMA results discussed in Chapter 3. The Autovibron plot for bis-GMA irradiated at 12 Mrads is given in Fig. 25. The softening point temperature is 183°C, as shown by the storage modulus curve (E′). The tan δ peaks exist at 84 and 198°C, indicating the initial T_g and the glass transition of the network after further crosslinking takes place. The T_g increases as crosslinking continues as molecules are thermally mobilized.

The softening points and T_g's are higher for the pure bis-GMA than for the rubbery modified materials. This indicates that the rubber modifier materials do not phase separate, but tend to crosslink into the system in a random manner. The rubbery component decreases the T_g and softening point temperature.

5.2.3 Morphology from Scanning Electron Microscopy

Scanning electron microscopy (SEM) was done for fractured samples of the 15% PTMO-MA / 85% bis-GMA and 15% PTMO-A / 85% bis-GMA. The networks were irradiated at 2 and 12 Mrads. In addition, SEM photographs were taken of thermally cured mixtures at the com-

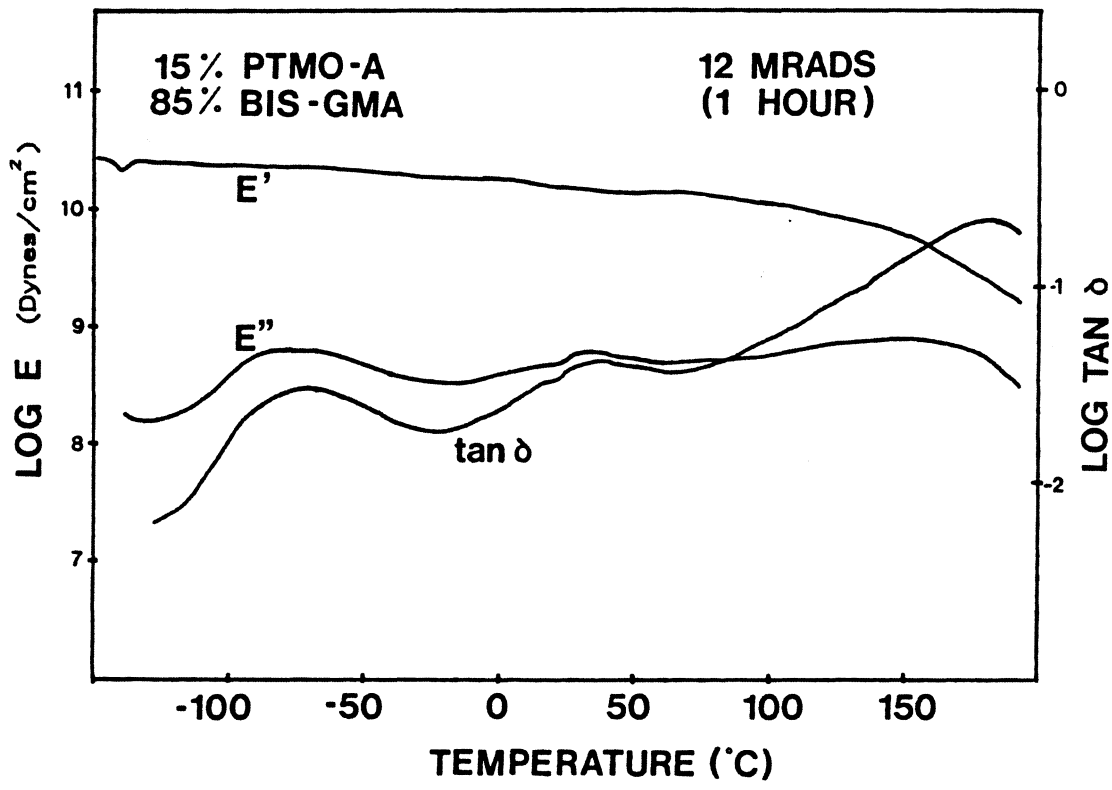

Figure 55. Dynamic Mechanical Spectrum for 15% PTMO-A/85% Bis-GMA Irradiated at 12 Mrads.: Values for E', E", and tan δ are give as a function of the temperature. Aging time after cure is one hour.

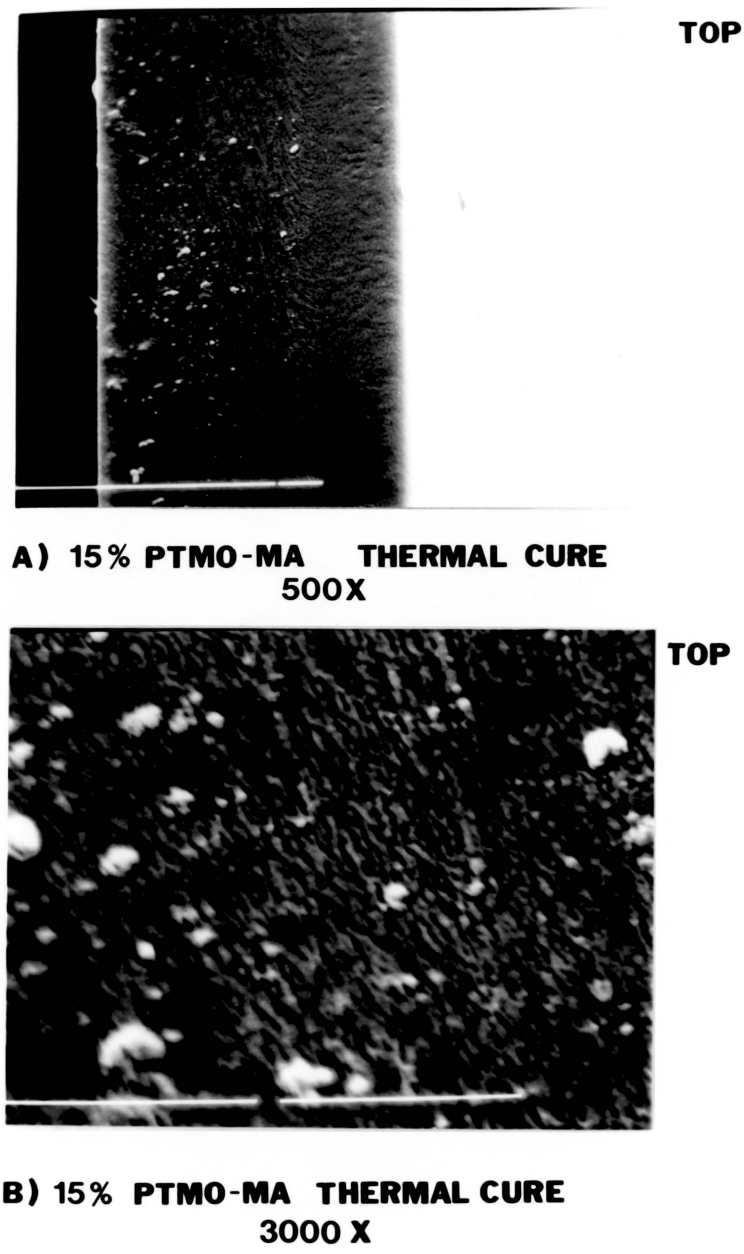

Figure 56. SEM Photographs for Thermally Cured 15% PTMO-MA / 85% bis-GMA Mixture.: Thermal curing was done at 150°C for 2 hours. Magnification for the pictures was a) 500 x, and b) 3000 x. Extraction was done in THF for 5 minutes.

positions above. The purpose of this series of experiments was to characterize morphology and supplement the dynamic mechanical spectroscopy results discussed in the previous section. The critical issue is whether or not the irradiated networks can undergo phase separation during cure. The alternative is that the rubbery component is randomly crosslinked into the glassy network, such that it acts as a plasticizer reducing the ultimate glass transition temperature ($T_{g\infty}$).

Photomicrographs are presented in Figure 56 on page 132 for the thermally cured PTMO-MA mixture. The crosslinking reaction was done at 150°C for 2 hours. The photographs were taken at x500 and x3000 magnification with a sample tilt of 45°. The phase separation of the rubbery component is quite evident.

Similar SEM photographs for the 2 and 12 Mrad irradiated samples are presented in Figure 57 on page 134 and Figure 58 on page 135. The rubbery domains seen in the thermally cured sample are not present in these networks. The irradiation process only takes a second, and from these data it appears that diffusion limitations occur before phase separation in the solid state can take place.

Electron microscopy was also done for the acrylate-capped modifier (the 15% PTMO-A/ 85% bis-GMA mixture). Figure 59 shows SEM photographs for fractured samples of films irradiated at 2 and 5 Mrads. The films do not show phase separation, indicating the rubbery material is randomly crosslinked into the bis-GMA. Figure 60 gives a similar photograph for the 12 Mrad sample. Again, no phase separation is evident here.

5.3 *Conclusions from the Rubber Modification Experiments*

The degree of crosslinking was determined by percent gel and FTIR techniques as was done for the other experiments discussed earlier. Percent gel values for the methacrylate-capped

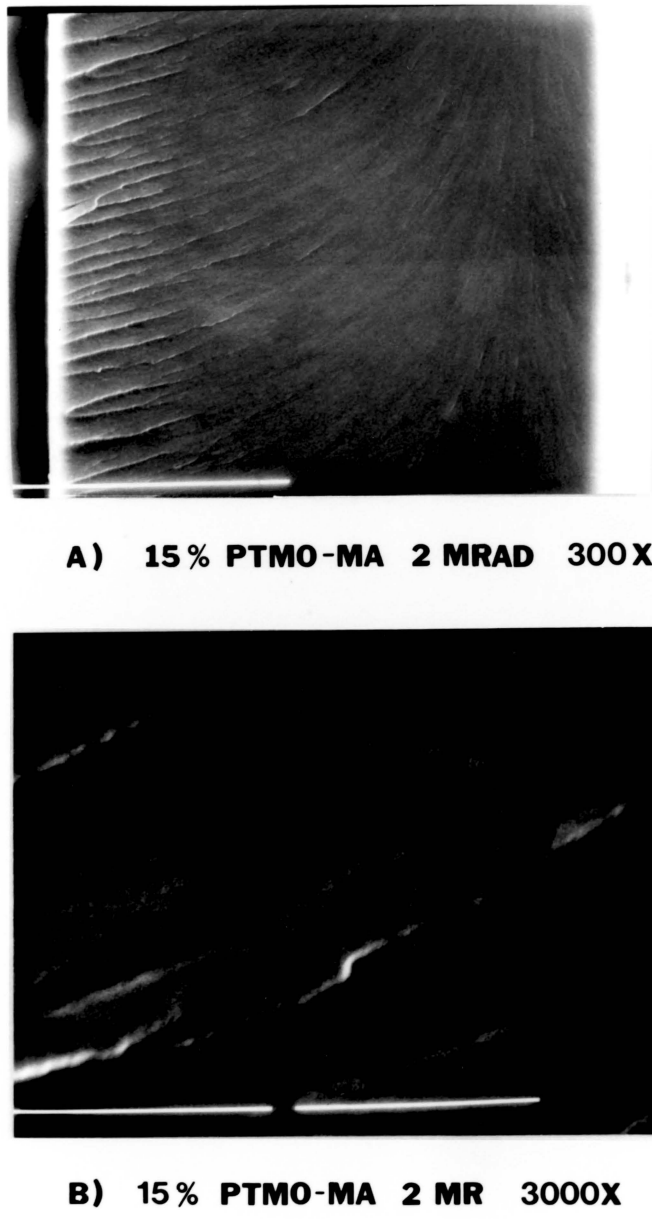

Figure 57. SEM Photographs for 15% PTMO-MA / 85% bis-GMA Mixture Irradiated at 2 Mrads.: Magnifications for the photographs were a) 300x and b) 3000x power. Extraction by THF was done for 5 minutes prior to SEM.

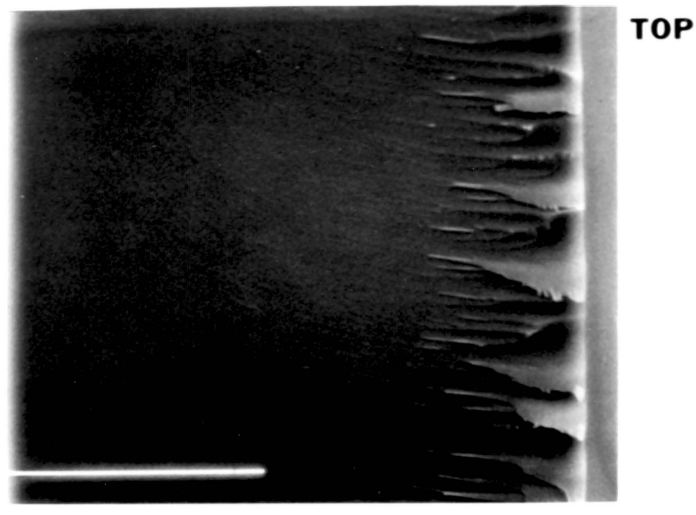

Figure 58. SEM Photographs for 15% PTMO-MA / 85% bis-GMA Mixture Irradiated at 12 Mrads.: Magnifications for the photographs were a) 300 x and b) 3000 x. Extraction in THF was done for 5 minutes.

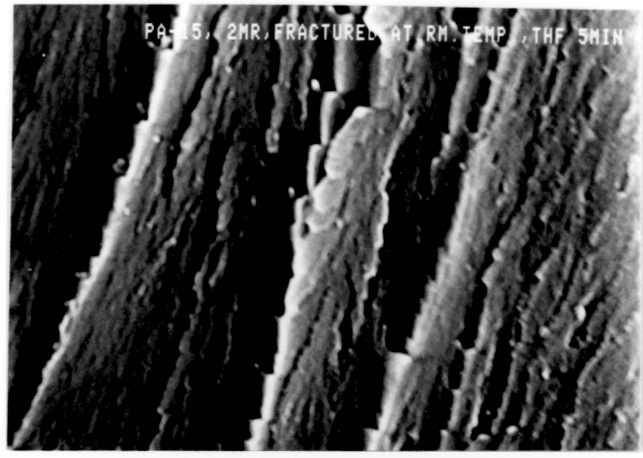

A) 15% PTMO-A 2 MRADS 3400X

B) 15% PTMO-A 5 MRADS 3600X

Figure 59. SEM Photograph for 15% PTMO-A / 85% Bis-GMA cured at 2 and 5 Mrads by electron beam.: The samples were irradiated at 2 and 5 Mrads. The photographs are taken at about 3400 x. Samples were extracted in THF for 5 minutes.

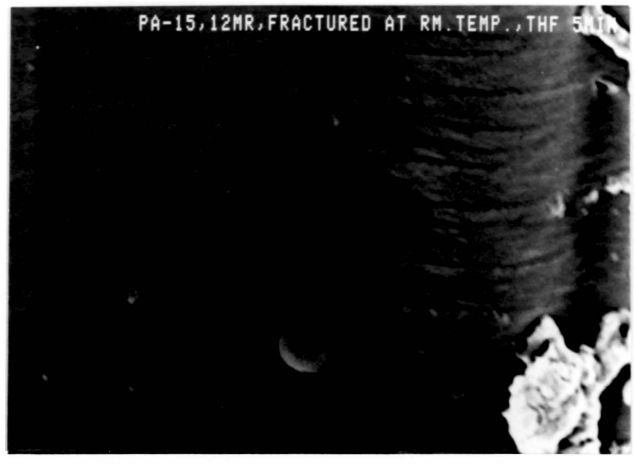

A) 15 % PTMO-A 12 MRADS 3400X

Figure 60. SEM Photographs for 15% PTMO-A / 85% bis-GMA.: The sample was irradiated at 12 Mrads, and the photograph is taken at 3600 x. Extraction was done in THF for 5 minutes.

modifier mixed with bis-GMA dropped as the composition of modifier increased. The residual double bond content did not quite follow, as the minimum values for percent double bonds were found for the 30% modified bis-GMA mixture (see Figure 45 on page 115 and Figure 47 on page 118). Although more double bonds were opened in the 30% PTMO-MA than in pure bis-GMA, the amount of gel formation was less. The higher molecular weight materials have longer chains such that it is more difficult for the radicals to find other reactive species for crosslinking. As such, more free radicals are trapped in the 30% PTMO-MA networks and less gelation occurs. The acrylate-modified mixtures of PTMO-A and bis-GMA were also tested. Percent gel values decreased as the content of the acrylate modifier increased. Again, the double bond content did not follow precisely, because the minimum values were found for the 30 and 50% PTMO-A mixtures. Again, the excited species are not able to react as much as analogous shorter chain materials because the excited species are on the average further away from each other.

DSC and dynamic mechanical tests were carried out to determine the effects of composition of rubbery modifier material on the glass transition temperatures at various dosages. Two series of DSC experiments were run; one on the methacrylate-capped modified mixtures, and the other on mixtures containing the acrylate-capped mixtures (PTMO-A/bis-GMA). The T_g's for the acrylate-capped mixtures were higher in general than the analogous PTMO-MA/bis-GMA mixtures. This is consistent with the other results, in that the acrylate species are more reactive than analogous acrylates. Again, the heat of reaction is also greater for acrylates than analogous methacrylates, so there is more of a temperature rise leading to more mobility in the chains and more crosslinking.

The glass transition temperatures from dynamic mechanical tests show that the bis-GMA/PTMO-MA and bis-GMA/PTMO-A mixtures have a T_g that is suppressed below that of the pure bis-GMA. This suggests that the phases are not separated but are randomly dispersed within each other. So, from a physical property standpoint, the irradiated mixtures will not have the benefit of the bis-GMA transition temperature around 190°C, but will soften

at the suppressed T_g of 161°C (for 15% PTMO-MA/ 85% bis-GMA) or 178°C (for 15% PTMO-A/ 85% bis-GMA). The rubber toughening effect is present, as some flexibility is gained in the irradiated films. However, the T_g of the film is not as high as it could be if phase separation had occurred.

Scanning electron microscopy was also done to supplement the findings of the dynamic mechanical tests. SEM photomicrographs were taken from bis-GMA/PTMO-MA mixtures cured thermally as well as by radiation crosslinking with 2 and 12 Mrad dosages. In addition, SEM photographs were obtained for bis-GMA/PTMO-A mixtures cured thermally and for mixtures crosslinked by EB, also at 2 and 12 Mrads. For the methacrylate-capped mixture cured thermally, phase separation occurred as shown by the SEM photomicrographs presented earlier (Fig. 56). However, phase separation was not seen from any of the rubbery modified mixtures cured by radiation crosslinking. It appears that the radiation crosslinking reaction reaches diffusion limitations (i.e., vitrification) before the phases can separate.

6.0 Summary and Conclusions

In the preceding three chapters, three sets of experiments were discussed. Bis-GMA systems were discussed in Chapter 3 while binary systems of bis-GMA and low molecular weight modifiers triethylene glycol dimethacrylate and polyethylene glycol diacrylate were detailed in Chapter 4. The topic of Chapter 5 consisted of bis-GMA mixtures with higher molecular weight rubbery modifiers. The purpose of this chapter is to "tie" all of this material together by means of a summary of the results and conclusions. Finally, some discussion will be given concerning future experimental work to be done based on these findings.

6.1 Bis-GMA Systems Cured by Electron Beam Irradiation

Bis-GMA, a diglycidyl ether of bisphenol-A, has been the featured component of the work reported by this author. The bis-GMA liquid was crosslinked by electron beam irradiation. A number of process variables were systematically studied, including dose, dose rate, aging time after EB cure, and the effects of post-cure annealing on physical properties.

It has been found that upon irradiation, bis-GMA crosslinks to form a clear, brittle, solid network. The amount of crosslinking increases as dosage increases (in a single pass experiment), up to a critical dosage near 10 Mrads. This was shown in Chapter 3 by three experimental techniques. First, values for percent gel from extraction in acetone increase as

dosage increases, indicating more network formation occurs at higher irradiation dosages. A similar test was performed to find the swelling ratio in these networks. The swelling ratio is inversely proportional to the crosslink density of the network system. Values for the equilibrium swelling ratio decreased as dosage increased. A third method to measure the amount of chemical crosslinking used FTIR to determine the quantity of double bonds remaining after irradiation. As expected, the number of residual double bonds decreased as dosage increased, indicating more double bonds are opened at higher irradiation dosage. Since the double bonds are involved in the crosslinking reaction, it follows that more crosslinks are formed at higher irradiation dosage.

Physical property tests, such as DSC and dynamic mechanical spectroscopy, were performed to measure glass transition temperature at various irradiation dosages. Other factors being constant, the T_g tends to increase as dosage is increased. Since the temperature of cure is higher at higher dosage, more crosslinking can occur before T_g increases to "run into the cure temperature". This was found experimentally for bis-GMA from DSC and dynamic mechanical tests (Chapter 3). The increased T_g is the result of more network formation.

Since the bis-GMA systems are diffusion limited and radicals can become trapped in the glassy networks, the effects of ambient aging on physical properties was studied. The trapped radicals were found to have a finite lifetime. Radicals trapped in bis-GMA irradiated at 2 Mrads had a life of approximately 80 hours based on DSC results (recall Figure 33 on page 80). Dynamic mechanical results supported this finding, as the T_g is lower at 48 and 120 hours after cure than at only one hour after cure. This reduction is due to the deactivation of free radicals from the system due to oxygen or other scavenger, as they are no longer available to contribute to the crosslinking of the network.

The final variable studied in bis-GMA systems was the effect of post-cure annealing on irradiated films of bis-GMA. Post-cure annealing can allow the crosslinking reaction to continue to raise T_g to the annealing (cure) temperature or to $T_{g\infty}$. From the Time-

Temperature-Transformation diagram discussed earlier, as the temperature of the network is increased above its T_g, the polymer chains acquire mobility. Any reactive species remaining can then react if it finds another suitable functional group. This is precisely what happens in the bis-GMA systems. This was shown by the DSC rescans (Fig. 33) and by the Autovibron scan run on the annealed sample (Fig. 35). At temperatures above 130°C, double bonds can be opened due to thermal energy as well as by reacting with residual free radicals. This explains the very low percent residual double bond content found for bis-GMA systems annealed at higher temperatures (180 and 200°C).

6.2 Bis-GMA and Low Molecular Weight Modifiers

Binary systems consisting of bis-GMA and either triethylene glycol dimethacrylate (TEGDMA) or polyethylene glycol diacrylate (PEGDA) were irradiated by an electron beam curtain. In addition to dosage, other variables studied in this series of experiments were the composition and the reactivity of acrylates vs. methacrylates in these systems. As was done previously for bis-GMA, tests were done to quantify the crosslinking reaction and to look at structure/property relationships from glass transition data from the DSC experiments. Some of the more detailed work which was done with bis-GMA, such as effects of dose rate, aging time after cure, or thermal annealing was not repeated for these binary systems. The following observations were made from these data:

1. The amount of network formation increases as dosage increases for the mixtures with high concentrations of bis-GMA. Again, 10 Mrads is sufficient to obtain a network with over 90% gel content for high bis-GMA mixtures. The dimethacrylate modifier (TEGDMA) was not as reactive to EB cure, such that crosslinking of pure TEGDMA even at high dosages was insufficient to form gels.

2. The diacrylate-capped species (PEGDA) was more reactive to EB cure than the analogous dimethacrylate (TEGDMA). For example, the 50% PEGDA had a residual double bond content of 4.7% at 12 Mrads, while the 50% TEGDMA/ 50% bis-GMA had 50% residual double bonds. Three reasons, which are discussed in Chapter 4, are apparent for this difference:
   a. The acrylate groups have a higher heat of polymerization than the methacrylate groups.
   b. PEGDA has a higher viscosity at room temperature than TEGDMA.
   c. The acrylate groups offer less steric hindrance for electrons or active groups than methacrylates.

3. The low molecular weight modifiers can increase the reactivity of bis-GMA in that the double bond density is higher for lower molecular weight prepolymers. The trade-off exists since more crosslinking reactions are needed for gelation to occur. Crosslinking reactions which form cyclic species are possible, since the prepolymers are flexible.

4. The composition variable is not a simple one, as the variables mentioned above (end-group reactivity, viscosity, and chain length) all influence the physical properties of the network. Thus, irradiated mixtures with high concentrations of PEGDA or TEGDMA may have a high percentage of double bonds broken but may not be high in gel content. Gel content is a probability problem complicated by entanglements, trapped free radicals, oligomers, etc.

5. At low dosages, DSC glass transition temperatures were higher for the mixtures than for pure bis-GMA. Temperatures for T_g were above 90°C for 15% modifier mixtures at or above 5 Mrads. This is mainly due to the lower viscosity from the low molecular weight modifiers, which allows more crosslinking to occur before diffusion limitations are reached. Due to the difference in the heats of reaction for the acrylate groups, T_g's for the bis-GMA/PEGDA mixtures were generally higher than the bis-GMA/TEGDMA mixtures.

6.3 *Bis-GMA and Higher Molecular Weight Rubbery Modifiers*

Bis-GMA, the featured material in this study, was mixed with higher molecular weight materials containing polytetramethylene oxide (PTMO) which was end-capped with either an acrylate or methacrylate species. The PTMO had a number average molecular weight of 1000 g/mol, such that the diacrylate and dimethacrylate-capped species averaged 1110 and 1138 g/mol respectively. Chemical structures for these species as well as the end-capping reaction procedure were discussed in Chapter 2. Similar studies were done as before to characterize the extent of crosslinking and the physical property relationships. The following results and conclusions were made based on data discussed in Chapter 5:

1. As in the previous studies, the amount of crosslinking in these systems is proportional to the irradiation dosage up to a critical dosage near 10 Mrads.

2. Again, the diacrylate material (PTMO-A) was more reactive to EB curing than the analogous dimethacrylate (PTMO-MA). This was shown by higher percent gel values, lower residual double bond content, and higher T_g's for PTMO-A than for the PTMO-MA mixtures at the same conditions. For example, the 30% PTMO-A mixture irradiated at 12 Mrads had a T_g at 93°C. The analogous methacrylate had its T_g at 80°C.

3. The maximum percentage of double bonds opened by the EB irradiation was found for the 30% methacrylate modifier. Compositions higher than 30% modifier (50 and 100% PTMO-MA) did not form a solid network upon irradiation at dosages up to 12 megarads.

4. Phase separation in the solid networks was not achieved, as shown by the depressed T_g from Autovibron results relative to pure bis-GMA. The networks formed were more randomly crosslinked, as the crosslinking and vitrification steps occur rapidly with electron beam curing. Phase separation was observed in thermally cured bis-GMA/PTMO-MA and bis-GMA/PTMO-A mixtures from SEM photomicrographs. Similar SEM photographs did not show phase separation in the EB cured films.

6.4 *Recommendations for Future Studies*

This research has raised many questions; some have been answered in the preceding text, and some require further work and insight. Some of the areas for future studies will be provided below.

6.4.1 Effect of Fillers in Electron Beam Cured Systems

The effects of fillers on electron beam cured bis-GMA systems have not been investigated. Fillers such as titanium oxide, carbon black, or various silicon products are commonly used

in many industrial coatings. Quartz is also used as a filler in dental resins. Fillers added to the bis-GMA could serve as a "heat sink" for the exotherm developed by the reaction. By utilizing a controlled surface area and a known content and thermal conductivity of filler species, an average heat of reaction could be calculated similarly to those done for pure bis-GMA developed in Appendix A. The composition of filler would have to be varied to ensure that the polymer chains surround the filler to form a solid, stable coating. Fillers can also absorb the electrons, possibly blocking them from penetrating the entire coating. This blocking effect is greater for higher density fillers (e.g., metallic oxides). The potential problem could be a gradient in the degree of cure as a function of coating depth, or a non-uniform curing with less cure underneath the filler molecules.

6.4.2 Higher Molecular Weight Rubbery Modifier Materials

Since the 1000 g/mol molecular weight end-capped PTMO did not phase separate from bis-GMA during irradiation crosslinking, a higher molecular weight oligomer, maybe 2000 or 3000 g/mol, could be mixed with bis-GMA and irradiated via electron beam to see if molecular weight is the critical variable. It must be remembered that the reactivity of the system will be reduced as the chain ends, which contain the reactive species in these prepolymer systems, are on average farther apart in higher molecular weight systems. The trade-off mentioned earlier for prepolymers in radiation curing is relevant here; that is, high double bond density for low molecular weight oligomers vs. gelation from fewer crosslinking reactions with high molecular weight materials. Due to the higher reactivity of the acrylate species, future work should concentrate on the acrylate-capped oligomers. Another possibility is to end-cap polyethylene glycol (PEG) rather than the PTMO material used in this research. The major hindrance to overcome with either component is that of diffusion limitations, which are reached quickly in many EB prepolymer crosslinking reactions.

6.4.3 Quantification of Free Radicals using Electron Spin Resonance

An additional way of understanding the diffusion limitations in the radiation crosslinking of the bis-GMA systems is to quantify the trapped free radical species in the glassy matrices. This was indirectly done in the DSC tests by observing the magnitude of the exothermic peaks from the lower temperature reactions (with onsets of T_g at 40-50°C or 90-100°C). These peaks were from the plots which were normalized to account for differences in sample weight. A more direct approach would utilize electron spin resonance (ESR). O'Donnell [39] has successfully studied free radicals in irradiated polybutadiene systems using ESR. In addition, Abraham et. al. [40] investigated irradiated poly(methyl methacrylate) with this instrument, suggesting that a degradation takes place through disproportionation reactions. A possible study could be done to quantify the residual trapped radicals in the irradiated bis-GMA mixtures with TEGDMA and PEGDA. Based on the percent gel and residual double bond data discussed in this thesis, one would expect to find more trapped radicals in the bis-GMA/TEGDMA mixtures than in bis-GMA/PEGDA. In addition, as the concentration of TEGDMA or PEGDA is increased, the number of trapped radicals should increase. This verification would help explain the discrepancy from the two test methods. The relative quantities could be found by comparing the areas under the absorption curves [41]. Electron spin resonance facilities do not presently exist at VPI, but future plans may include the purchase of an ESR instrument.

6.4.4 Temperature Rise in Electron Beam Curing

A final focus of study to be mentioned here is to quantify the temperature rise during electron beam cure. Although Degnan's paper utilized a model based on solid engineering principles, little has been done to this author's knowledge to investigate other systems to determine its predictive capabilities. As thermal instrumentation becomes smaller, it will be feasible to run

the thermocouple (some thermal chip) through the electron beam chamber along with the coating. Another possibility is to insert infrared thermocouples in the chamber before and immediately after the electron beam curtain. It is the peak temperature and temperature of vitrification that are of interest, not that of the sample film as it comes out of the chamber. Thus, the thermal device would need to record the peak temperature during this process. In light of the discussion of the Time-Temperature-Transformation diagram alluded to before, this temperature of cure where the T_g of the crosslinking network increases to reach diffusion limitations becomes important because of its effect on physical properties.

Bibliography

1. G.A. Senich and R.E. Florin, JMS-Rev. Macromol. Chem. Phys. C24(2), 239 (1984).

2. W.J. Ramler, Private Communication, RPC Equipment, PPG Industries, Inc.

3. S.V. Nablo, J.R. Uglum, and B.S. Quintal in Non-Polluting coatings and Coating Processes (J.L. Gardon and J.W. Prane, eds.) Plenum Press, New York, 1973, p. 179.

4. R.C. Becker, J.H. Bly, M.R. Clelland, and J.P. Farrell, Radiation Phys. Chem., 14, 353 (1975).

5. E. Pollard and W.L. Davidson,Jr., Applied Nuclear Physics, Wiley, New York, 1942, p. 127.

6. R.S. Tu, 1982 Symposium on Radiation Curing, p. 10-1.

7. J.H. O'Donnell and A.K. Whitaker, British Polymer J., 17, 51 (1985).

8. N. Sagane and H. Harayama, Radiat. Phys. Chem., 18, 99 (1981). (1981).

9. A. Barlow, J.W. Biggs, and L.A. Meeks, Radiat. Phys. Chem., 18, 267 (1981).

10. L. Spenadel, Radiat. Phys. Chem., 14, 683 (1977).

11. A. Charlesby, Radiat. Phys. Chem., 18, 59 (1981).

12. A.A. Miller, E.J. Lawton, and J.S. Balwitt, J. Polym. Sci., 14, 50 (1954).

13. E.P. Tripp and S.V. Nablo, J. Coated Fabrics, 8, 144 (1978).

14. J.E. Mark, Adv. in Polymer Sciences, 44, 3 (1982).

15. A. Charlesby, *Atomic Radiation and Polymers*, Pergamon Press, New York (1960).

16. A. Rudin, *The Elements of Polymer Science and Engineering*, Academic Press, Inc., New York (1982), p. 192.

17. I. Mita, in *Aspects of Degradation and Stabilization of Polymers* (H.H.G. Jellink, ed.) Elsevier, Amsterdam, 1978, p. 247.

18. K.H. Sun, Mod. Plast., 32, 141, Ser.1 (1954).

19. M. Dole and C.D. Keeling, J. Amer. Chem. Soc., 75, 6082 (1953).

20. L.A. Wall, J. Polym. Sci., 17, 141 (1955).

21. R.W. Pearson, J. Polym. Sci., 25, 189 (1955).

22. B.G. Collyns, J.F. Fowler, and J. Weiss, Chem. and Ind. (Rev.) 3, 74 (1957).

23. J.K. Gillham, AIChE Journal, 20, 1056 (1974).

24. J.K. Gillham, Polym. Engr. and Science, 16, 353 (1976).

25. E.S.W. Kong, T.N. Snow, R. Redd, and G.L. Wilkes, Private Communication (1979).

26. J.B. Enns and J.K. Gillham, ONR Technical Report No. 25, Task No. NR-356-504 (1982).

27. J.B. Enns and J.K. Gillham, ONR Technical Report No. 26, Task No. NR-1356-504 (1983).

28. J.K. Gillham, ONR Technical Report No. 27 (1985).

29. E.B. Orler, G.L. Wilkes, and N.G. Kumar, Polymer Preprints, 26, 281 (1985).

30. A.M. Torgalkar, J. Dent. Res., 52, 483 (1973).

31. T.F. Degnan, Radiat. Phys. Chem., 19, 393 (1982).

32. W.H.T. Davison, J. Oil Col. Chem. Assoc., 52, 946 (1963).

33. D.R. Bailey, Paint Technol., 35(11), 12 (1971).

34. R.V. Milby, *Plastics Technology*. McGraw-Hill, New York, 1973.

35. I. Yilgor, E. Yilgor, A.K. Banthia, G.L. Wilkes, and J.E. McGrath, Polymer Composites, 4, 120 (1983).

36. W. Wu and B.M. Fanconi, Polym. Engr. and Sci., 23, 13 (1983).

37. R. Takiguchi and T. Uryu, J. App. Polym. Sci., 30, 709 (1985).

38. W. Oraby and W.K. Walsh, J. App. Polym. Sci., 23, 3227 (1979).

39. P.J. Flory, *Principles of Polymer Chemistry*, Cornell University Press, Ithaca, 1953.

40. P.F. Barron and J.H. O'Donnell, Polymer Bull. (Berlin), 14, 339 (1985).

41. R.J. Abraham, H.W. Melville, D.W. Ovenall, and D.H. Whiffen, Trans. Faraday Soc., 54, 1133 (1958).

42. E. Lifshin, E.A. Williams, "Analytical Methods", *Encyclopedia of Chemical Technology*, Kirk and Othmer (eds.), 3rd ed., Vol. 2, p. 668.

43. A.J. Swallow, *Radiation Chemistry of Organic Compounds*, Pergamon Press, Oxford, 1960.

44. A. Chapiro, *Radiation Chemistry of Polymeric Systems*, Wiley and Sons, New York, 1962.

Appendix A. Calculation of Temperature Rise During EB Cure

First, a simple model is in order to begin this evaluation. The assumptions are listed as follows:

1. No heat transfer to substrate or gas (adiabatic).
2. A volume element of the coating is selected (1 cm^3).
3. Residual double bond content is 55%, which means 45% of the double bonds have reacted. This is the result from FTIR testing on bis-GMA irradiated at 2 Mrads. Other dosages will be investigated as well.
4. Temperature rise calculations will be done based on the heats of reaction for the methacrylate or acrylate groups.
5. The temperature rise due to the energy of the electrons themselves is not considered.

Select a volume element. As mentioned above, the element selected is 1 cm^3. For bis-GMA, some physical constants are needed.

Density (bis-GMA) = 1.152 g/cm^3

Molecular Weight of bis-GMA = 512 g/gmol

ΔH = 26.0 $\pm$ 0.2 kcal/mole = 108 $\pm$ 0.6 kJ/mole

$\cong$ 4.319 (10^{-20}) cal/ molecule bis-GMA

The heat capacity of bis-GMA is found using Kopp's Rule:

$$C_p(\text{bis-GMA}) = [29(C_{pa})_C + 36(C_{pa})_H + 8(C_{pa})_O]\ \text{J/mol°C.}$$

$$= [29(12) + 36(18) + 8(25)]\text{J/mol°C}$$

$$= 1196\text{J/mol°C}$$

$$= 0.485\text{cal/g °C}$$

$$= 0.559\text{cal/cm}^3\ \text{°C}$$

Degnan [31] reports a general C_p for polymers of 0.4 ± 0.1 cal/g °C. The equation of energy includes an unsteady state term, a conduction term, and a heat generation term, as follows:

$$\rho C_p \frac{\partial T}{\partial t} = k\frac{\partial^2 T}{\partial y^2} + S_c \qquad (A - 2)$$

The heat generation term is defined by

$$S_c = \rho \Delta H_{pzn} \frac{dN}{dt} = \rho \Delta H_{pzn} k_c \qquad (A - 3)$$

From the boundary conditions it can be shown that the conduction term is zero for the adiabatic assumption, and the energy equation is then reduced to a separable first order equation:

$$C_p \frac{dT}{dt} = \Delta H_{pzn} k_c \qquad (A - 4)$$

Integrating and solving for ΔT leads to

$$\Delta T = \frac{\Delta H_{pzn} k_c t}{C_p} \qquad (A - 1).$$

A sample calculation for bis-GMA irradiated at 2 Mrads proceeds as follows:

$$\Delta H_{pzn} = \frac{26.0\ \text{kcal}}{\text{mole}} \left| \frac{\text{mole}}{6.02(10^{23})\text{molecules}} \right| \frac{10^3\text{cal}}{\text{kcal}}$$
$$= 4.319(10^{-20})\frac{\text{cal}}{\text{molecule}}$$

$$k_c = \frac{dN}{dt} = \frac{1.152\text{g}}{\text{cm}^3} \left| \frac{\text{gmole}}{512\text{g}} \right| \frac{6.02(10^{23})\text{molecules}}{\text{mole}} \left| \frac{0.225}{\text{sec}} \right.$$
$$= 3.05(10^{20})\frac{\text{molecules}}{\text{cm}^3\ \text{sec}}$$

$$\Delta T = \frac{4.319(10^{-20})\text{cal}}{\text{molecule}} \left| \frac{3.05(10^{20})\text{molecules}}{\text{cm}^3\ \text{sec}} \right| \frac{\text{cm}^3\ °\text{C}}{0.559\text{cal}} t$$
$$= 23.57t°\text{C}$$

where t is the time of reaction in seconds. At 2 seconds, this corresponds to a temperature rise of 47°C.

Tabulated below are similar results at the other dosages:

Table 1. Temperature Rise for Irradiated Bis-GMA (Calculated)

Irradiation Dosage (MR)	Percent Double Bonds Reacted (%)	Temperature Rise (K)
2 MR	45%	47°C
5 MR	57%	60°C
12 MR	70%	73°C

This model was also applied to polyethylene glycol diacrylate (PEGDA), discussed in Chapter 4 of this thesis. Physical properties are as follows:

Density (25°C) = ρ = 1.120 g/cm^3

Viscosity (25°C) = μ = 50 cps

Molecular Weight = 302 g/gmol

Heat Capacity = c_p = 0.585 cal /gmol (from Kopp's Rule)

ΔH = 37.4 kcal/gmol PEGDA

Similar calculations as those performed for bis-GMA at a reaction time of 2 seconds leads to:

Table 2. Temperature Rise in PEGDA Irradiated at 2, 5, and 12 Mrads.

Irradiation Dosage (MR)	Percent Double Bonds Reacted (%)	Temperature Rise (°C)
2 MR	65%	138°C
5 MR	88%	186°C
12 MR	89%	188°C

Appendix B. Calculation of Residual Double Bond Content from FTIR

Shown below is the calculation procedure to determine the residual double bond content in bis-GMA. The sample calculation given is for an irradiation dosage of 5 Mrad. The alkene peak is ratioed to the phenyl ring peak for normalization and compared to a similar ratio for unirradiated bis-GMA. The absorption spectra were used in these calculations.

Average Baseline

Alkene Peak (1638 cm ^{1})

$$\bar{Y} = \frac{A + B}{2}$$

Peak (1638 cm^{-1}) = C - $\bar{Y}$

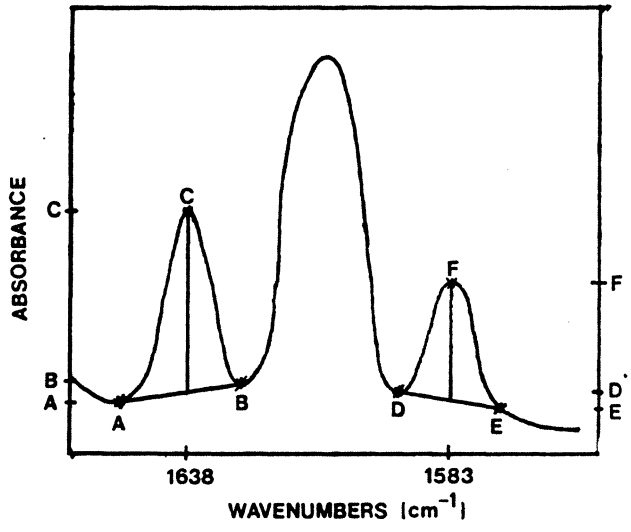

Phenyl Ring Peak (1583 cm ^{1})

$$\bar{Z} = \frac{D + E}{2}$$

Peak (1583 cm^{-1}) = F - $\bar{Z}$

$$\text{Ratio} = \frac{\text{Peak}(1638\text{cm}^{-1})}{\text{Peak}(1583\text{cm}^{-1})} = \frac{C - \bar{Y}}{F - \bar{Z}} = 1.1091(5\ \text{Mrad, 1 hour after cure})$$

The ratio is divided by a similar ratio for unirradiated bis-GMA.

$$\%\ \text{Double Bonds} = \frac{\text{Ratio (5 MR)}}{\text{Ratio (No EB)}} \times 100 = \frac{1.1091}{2.350} \times 100 = 47.2$$

Percent Double Bonds = 47%.

The vita has been removed
from the scanned document